

# CP Factor Model for Dynamic Tensors\*

Yuefeng Han<sup>1</sup>, Dan Yang<sup>2</sup>, Cun-Hui Zhang<sup>3</sup> and Rong Chen<sup>3</sup>

<sup>1</sup>Department of Applied and Computational Mathematics and Statistics, University of Notre Dame, Notre Dame, IN 46556, USA

<sup>2</sup>Business School, The University of Hong Kong, Hong Kong

<sup>3</sup>Department of Statistics, Rutgers University, Piscataway, NJ 08854, USA

## Abstract

Observations in various applications are frequently represented as a time series of multidimensional arrays, called tensor time series, preserving the inherent multidimensional structure. In this paper, we present a factor model approach, in a form similar to tensor CP decomposition, to the analysis of high-dimensional dynamic tensor time series. As the loading vectors are uniquely defined but not necessarily orthogonal, it is significantly different from the existing tensor factor models based on Tucker-type tensor decomposition. The model structure allows for a set of uncorrelated one-dimensional latent dynamic factor processes, making it much more convenient to study the underlying dynamics of the time series. A new high order projection estimator is proposed for such a factor model, utilizing the special structure and the idea of the higher order orthogonal iteration procedures commonly used in Tucker-type tensor factor model and general tensor CP decomposition procedures. Theoretical investigation provides statistical error bounds for the proposed methods, which shows the significant advantage of utilizing the special model structure. Simulation study is conducted to further demonstrate the finite sam-

---

\* Yuefeng Han is Assistant Professor, Department of Applied and Computational Mathematics and Statistics, University of Notre Dame, Notre Dame, IN 46556. Email: yuefeng.han@nd.edu. Dan Yang is Associate Professor, Business School, The University of Hong Kong, Hong Kong. Email: dyanghku@hku.hk. Cun-Hui Zhang is Professor, Department of Statistics, Rutgers University, Piscataway, NJ 08854. E-mail: czhang@stat.rutgers.edu. Rong Chen is Professor, Department of Statistics, Rutgers University, Piscataway, NJ 08854. E-mail: rongchen@stat.rutgers.edu. Rong Chen is the corresponding author. Han's research was supported in part by National Science Foundation grant IIS-1741390. Yang's research was supported in part by NSF grant IIS-1741390, Hong Kong grant GRF 17301620, Hong Kong grant CRF C7162-20GF and Shenzhen grant SZRI2023-TBRF-03. Zhang's research was supported in part by NSF grants DMS-1721495, IIS-1741390, CCF-1934924, DMS-2052949 and DMS-2210850. Chen's research was supported in part by National Science Foundation grants DMS-1737857, IIS-1741390, CCF-1934924, DMS-2027855 and DMS-2319260.

ple properties of the estimators. Real data application is used to illustrate the model and its interpretations.

**Keywords:** Tensor Factor Model, CP Decomposition, Tensor Time Series, Dimension Reduction, Orthogonal Projection.

## 1 Introduction

In recent years, information technology has made tensors or high-order arrays observations routinely available in applications. For example, such data arises naturally from genomics ([Alter and Golub, 2005](#), [Omberg et al., 2007](#)), neuroimaging analysis ([Sun and Li, 2017](#), [Zhou et al., 2013](#)), recommender systems ([Bi et al., 2018](#)), computer vision ([Liu et al., 2012](#)), community detection ([Anandkumar et al., 2014a](#)), longitudinal data analysis ([Hoff, 2015](#)), among others. Most of the developed tensor-based methods were designed for independent and identically distributed (i.i.d.) tensor data or tensor data with i.i.d. noise.

On the other hand, in many applications, the tensors are observed over time, and hence form a tensor-valued time series. For example, the monthly import export volumes of multi-categories of products (e.g. Chemical, Food, Machinery and Electronic, and Footwear and Headwear) among countries naturally form a dynamic sequence of 3-way tensor-variates, each of which representing a weighted directional transportation network. Another example is functional MRI, which typically consists hundreds of thousands of voxels observed over time. A sequence of 2-D or 3-D images can also be modeled as matrix or tensor time series to preserve temporal structure. Development of statistical methods for analyzing such large scale tensor-valued time series is still in its infancy.

In many settings, although the observed tensors are of high order and high dimension, there is often hidden low-rank structures in the tensors that can be exploited to facilitate the data analysis. Such a low-rank condition provides convenient decomposable structures and has been widely used in tensor data analysis. Two common choices of low-rank tensor structures are CANDECOMP/PARAFAC (CP) structure and multilinear/Tucker structure, and each of them has their respective benefits; see the survey in [Kolda and Bader \(2009\)](#).

In dynamic data, the low-rank structures are often realized through factor models, one of the most effective and popular dimension reduction tools. Over the past few decades, there has been a large body of literature in the statistics and econometrics communities on factor models for vector time series. An incomplete list of the publications includes [Bai \(2003\)](#), [Bai and Ng \(2002\)](#), [Chamberlain and Rothschild \(1983\)](#), [Fan et al. \(2011, 2013, 2016\)](#), [Forni et al. \(2000, 2004, 2005\)](#), [Lam and Yao \(2012\)](#), [Lam et al. \(2011\)](#), [Pan and Yao \(2008\)](#), [Pena and Box \(1987\)](#), [Stock and Watson \(2002\)](#). Recently, the factor model approach has been developed for analyzing high

dimensional dynamic tensor time series (Chang et al., 2023, Chen and Fan, 2023, Chen et al., 2019, 2024, 2022, Han et al., 2020, 2022, Wang et al., 2019). These existing works utilize the Tucker low-rank structure in formulating the factor models. Such Tucker type tensor factor model is also closely related to separable factor analysis in Fosdick and Hoff (2014) under the array Normal distribution of Hoff (2011).

In this paper, we investigate a tensor factor model with a CP type low-rank structure, called TFM-cp. Specifically, let  $\mathcal{X}_t$  be an order  $K$  tensor of dimensions  $d_1 \times d_2 \times \dots \times d_K$ . We assume

$$\mathcal{X}_t = \sum_{i=1}^r w_i f_{it} \mathbf{a}_{i1} \otimes \mathbf{a}_{i2} \otimes \dots \otimes \mathbf{a}_{iK} + \mathcal{E}_t, \quad t = 1, \dots, T, \quad (1)$$

where  $\otimes$  denotes tensor product,  $w_i > 0$  represents the signal strength,  $\mathbf{a}_{ik}$ ,  $i = 1, \dots, r$ , are unit vectors of dimension  $d_k$ , with  $\|\mathbf{a}_{ik}\|_2 = 1$ ,  $\mathcal{E}_t$  is a noise tensor of the same dimension as  $\mathcal{X}_t$ , and  $\{f_{it}, i = 1, \dots, r\}$  is a set of uncorrelated univariate latent factor processes. That is, the signal part of the observed tensor at time  $t$  is a linear combination of  $r$  rank-one tensors,  $w_i \mathbf{a}_{i1} \otimes \mathbf{a}_{i2} \otimes \dots \otimes \mathbf{a}_{iK}$ . These rank-one tensors are fixed and do not change over time. Here,  $\{\mathbf{a}_{ik}, 1 \leq i \leq r, 1 \leq k \leq K\}$  are called loading vectors and the loading vectors for each mode,  $\{\mathbf{a}_{ik}, 1 \leq i \leq r\}$ , are not necessarily orthogonal. The dynamics of the tensor time series are driven by the  $r$  univariate latent processes  $f_{it}$ . By stacking the fibers of the tensor  $\mathcal{X}_t$  into a vector, the TFM-cp can be written as a vector factor model, with  $r$  factors and a  $d \times r$  (where  $d = d_1 \dots d_K$ ) loading matrix of a special structure induced by the TFM-cp. More detailed discussion of the model is given in Section 2.

A standard approach for dynamic factor model estimation is through the analysis of the covariance or autocovariance of the observed process. The autocovariance of a TFM-cp process in (1) is also a tensor with a low-rank CP structure. Hence, potentially the estimation of (1) can be done with a tensor CP decomposition procedure. However, tensor CP decomposition is well known to be a notoriously challenging problem as it is in general NP hard to compute and the CP rank is not lower semi-continuous (Håstad, 1990, Hillar and Lim, 2013, Kolda and Bader, 2009). There are a number of works on tensor CP decomposition, which is often called tensor principal component analysis (PCA) in the literature, including alternating least squares (Comon et al., 2009), robust tensor power methods with orthogonal components (Anandkumar et al., 2014b), tensor unfolding approaches (Richard and Montanari, 2014, Wang and Lu, 2017), rank-one alternating least squares (Anandkumar et al., 2014c, Sun et al., 2017), and simultaneous matrix diagonalization (Kuleshov et al., 2015). See also Auddy and Yuan (2023b), Han et al. (2023), Hao et al. (2020), Wang and Li (2020), Wang and Song (2017), Zhou et al. (2013), among others. Although these methods can be used directly to obtain the low-rank CP components of the autocovariance tensors, they have been designed for general tensors and do not utilize the special structure embedded in the TFM-cp.

In this paper, we develop a new estimation procedure, named as **High-Order Projection**

Estimators (HOPE), for TFM-cp in (1). The procedure includes a warm-start initialization using a newly developed composite principal component analysis (cPCA), and an iterative simultaneous orthogonalization scheme to refine the estimator. The procedure is designed to take the advantage of the special structure of TFM-cp whose autocovariance tensor has a specific CP structure with components close to being orthogonal and of a high-order coherence in a multiplicative form. The proposed cPCA takes advantage of this feature so the initialization is better than using random projection initialization often used in generic CP decomposition algorithms. The refinement step makes use of the multiplicative coherence again and is better than the alternating least squares, the iterative projection algorithm (Han et al., 2020), and other forms of the high order orthogonal iteration (HOOI) (De Lathauwer et al., 2000, Liu et al., 2014, Zhang and Xia, 2018). Our theoretical analysis provides details of these improvements.

In the theoretical analysis, we establish statistical upper bounds on the estimation errors of the factor loading vectors for the proposed algorithms. The cPCA yields useful and good initial estimators with less restrictive conditions, and the iterative algorithm provides faster statistical error rates under weaker conditions than the generic CP decomposition algorithms. For cPCA, the number of factors  $r$  can increase with the dimensions of the tensor time series and is allowed to be larger than  $\max_k d_k$ . We also derive the statistical guarantees of the iterative algorithm under the settings where the tensor is (sufficiently) undercomplete ( $r \ll \min_k d_k$ ). It is worth noting that the iterative refinement algorithm has much sharper upper bounds for the statistical error than the cPCA initial estimators.

The TFM-cp in (1) can also be written as a tensor factor model with a Tucker form (TFM-tucker) of a special structure. See (3) for the definition of TFM-tucker and Remark 3 below for the comparison between TFM-cp and TFM-tucker from the perspectives of modeling assumptions and interpretations. Potentially, the iterative estimation procedures designed for TFM-tucker can also be used here (Han et al., 2020), ignoring the special TFM-cp structure. However, HOPE has lower computational complexity per iteration, requires less restrictive conditions and exhibits faster convergence rate, by fully utilizing the structure of TFM-cp. See Remark 16 for further discussion. They also share the nice properties that the increase in either the dimensions  $d_1, \dots, d_k$ , or the sample size can improve the estimation of the factor loading vectors or spaces.

The rest of the paper is organized as follows. After a brief introduction of the basic notations and preliminaries of tensor analysis in Section 1.1, we introduce a tensor factor model with CP low-rank structure in Section 2. The estimation procedures of the factors and the loading vectors are presented in Section 3. Section 4 investigates the theoretical properties of the proposed methods. Section 5 develops some alternative algorithms to tensor factor models, which extend existing popular CP methods to the auto-covariance tensors with cPCA as initialization, and provides some

simulation studies to demonstrate the numerical performance of all the estimation procedures. Section 6 illustrates the model and its interpretations in real data applications. Section 7 provides a short concluding remark. All technical details and more simulation results are relegated to the supplementary materials.

## 1.1 Notations and preliminaries

The following basic notations and preliminaries will be used throughout the paper. Define  $\|x\|_q = (x_1^q + \dots + x_p^q)^{1/q}$ ,  $q \geq 1$ , for any vector  $x = (x_1, \dots, x_p)^\top$ . The matrix spectral norm is denoted as

$$\|A\|_S = \max_{\|x\|_2=1, \|y\|_2=1} \|x^\top A y\|_2.$$

For two sequences of real numbers  $\{a_n\}$  and  $\{b_n\}$ , write  $a_n = O(b_n)$  (resp.  $a_n \asymp b_n$ ) if there exists a constant  $C$  such that  $|a_n| \leq C|b_n|$  (resp.  $1/C \leq a_n/b_n \leq C$ ) holds for all sufficiently large  $n$ , and write  $a_n = o(b_n)$  if  $\lim_{n \rightarrow \infty} a_n/b_n = 0$ . Write  $a_n \lesssim b_n$  (resp.  $a_n \gtrsim b_n$ ) if there exists a constant  $C$  such that  $a_n \leq Cb_n$  (resp.  $a_n \geq Cb_n$ ).

For any two tensors  $\mathcal{A} \in \mathbb{R}^{m_1 \times m_2 \times \dots \times m_K}$ ,  $\mathcal{B} \in \mathbb{R}^{r_1 \times r_2 \times \dots \times r_N}$ , denote the tensor product  $\otimes$  as  $\mathcal{A} \otimes \mathcal{B} \in \mathbb{R}^{m_1 \times \dots \times m_K \times r_1 \times \dots \times r_N}$ , such that

$$(\mathcal{A} \otimes \mathcal{B})_{i_1, \dots, i_K, j_1, \dots, j_N} = (\mathcal{A})_{i_1, \dots, i_K} (\mathcal{B})_{j_1, \dots, j_N}.$$

The  $k$ -mode product of  $\mathcal{A} \in \mathbb{R}^{r_1 \times r_2 \times \dots \times r_K}$  with a matrix  $U \in \mathbb{R}^{m_k \times r_k}$  is an order  $K$ -tensor of size  $r_1 \times \dots \times r_{k-1} \times m_k \times r_{k+1} \times \dots \times r_K$  and will be denoted as  $\mathcal{A} \times_k U$ , such that

$$(\mathcal{A} \times_k U)_{i_1, \dots, i_{k-1}, j, i_{k+1}, \dots, i_K} = \sum_{i_k=1}^{r_k} \mathcal{A}_{i_1, i_2, \dots, i_K} U_{j, i_k}.$$

Given  $\mathcal{A} \in \mathbb{R}^{m_1 \times \dots \times m_K}$  and  $m = \prod_{j=1}^K m_j$ , let  $\text{vec}(\mathcal{A}) \in \mathbb{R}^m$  be vectorization of the matrix/tensor  $\mathcal{A}$ ,  $\text{mat}_k(\mathcal{A}) \in \mathbb{R}^{m_k \times (m/m_k)}$  the mode- $k$  matrix unfolding of  $\mathcal{A}$ , and  $\text{mat}_k(\text{vec}(\mathcal{A})) = \text{mat}_k(\mathcal{A})$ .

## 2 A tensor factor model with a CP low rank structure

Again, we specifically consider the following tensor factor model with CP low-rank structure (TFM-cp) for observations  $\mathcal{X}_t \in \mathbb{R}^{d_1 \times \dots \times d_K}$ ,  $1 \leq t \leq T$ ,

$$\mathcal{X}_t = \sum_{i=1}^r w_i f_{it} \mathbf{a}_{i1} \otimes \mathbf{a}_{i2} \otimes \dots \otimes \mathbf{a}_{iK} + \mathcal{E}_t,$$

where  $f_{it}$  is the unobserved latent factor process and  $\mathbf{a}_{ik}$  are the fixed unknown factor loading vectors. We assume without loss of generality,  $\mathbb{E}f_{it}^2 = 1$ ,  $\|\mathbf{a}_{ik}\|_2 = 1$ , for all  $1 \leq i \leq r$  and

$1 \leq k \leq K$ . Then, all the signal strengths are contained in  $w_i$ . A key assumption of TFM-cp is that the factor process  $f_{it}$  is assumed to be uncorrelated across different factor processes, e.g.,  $\mathbb{E}f_{it-h}f_{jt} = 0$  for  $i \neq j$  and  $h \geq 1$ . In addition, we assume that the noise tensor  $\mathcal{E}_t$  are uncorrelated (white) across time, but with an arbitrary contemporary covariance structure, following [Lam and Yao \(2012\)](#), [Chen et al. \(2022\)](#). In this paper, we consider the case that the order of the tensor  $K$  is fixed but the dimensions  $d_1, \dots, d_K \rightarrow \infty$  and rank  $r$  can be fixed or diverging.

**Remark 1.** By incorporating time, we may stack  $\mathcal{X}_t$  into an order- $(K+1)$  tensor  $\mathcal{Y} \in \mathbb{R}^{d_1 \times \dots \times d_K \times T}$ , with time  $t$  as the  $(K+1)$ -th mode, referred to as the time-mode. Subsequently, model (1) can be reformulated as

$$\mathcal{Y} = \sum_{i=1}^r w_i \mathbf{a}_{i1} \otimes \mathbf{a}_{i2} \otimes \dots \otimes \mathbf{a}_{iK} \otimes \mathbf{f}_i + \mathcal{E}, \quad (2)$$

where  $\mathbf{f}_i = (f_{i1}, \dots, f_{iT})^\top$ . While it is enticing to directly estimate the signal part in (2) with standard tensor CP decomposition approaches based on the assumed CP structure, the dynamics and dependencies in the time direction (auto-dependency) are pivotal and warrant a distinct treatment. In our model, the component in the time direction is deemed latent and random. Consequently, it is crucial to examine the unique role of the time-mode and the (auto)-covariance structure in the time direction. The assumptions and interpretations inherent in our model, along with the corresponding estimation procedures and theoretical properties, markedly diverge from those of using the standard CP decompositions.

**Remark 2.** Ignoring the random noise  $\mathcal{E}$ , the CP decomposition in (2) is unique up to scaling and permutation indeterminacy if  $\sum_{k=1}^K \mathcal{R}(\mathbf{A}_k) + \mathcal{R}(\mathbf{F}) \geq 2r + K$ , where  $\mathbf{A}_k = (\mathbf{a}_{1k}, \dots, \mathbf{a}_{rk})$ ,  $\mathbf{F} = (\mathbf{f}_1, \dots, \mathbf{f}_r)$  and  $\mathcal{R}(\mathbf{A}) = \max\{s : \text{any } s \text{ columns of the matrix } \mathbf{A} \text{ are linearly independent}\}$ . Such a requirement provides a sufficient condition for uniqueness as per [Kolda and Bader \(2009\)](#). In the subsequent estimation procedure, we delve into the estimation of the auto-covariance tensor  $\boldsymbol{\Sigma}_h$  in (5) below. The sufficient identifiability condition for the CP decomposition of the auto-covariance tensor becomes  $2 \sum_{k=1}^K \mathcal{R}(\mathbf{A}_k) \geq 2r + 2K - 1$ . This condition is significantly milder compared to the condition necessary to ensure statistical convergence.

**Remark 3 (Comparison of TFM-cp with a Tucker low-rank structure).** [Chen and Fan \(2023\)](#), [Chen et al. \(2022\)](#), [Han et al. \(2020, 2022\)](#) studied the following tensor factor models with a Tucker low-rank structure (TFM-tucker):

$$\mathcal{X}_t = \mathcal{F}_t \times_1 \mathbf{A}_1 \times \dots \times \mathbf{A}_K + \mathcal{E}_t, \quad (3)$$

where the core tensor  $\mathcal{F}_t \in \mathbb{R}^{r_1 \times \dots \times r_K}$  is the latent factor process in a tensor form, and  $\mathbf{A}_i$ 's are  $d_i \times r_i$  loading matrices. For example, when  $K = 2$  (matrix time series), the TFM-cp can be

rewritten as a TFM-tucker,

$$\mathbf{X}_t = \mathbf{A}_1 \mathbf{F}_t \mathbf{A}_2^\top + \mathbf{E}_t, \quad (4)$$

where  $\mathbf{F}_t = \text{diag}(f_{1t}, \dots, f_{rt})$ , and  $\mathbf{A}_1 = (\mathbf{a}_{11}, \dots, \mathbf{a}_{r1})$  and  $\mathbf{A}_2 = (\mathbf{a}_{12}, \dots, \mathbf{a}_{r2})$  are matrices with the column vectors being  $\mathbf{a}_{ik}$ 's. There are four major differences between TFM-tucker and TFM-cp. First, TFM-tucker suffers from a severe identification problem, as the model remains equivalent if  $\mathcal{F}_t$  is replaced by  $\mathcal{F}_t \times_k \mathbf{R}$  and  $\mathbf{A}_k$  replaced by  $\mathbf{A}_k \mathbf{R}^{-1}$  for any invertible  $r_k \times r_k$  matrix  $\mathbf{R}$ . For the  $K = 2$  case,  $\mathbf{X}_t = (\mathbf{A}_1 \mathbf{R}_1^{-1})(\mathbf{R}_1 \mathbf{F}_t \mathbf{R}_2^\top)(\mathbf{A}_2 \mathbf{R}_2^{-1})^\top + \mathbf{E}_t$  are all equivalent under TFM-tucker. Such ambiguity makes it difficult to find an ‘optimal’ representation of the model, which often leads to *ad hoc* and convenient representations that are difficult to interpret (Bai and Wang, 2014, 2015, Bekker, 1986, Neudecker, 1990). On the other hand, TFM-cp is uniquely defined up to sign changes, under an ordering of the signal strengths  $w_1 \geq w_2 \geq \dots \geq w_r$ . As a result, the interpretation of the model becomes much easier. Second, although TFM-cp can be rewritten in the form of (3) with a *diagonal* core latent tensor consisting of the individual  $f_{it}$ 's, it is not under a typical Tucker form since TFM-tucker typically adopts the representation that the loading matrices  $\mathbf{A}_k$ 's are orthonormal, due to its identification problem. In TFM-cp, the loading vectors  $\{\mathbf{a}_{ik}, 1 \leq i \leq r\}$  are not necessarily orthogonal vectors. In the  $K = 2$  example in (4), if we find rotation matrices  $\mathbf{R}_1$  and  $\mathbf{R}_2$  so that  $\mathbf{A}_1 \mathbf{R}_1^{-1}$  and  $\mathbf{A}_2 \mathbf{R}_2^{-1}$  are orthonormal, then the corresponding core factor process in (4) becomes  $\mathbf{R}_1 \mathbf{F}_t \mathbf{R}_2^\top$ , no longer diagonal and with  $r^2$  heavily correlated components, rather than  $r$  uncorrelated components. Third, TFM-cp separates the factor processes into a set of univariate time series, which enjoys great advantages over the tensor-valued factor processes in TFM-tucker. Modelling univariate time series are much easier and more flexible due to the vast repository of linear and nonlinear options. Lastly, TFM-cp is often much more parsimonious due to its restrictions, while enjoying great flexibility. Note that TFM-tucker is also a special case of TFM-cp, as it can be written as a sum of  $r = r_1 \dots r_K$  rank-one tensors, albeit with many repeated loading vectors. With its condensed formulation, in practical applications, the number of factors  $r$  needed under TFM-cp is typically much smaller than the total number  $r_1 \dots r_K$  of factors needed in TFM-tucker.

**Remark 4.** There are two different types of factor model assumptions in the literature. One type of factor models assumes that the common factors must have impact on ‘most’ (defined asymptotically) of the time series, but allows the idiosyncratic noise ( $\mathcal{E}_t$ ) to have weak cross-correlations and weak auto-correlations; see, e.g., Bai and Ng (2002), Chen and Fan (2023), Fan et al. (2011, 2013), Forni et al. (2000), Stock and Watson (2002). PCA of the sample covariance matrix is typically used to estimate the factor loading space, with various extensions. The other type of factor models assumes that the factors accommodate all dynamics, making the idiosyncratic noise ‘white’ with no auto-correlation, but allows substantial contemporary cross-correlation among the error process; see, e.g., Lam and Yao (2012), Lam et al. (2011), Pan and Yao (2008), Pena and

Box (1987), Wang et al. (2019). Under such assumptions, PCA is applied to the non-zero lagged autocovariance matrices. In this paper, we adopt the latter type of assumptions in our model development.

### 3 Estimation procedures

In this section, we focus on the estimation of the factors and loading vectors of model (1). The proposed procedure includes two steps: an initialization step using a new composite PCA (cPCA) procedure, presented in Algorithm 1, and an iterative refinement step using a new iterative simultaneous orthogonalization (ISO) procedure, presented in Algorithm 2. We call this two-step procedure HOPE (**H**igh-**O**rders **P**rojection **E**stimators) as it repeatedly perform high order projections on high order moments of the tensor observations. It utilizes the special structure of the model and leads to higher statistical and computational efficiency, which will be demonstrated later.

For  $\mathcal{X}_t$  following (1), the lagged cross-product operator, denoted by  $\boldsymbol{\Sigma}_h$ , is the  $(2K)$ -tensor satisfying

$$\begin{aligned} \boldsymbol{\Sigma}_h &= \mathbb{E} \left[ \sum_{t=h+1}^T \frac{\mathcal{X}_{t-h} \otimes \mathcal{X}_t}{T-h} \right] \\ &= \sum_{i=1}^r \lambda_{i,h} (\mathbf{a}_{i1} \otimes \mathbf{a}_{i2} \otimes \cdots \otimes \mathbf{a}_{iK})^{\otimes 2} \in \mathbb{R}^{d_1 \times \cdots \times d_K \times d_1 \times \cdots \times d_K}, \end{aligned} \quad (5)$$

for a given  $h \geq 1$ , where  $\lambda_{i,h} = w_i^2 \mathbb{E} f_{i,t-h} f_{i,t}$ . Note that the tensor  $\boldsymbol{\Sigma}_h$  is expressed in a CP-decomposition form with each  $\mathbf{a}_{ik}$  used twice. Let  $\hat{\boldsymbol{\Sigma}}_h$  be the sample version of  $\boldsymbol{\Sigma}_h$ ,

$$\hat{\boldsymbol{\Sigma}}_h = \sum_{t=h+1}^T \frac{\mathcal{X}_{t-h} \otimes \mathcal{X}_t}{T-h}. \quad (6)$$

When  $\mathcal{X}_t$  is weakly stationary and  $\mathcal{E}_t$  is white noise, a natural approach to estimating the loading vectors is via minimizing the empirical squared loss

$$(\mathbf{a}_{i1}, \mathbf{a}_{i2}, \dots, \mathbf{a}_{iK}, 1 \leq i \leq r) = \arg \min_{\substack{\mathbf{a}_{i1}, \mathbf{a}_{i2}, \dots, \mathbf{a}_{iK}, 1 \leq i \leq r, \\ \|\mathbf{a}_{i1}\|_2 = \dots = \|\mathbf{a}_{iK}\|_2 = 1}} \left\| \hat{\boldsymbol{\Sigma}}_h - \sum_{i=1}^r \lambda_{i,h} (\mathbf{a}_{i1} \otimes \mathbf{a}_{i2} \otimes \cdots \otimes \mathbf{a}_{iK})^{\otimes 2} \right\|_{\text{HS}}^2, \quad (7)$$

where the Hilbert Schmidt norm for a tensor  $\mathcal{A}$  is defined as  $\|\mathcal{A}\|_{\text{HS}} = \|\text{vec}(\mathcal{A})\|_2$ . In other words,  $\mathbf{a}_{i1} \otimes \mathbf{a}_{i2} \otimes \cdots \otimes \mathbf{a}_{iK}$  can be estimated by the leading *principal component* of the sample autocovariance tensor  $\hat{\boldsymbol{\Sigma}}_h$ . However, due to the non-convexity of (7) or its variants, a straightforward implementation of many local search algorithms, such as gradient descent and alternating minimization, may easily get trapped into local optima and result in sub-optimal statistical performance. As shown by Auffinger et al. (2013), there could be an exponential number of local optima and the

great majority of these local optima are far from the best low rank approximation. However, if we start from an appropriate initialization not too far from the global optimum, then a local optimum reached may be as good an estimator as the global optimum. A critical task in estimating the factor loading vectors is thus to obtain good initialization.

We develop a warm initialization procedure, the composite PCA (cPCA) procedure. Note that, if we unfold  $\Sigma_h$  into a  $d \times d$  matrix  $\Sigma_h^*$ , where  $d = d_1 \dots d_K$ , then (5) implies that

$$\Sigma_h^* = \sum_{i=1}^r \lambda_{i,h} \mathbf{a}_i \mathbf{a}_i^\top, \quad (8)$$

a sum of  $r$  rank-one matrices, each of the form  $\mathbf{a}_i \mathbf{a}_i^\top$ , where  $\mathbf{a}_i = \text{vec}(\otimes_{k=1}^K \mathbf{a}_{ik})$ . This is very close to the principal component decomposition of  $\Sigma_h^*$ , except that  $\mathbf{a}_i$ 's are not necessarily orthogonal in this case. However, the following intuition provides a solid justification of using PCA to obtain an estimate of  $\mathbf{a}_i$ . We call this estimator the cPCA estimator.

The accuracy of using the principal components of  $\Sigma_h^*$  as the estimate of  $\mathbf{a}_i$  heavily depends on the coherence of the components, defined as  $\vartheta = \max_{1 \leq i < j \leq r} |\mathbf{a}_i^\top \mathbf{a}_j|$ , the maximum pairwise correlation among the  $\mathbf{a}_i$ 's. When the components are orthogonal ( $\vartheta = 0$ ), there is no error in using PCA. The main idea of cPCA is to take advantage of the special structure of TFM-cp, which leads to a multiplicative high-order coherence of the CP components. In the following, we provide an analysis of  $\vartheta$  under TFM-cp.

Let  $\mathbf{A}_k = (\mathbf{a}_{1k}, \dots, \mathbf{a}_{rk}) \in \mathbb{R}^{d_k \times r}$  be the matrix with  $\mathbf{a}_{ik}$  as its columns, and  $\mathbf{A}_k^\top \mathbf{A}_k = (\sigma_{ij,k})_{r \times r}$ . As  $\sigma_{ii,k} = \|\mathbf{a}_{ik}\|_2^2 = 1$ , the correlation among columns of  $\mathbf{A}_k$  can be measured by

$$\vartheta_k = \max_{1 \leq i < j \leq r} |\sigma_{ij,k}|, \quad \delta_k = \|\mathbf{A}_k^\top \mathbf{A}_k - I_r\|_S, \quad \eta_{jk} = \left( \sum_{i \in [r] \setminus \{j\}} \sigma_{ij,k}^2 \right)^{1/2}. \quad (9)$$

Similarly we use

$$\vartheta = \max_{1 \leq i < j \leq r} |\mathbf{a}_i^\top \mathbf{a}_j|, \quad \delta = \|\mathbf{A}^\top \mathbf{A} - I_r\|_S, \quad (10)$$

to measure the correlation of the matrix  $\mathbf{A} = (\mathbf{a}_1, \dots, \mathbf{a}_r) \in \mathbb{R}^{d \times r}$  with  $\mathbf{a}_i = \text{vec}(\otimes_{k=1}^K \mathbf{a}_{ik})$  and  $d = \prod_{k=1}^K d_k$ . It can be seen that the coherence  $\vartheta$  has the bound  $\vartheta \leq \prod_{k=1}^K \vartheta_k \leq \vartheta_{\max}^K$ , due to  $\mathbf{a}_i^\top \mathbf{a}_j = \prod_{k=1}^K \mathbf{a}_{ik}^\top \mathbf{a}_{jk} = \prod_{k=1}^K \sigma_{ij,k}$ . The spectrum norm  $\delta$  is also bounded by the multiplicative of correlation measures in (9). More specifically, we have the following proposition.

**Proposition 1.** Define  $\mu_* = \max_j \min_{k_1, k_2} \max_{i \neq j} \prod_{k \neq k_1, k \neq k_2, k \in [K]} \sqrt{r} |\sigma_{ij,k}| / \eta_{jk} \in [1, r^{K/2-1}]$  as

the (leave-two-out) mutual coherence of  $\mathbf{A}_1, \dots, \mathbf{A}_K$ . Then,  $\delta \leq \min_{1 \leq k \leq K} \delta_k$  and

$$\delta \leq (r-1)\vartheta, \quad \text{and} \quad \vartheta \leq \prod_{k=1}^K \vartheta_k \leq \vartheta_{\max}^K, \quad (11)$$

$$\delta \leq \mu_* r^{1-K/2} \max_{j \leq r} \prod_{k=1}^K \eta_{jk} \leq \mu_* r^{1-K/2} \prod_{k=1}^K \delta_k. \quad (12)$$

When (most of) the quantities in (9) are small, the products in (11) would be very small so that the  $\mathbf{a}_i$ 's are nearly orthogonal. For example, if  $(\mathbf{a}_{11}, \mathbf{a}_{21})$  and  $(\mathbf{a}_{12}, \mathbf{a}_{22})$  both have i.i.d. bivariate random rows with correlation coefficients  $\rho_1$  and  $\rho_2$ , and independent, then the population correlation coefficient of  $\text{vec}(\mathbf{a}_{11} \otimes \mathbf{a}_{12})$  and  $\text{vec}(\mathbf{a}_{21} \otimes \mathbf{a}_{22})$  is  $\rho_1 \rho_2$ , though the variation of the sample correlation coefficient depends on the length of the  $\mathbf{a}_{ik}$ 's.

**Remark 5.** Let polylog denote the polynomial of the logarithm. The incoherence condition such as  $\vartheta_{\max} \lesssim \text{polylog}(d_{\min})/\sqrt{d_{\min}}$  is commonly imposed in the literature for generic CP decomposition; see e.g. Anandkumar et al. (2014b,c), Hao et al. (2020), Sun et al. (2017). Proposition 1 establishes a connection between  $\delta$ ,  $\delta_k$  and the  $\vartheta_k$  in the same framework of incoherence considerations. The parameters  $\delta_k$  and  $\delta$  quantify the non-orthogonality of the factor loading vectors, and play a key role in our theoretical analysis, as the performance bound of cPCA estimators involves  $\delta$ . Differently from the existing literature depending on  $\vartheta_{\max}$ , the cPCA exploits  $\delta$  or the much smaller  $\vartheta$  (comparing to  $\vartheta_{\max}$ ), thus has better properties when  $K \geq 2$ . Note that the idea of using tensor unfolding to enhance incoherence can be traced back to Allman et al. (2009), Huang et al. (2015), Jain and Oh (2014), though their incoherence measure is slightly different from ours. The most notable advances from these studies is that we establish a non-asymptotic bound for the estimated loading vectors in the presence of noise (c.f. Theorem 1).

The pseudo-code of cPCA is provided in Algorithm 1. Though  $\boldsymbol{\Sigma}_h^*$  is symmetric, its sample version  $\hat{\boldsymbol{\Sigma}}_h^*$  in general is not. We use  $(\hat{\boldsymbol{\Sigma}}_h^* + \hat{\boldsymbol{\Sigma}}_h^{*\top})/2$  to ensure symmetry and reduce the noise. The cPCA produces definitive initialization vectors up to the sign change.

---

**Algorithm 1** Initialization based on composite PCA (cPCA)

---

**Input:** The observations  $\mathcal{X}_t \in \mathbb{R}^{d_1 \times \dots \times d_K}$ ,  $t = 1, \dots, T$ , the number of factors  $r$ , and the time lag  $h$ .

- 1: Evaluate  $\hat{\boldsymbol{\Sigma}}_h$  in (6), and unfold it to  $d \times d$  matrix  $\hat{\boldsymbol{\Sigma}}_h^*$ .
- 2: Obtain  $\hat{\mathbf{u}}_i$ ,  $1 \leq i \leq r$ , the top  $r$  eigenvectors of  $(\hat{\boldsymbol{\Sigma}}_h^* + \hat{\boldsymbol{\Sigma}}_h^{*\top})/2$ .
- 3: Compute  $\hat{\mathbf{a}}_{ik}^{\text{cpca}}$  as the top left singular vector of  $\text{mat}_k(\hat{\mathbf{u}}_i) \in \mathbb{R}^{d_k \times (d/d_k)}$ , for all  $1 \leq k \leq K$ .

**Output:**  $\hat{\mathbf{a}}_{ik}^{\text{cpca}}$ ,  $i = 1, \dots, r$ ,  $k = 1, \dots, K$ .

---

After obtaining a warm start via cPCA (Algorithm 1), we engage an iterative simultaneous orthogonalization (ISO) algorithm (Algorithm 2) to refine the solution of  $\mathbf{a}_{ik}$  and obtain estimations

of the factor process  $f_{it}$  and the signal strength  $w_i$ . Algorithm 2 can be viewed as an extension of HOOI (De Lathauwer et al., 2000, Zhang and Xia, 2018) and the iterative projection algorithm in Han et al. (2020) to undercomplete ( $r < d_{\min}$ ) and non-orthogonal CP decompositions. It is motivated by the following observation. Define  $\mathbf{A}_k = (\mathbf{a}_{1k}, \dots, \mathbf{a}_{rk})$  and  $\mathbf{B}_k = \mathbf{A}_k(\mathbf{A}_k^\top \mathbf{A}_k)^{-1} = (\mathbf{b}_{1k}, \dots, \mathbf{b}_{rk}) \in \mathbb{R}^{d_k \times r}$ . Let

$$\mathcal{Z}_{t,ik} = \mathcal{X}_t \times_1 \mathbf{b}_{i1}^\top \times_2 \cdots \times_{k-1} \mathbf{b}_{i,k-1}^\top \times_{k+1} \mathbf{b}_{i,k+1}^\top \times_{k+2} \cdots \times_K \mathbf{b}_{iK}^\top, \quad (13)$$

$$\mathcal{E}_{t,ik}^* = \mathcal{E}_t \times_1 \mathbf{b}_{i1}^\top \times_2 \cdots \times_{k-1} \mathbf{b}_{i,k-1}^\top \times_{k+1} \mathbf{b}_{i,k+1}^\top \times_{k+2} \cdots \times_K \mathbf{b}_{iK}^\top. \quad (14)$$

Since  $\mathbf{a}_{jk}^\top \mathbf{b}_{ik} = I_{\{i=j\}}$ , model (1) implies that

$$\mathcal{Z}_{t,ik} = w_i f_{it} \mathbf{a}_{ik} + \mathcal{E}_{t,ik}^*. \quad (15)$$

Here  $\mathcal{Z}_{t,ik}$  is a vector, and (15) is in a factor model form with a univariate factor. The estimation of  $\mathbf{a}_{ik}$  can be done easily and much more accurately than dealing with the much larger  $\mathcal{X}_t$ . The operation in (13) achieves two objectives. First, by multiplying a vector on every mode except the  $k$ -th mode to  $\mathcal{X}_t$ , it reduces the tensor to a vector. It also serves as an averaging operation to reduce the noise variation. Second, as  $\mathbf{b}_{ik}$  is orthogonal to all  $\mathbf{a}_{jk}$  except  $\mathbf{a}_{ik}$ , it is an orthogonal projection operation that eliminates all  $\otimes_{k=1}^K \mathbf{a}_{jk}$  terms in (1) except the  $i$ -th term, resulting in (15). If the matrix  $\mathbf{A}_k^\top \mathbf{A}_k$  is not ill-conditioned, *i.e.*  $\{\mathbf{a}_{ik}, 1 \leq i \leq r\}$  are not highly correlated, then  $\mathbf{B}_k$  and all individual  $\mathbf{b}_{jk}$  are well defined and this procedure shall work well. Under proper conditions on the combined noise tensor  $\mathcal{E}_{t,ik}^*$ , estimation of the loading vectors  $\mathbf{a}_{ik}$  based on  $\mathcal{Z}_{t,ik}$  can be made significantly more accurate, as the statistical error rate now depends on  $d_k$  rather than  $d_1 d_2 \dots d_k$ . Intuitively,  $\mathbf{b}_{ik}$  can also be viewed as a form of (normalized) residuals of  $\mathbf{a}_{ik}$  projected onto the space spanned by  $\{\mathbf{a}_{jk}, j \neq i, 1 \leq j \leq r\}$ .

In practice we do not know  $\mathbf{b}_{il}$ , for  $1 \leq i \leq r$ ,  $1 \leq l \leq K$  and  $l \neq k$ . Similar to back-fitting algorithms, we iteratively estimate the loading vector  $\mathbf{a}_{ik}$  at iteration number  $m$  based on

$$\mathcal{Z}_{t,ik}^{(m)} = \mathcal{X}_t \times_1 \hat{\mathbf{b}}_{i1}^{(m)\top} \times_2 \cdots \times_{k-1} \hat{\mathbf{b}}_{i,k-1}^{(m)\top} \times_{k+1} \hat{\mathbf{b}}_{i,k+1}^{(m-1)\top} \times_{k+2} \cdots \times_K \hat{\mathbf{b}}_{iK}^{(m-1)\top},$$

using the estimate  $\hat{\mathbf{b}}_{il}^{(m-1)}$ ,  $k < l \leq K$ , obtained in the previous iteration and the estimate  $\hat{\mathbf{b}}_{il}^{(m)}$ ,  $1 \leq l < k$ , obtained in the current iteration. As we shall show in the next section, such an iterative procedure leads to a much improved statistical rate in the high dimensional tensor factor model scenarios, as if all  $\mathbf{b}_{il}$ ,  $1 \leq i \leq r$ ,  $1 \leq l \leq K$ ,  $l \neq k$ , are known and we indeed observe  $\mathcal{Z}_{t,ik}$  that follows model (15). Note that the projection error is

$$\mathcal{Z}_{t,ik}^{(m)} - \mathcal{Z}_{t,ik} = \sum_{j=1}^r w_j f_{j,t} \xi_{ij}^{(m)} \mathbf{a}_{jk} + \mathcal{E}_{t,ik}^{*(m)} - \mathcal{E}_{t,ik}^*$$

where

$$\xi_{ij}^{(m)} = \prod_{\ell=1}^{k-1} [\mathbf{a}_{j\ell}^\top \hat{\mathbf{b}}_{i\ell}^{(m)}] \prod_{\ell=k+1}^K [\mathbf{a}_{j\ell}^\top \hat{\mathbf{b}}_{i\ell}^{(m-1)}] - I_{\{i=j\}}, \quad (16)$$

and  $\mathcal{E}_{t,ik}^{*(m)}$  is that in (14) with  $\mathbf{b}_{ik}$  replaced with  $\hat{\mathbf{b}}_{ik}^{(m-1)}$  or  $\hat{\mathbf{b}}_{ik}^{(m)}$ . The multiplicative measure of projection error  $|\xi_{ij}^{(m)}|$  decays rapidly since, for  $j \neq i$ ,  $\mathbf{a}_{j\ell}^\top \hat{\mathbf{b}}_{i\ell}^{(m)}$  goes to zero quickly as the iteration  $m$  increases, and  $\xi_{ij}^{(m)}$  is a product of  $K - 1$  such terms. In fact, the higher the tensor order  $K$  is, the faster the error goes to zero.

**Remark 6 (Comparison with alternating least square).** The updates in Algorithm 2 can be viewed as a variant of the standard alternating least squares procedure. For example, suppose that  $\hat{\mathbf{b}}_{ik}^{(m-1)}$ ,  $1 \leq i \leq r$ ,  $2 \leq k \leq K$ , are fixed. Then the optimization problem to update  $\mathbf{a}_{i1}^{(m)}$  for each  $1 \leq i \leq r$  can be rewritten as

$$\arg \min_{\mathbf{a}_{i1} \in \mathbb{R}^{d_1}} \left\| \hat{\Sigma}_h \times_{k=2}^K \hat{\mathbf{b}}_{ik}^{(m-1)} \times_{k=K+2}^{2K} \hat{\mathbf{b}}_{i,k-K}^{(m-1)} - w_i \mathbf{a}_{i1} \mathbf{a}_{i1}^\top \right\|_F.$$

This is a least-squares problem. However, the algorithm cannot be viewed as an alternating least square procedure since we do not have an over-arching (least square) objective function such that every iteration is done to minimize the objective function given other components. This is due to the construction and involvement of  $\mathbf{b}_{ik}$  in the algorithm. As a matter of fact, if one uses standard ALS to minimize the objective function in (7), to update mode  $k$ , it would involve the inverse of the Hadamard product of  $\mathbf{A}_{k'}^\top \mathbf{A}_{k'}$  for  $k' \neq k$ . In contrast, due to the nice property of  $\mathcal{Z}_{t,ik}$  (defined based on  $\mathbf{B}_{k'}$  for  $k' \neq k$ ), we only need to compute the inverse of  $\mathbf{A}_{k'}^\top \mathbf{A}_{k'}$  for each  $k' \neq k$ , not their Hadamard product.

**Remark 7 (The role of  $h$ ).** In Algorithm 1, we use a fixed  $h \geq 1$ . Let  $\hat{\lambda}_{1,h} \geq \hat{\lambda}_{2,h} \geq \dots \geq \hat{\lambda}_{d,h}$  be the eigenvalues of  $\tilde{\Sigma}_h^* := (\hat{\Sigma}_h^* + \hat{\Sigma}_h^{*\top})/2$ . In practice, we may select  $h$  to maximize the fraction of the explained variance  $\sum_{i=1}^r \hat{\lambda}_{i,h}^2 / \sum_{i=1}^d \hat{\lambda}_{i,h}^2$  under different lag values  $1 \leq h \leq h_0$ , given some pre-specified maximum allowed lag  $h_0$ . Step 2 in Algorithm 1 can be improved by accumulating information from different time lags. For example, let  $\hat{\mathbf{U}}^{(0)} \in \mathbb{R}^{d \times r}$  be a matrix with its columns  $\hat{\mathbf{u}}_i$ 's being the top  $r$  eigenvectors of  $\tilde{\Sigma}_h^*$ . With such  $\hat{\mathbf{U}}^{(0)}$  as the initialization, we may iteratively refine  $\hat{\mathbf{U}}^{(m)}$  to be the top  $r$  eigenvectors of  $\sum_{h=1}^{h_0} \tilde{\Sigma}_h^* \hat{\mathbf{U}}^{(m-1)} \hat{\mathbf{U}}^{(m-1)\top} \tilde{\Sigma}_h^*$ .

**Remark 8 (Condition number of  $\hat{\mathbf{A}}_k^{(m)\top} \hat{\mathbf{A}}_k^{(m)}$ ).** Our theoretical analysis assumes that the condition number of the matrix  $\mathbf{A}_k^\top \mathbf{A}_k$  is bounded. However, in practice, the condition number of  $\hat{\mathbf{A}}_k^{(m)\top} \hat{\mathbf{A}}_k^{(m)}$  in Algorithm 2 may be very large, especially when  $m = 0$ . We suggest a simple regularized strategy. Define the eigen decomposition  $\hat{\mathbf{A}}_k^{(m)\top} \hat{\mathbf{A}}_k^{(m)} = \mathbf{V}_k^{(m)} \mathbf{\Lambda}_k^{(m)} \mathbf{V}_k^{(m)\top}$ . For all eigenvalues in  $\mathbf{\Lambda}_k^{(m)}$  that are smaller than a numeric constant  $c$  (e.g.,  $c = 0.1$ ), we set them to  $c$ . Denote the

---

**Algorithm 2** Iterative Simultaneous Orthogonalization (ISO)

**Input:** The observations  $\mathcal{X}_t \in \mathbb{R}^{d_1 \times \dots \times d_K}$ ,  $t = 1, \dots, T$ , the number of factors  $r$ , the warm-start initial estimates  $\hat{\mathbf{a}}_{ik}^{(0)}$ ,  $1 \leq i \leq r$  and  $1 \leq k \leq K$ , the time lag  $h$ , the tolerance parameter  $\epsilon > 0$ , and the maximum number of iterations  $M$ .

1: Compute  $\hat{\mathbf{B}}_k^{(0)} = \hat{\mathbf{A}}_k^{(0)} (\hat{\mathbf{A}}_k^{(0)\top} \hat{\mathbf{A}}_k^{(0)})^{-1} = (\hat{\mathbf{b}}_{1k}^{(0)}, \dots, \hat{\mathbf{b}}_{rk}^{(0)})$  with  $\hat{\mathbf{A}}_k^{(0)} = (\hat{\mathbf{a}}_{1k}^{(0)}, \dots, \hat{\mathbf{a}}_{rk}^{(0)}) \in \mathbb{R}^{d_k \times r}$  for  $k = 1, \dots, K$ . Set  $m = 0$ .

2: **repeat**

3:     Let  $m = m + 1$ .

4:     **for**  $k = 1$  to  $K$ .

5:         **for**  $i = 1$  to  $r$ .

6:             Given previous estimates  $\hat{\mathbf{a}}_{ik}^{(m-1)}$ , calculate

$$\mathcal{Z}_{t,ik}^{(m)} = \mathcal{X}_t \times_1 \hat{\mathbf{b}}_{i1}^{(m)\top} \times_2 \dots \times_{k-1} \hat{\mathbf{b}}_{i,k-1}^{(m)\top} \times_{k+1} \hat{\mathbf{b}}_{i,k+1}^{(m-1)\top} \times_{k+2} \dots \times_K \hat{\mathbf{b}}_{iK}^{(m-1)\top},$$

for  $t = 1, \dots, T$ . Let

$$\hat{\Sigma}_h \left( \mathcal{Z}_{1:T,ik}^{(m)} \right) = \frac{1}{T-h} \sum_{t=h+1}^T \mathcal{Z}_{t-h,ik}^{(m)} \otimes \mathcal{Z}_{t,ik}^{(m)}.$$

Compute  $\hat{\mathbf{a}}_{ik}^{(m)}$  as the top eigenvector of  $\hat{\Sigma}_h(\mathcal{Z}_{1:T,ik}^{(m)})/2 + \hat{\Sigma}_h(\mathcal{Z}_{1:T,ik}^{(m)})^\top/2$ .

7:     **end for**

8:     Compute  $\hat{\mathbf{B}}_k^{(m)} = \hat{\mathbf{A}}_k^{(m)} (\hat{\mathbf{A}}_k^{(m)\top} \hat{\mathbf{A}}_k^{(m)})^{-1} = (\hat{\mathbf{b}}_{1k}^{(m)}, \dots, \hat{\mathbf{b}}_{rk}^{(m)})$  with  $\hat{\mathbf{A}}_k^{(m)} = (\hat{\mathbf{a}}_{1k}^{(m)}, \dots, \hat{\mathbf{a}}_{rk}^{(m)})$ .

9:     **end for**

10: **until**  $m = M$  or

$$\max_{1 \leq i \leq r} \max_{1 \leq k \leq K} \|\hat{\mathbf{a}}_{ik}^{(m)} \hat{\mathbf{a}}_{ik}^{(m)\top} - \hat{\mathbf{a}}_{ik}^{(m-1)} \hat{\mathbf{a}}_{ik}^{(m-1)\top}\|_S \leq \epsilon,$$

**Output:** Estimates

$$\begin{aligned} \hat{\mathbf{a}}_{ik}^{\text{iso}} &= \hat{\mathbf{a}}_{ik}^{(m)}, \quad i = 1, \dots, r, \quad k = 1, \dots, K, \\ \hat{w}_i^{\text{iso}} &= \left( T^{-1} \sum_{t=1}^T \left( \mathcal{X}_t \times_{k=1}^K \hat{\mathbf{b}}_{ik}^{(m)\top} \right)^2 \right)^{1/2}, \quad i = 1, \dots, r, \\ \hat{f}_{it}^{\text{iso}} &= (\hat{w}_i^{\text{iso}})^{-1} \cdot \mathcal{X}_t \times_{k=1}^K \hat{\mathbf{b}}_{ik}^{(m)\top}, \quad i = 1, \dots, r, \quad t = 1, \dots, T, \\ \hat{\mathcal{X}}_t^{\text{iso}} &= \sum_{i=1}^r \mathcal{X}_t \times_{k=1}^K \hat{\mathbf{b}}_{ik}^{(m)\top} \times_{k=1}^K \hat{\mathbf{a}}_{ik}^{(m)}, \quad t = 1, \dots, T. \end{aligned}$$


---

resulting matrix as  $\tilde{\mathbf{A}}_k^{(m)}$  and get the corresponding  $\hat{\mathbf{B}}_k^{(m)}$  by  $\hat{\mathbf{A}}_k^{(m)\top} (\mathbf{V}_k^{(m)} \tilde{\mathbf{A}}_k^{(m)} \mathbf{V}_k^{(m)\top})^{-1}$ . Many alternative empirical methods can also be applied to bound the condition number.

**Remark 9.** Algorithm 1 requires that  $\delta < 1$  in order to obtain reasonable estimates. And it can accommodate the case that  $r \geq d_{\max}$ . In contrast, Algorithm 2 needs stronger conditions that  $\delta_k < 1$  and  $r \leq d_{\min}$  to rule out the possibility of co-linearity, as  $\mathbf{A}_k^\top \mathbf{A}_k$  needs to be invertible. It may not hold under certain situations. For example,  $\mathbf{a}_{1k} = \mathbf{a}_{2k}$  would lead to an ill-conditioned  $\mathbf{A}_k^\top \mathbf{A}_k$ . In such cases, the incoherence condition commonly required in the literature, e.g.,  $\vartheta_{\max} \ll 1$ , is also violated. It is possible to extend our approach to a more sophisticated projection scheme so the conditions can be weakened. As it requires more sophisticated analysis both on the methodology and on the theory, we do not pursue this direction in this paper.

**Remark 10.** As mentioned before,  $\mathbf{a}_{i1} \otimes \mathbf{a}_{i2} \otimes \cdots \otimes \mathbf{a}_{iK}$  can be regarded as the *principal component* of the auto-covariance tensor  $\boldsymbol{\Sigma}_h$ . Hence, our HOPE estimators (Algorithms 1 and 2 together) can also be characterized as a procedure of *principal component analysis* for order  $2K$  auto-covariance tensor, albeit with a special structure in (5).

**Remark 11 (The number of factors).** Here the estimators are constructed with given rank  $r$ , though in the theoretical analysis it is allowed to diverge. Determining the number of factors in a data-driven way has been an important research topic in the factor model literature. Bai and Ng (2002, 2007), Hallin and Liška (2007) proposed consistent estimators in the vector factor models based on the information criteria approach. Ahn and Horenstein (2013), Lam and Yao (2012) developed an alternative approach to study the ratio of each pair of adjacent eigenvalues. Recently, Han et al. (2022) established a class of rank determination approaches for the factor models with Tucker low-rank structure, based on both the information criterion and the eigen-ratio criterion. Those procedures can be extended to TFM-cp.

## 4 Theoretical Properties

In this section, we shall investigate the statistical properties of the proposed algorithms described in the last section. Our theories provide theoretical guarantees for consistency and present statistical error rates in the estimation of the factor loading vectors  $\mathbf{a}_{ik}$ ,  $1 \leq i \leq r, 1 \leq k \leq K$ , under proper regularity conditions. As the loading vector  $\mathbf{a}_{ik}$  is identifiable only up to the sign change, we use

$$\|\hat{\mathbf{a}}_{ik} \hat{\mathbf{a}}_{ik}^\top - \mathbf{a}_{ik} \mathbf{a}_{ik}^\top\|_S = \sqrt{1 - (\hat{\mathbf{a}}_{ik}^\top \mathbf{a}_{ik})^2} = \sup_{\mathbf{z} \perp \mathbf{a}_{ik}} |\mathbf{z}^\top \hat{\mathbf{a}}_{ik}|$$

to measure the distance between  $\hat{\mathbf{a}}_{ik}$  and  $\mathbf{a}_{ik}$ .

Recall  $\Sigma_h = \mathbb{E}\widehat{\Sigma}_h = \sum_{i=1}^r \lambda_{i,h}(\mathbf{a}_{i1} \otimes \mathbf{a}_{i2} \otimes \cdots \otimes \mathbf{a}_{iK})^{\otimes 2}$ , as in (5) and  $\lambda_{i,h} = w_i^2 \mathbb{E}f_{i,t-h}f_{i,t}$ . We will also continue to use the notations  $\mathbf{A}_k = (\mathbf{a}_{1k}, \dots, \mathbf{a}_{rk}) \in \mathbb{R}^{d_k \times r}$ , and  $\mathbf{B}_k = \mathbf{A}_k(\mathbf{A}_k^\top \mathbf{A}_k)^{-1} = (\mathbf{b}_{1k}, \dots, \mathbf{b}_{rk}) \in \mathbb{R}^{d_k \times r}$ . Let  $d = \prod_{k=1}^K d_k$ ,  $d_{\min} = \min\{d_1, \dots, d_K\}$ ,  $d_{\max} = \max\{d_1, \dots, d_K\}$  and  $d_{-k} = \prod_{j \neq k} d_j$ .

To present theoretical properties of the proposed procedures, we impose the following assumptions.

**Assumption 1.** The error process  $\mathcal{E}_t$  are independent Gaussian tensors, conditioning on the factor process  $\{f_{it}, 1 \leq i \leq r, t \in \mathbb{Z}\}$ . In addition, there exists some constant  $\sigma > 0$ , such that

$$\mathbb{E}(u^\top \text{vec}(\mathcal{E}_t))^2 \leq \sigma^2 \|u\|_2^2, \quad u \in \mathbb{R}^d.$$

**Assumption 2.** Assume the factor process  $f_{it}, 1 \leq i \leq r$  is stationary and strong  $\alpha$ -mixing in  $t$ , with  $\mathbb{E}f_{it}^2 = 1$ ,  $\mathbb{E}f_{it-h}f_{it} \neq 0$ ,  $\mathbb{E}f_{it-h}f_{jt} = 0$  for all  $i \neq j$  and  $h \geq 1$ . Let  $F_t = (f_{1t}, \dots, f_{rt})^\top$ . For any  $v \in \mathbb{R}^r$  with  $\|v\|_2 = 1$ ,

$$\max_t \mathbb{P}(|v^\top F_t| \geq x) \leq c_1 \exp(-c_2 x^{\gamma_2}), \quad (17)$$

where  $c_1, c_2$  are some positive constants and  $0 < \gamma_2 \leq 2$ . In addition, the mixing coefficient satisfies

$$\alpha(m) \leq \exp(-c_0 m^{\gamma_1}) \quad (18)$$

for some constant  $c_0 > 0$  and  $0 < \gamma_1 \leq 1$ , where

$$\alpha(m) = \sup_t \left\{ \left| \mathbb{P}(A \cap B) - \mathbb{P}(A)\mathbb{P}(B) \right| : A \in \sigma(f_{is}, 1 \leq i \leq r, s \leq t), B \in \sigma(f_{is}, 1 \leq i \leq r, s \geq t + m) \right\}.$$

**Assumption 3.** Assume  $h \leq T/4$  is fixed, and  $\lambda_{1,h}, \dots, \lambda_{r,h}$  are all distinct. Without loss of generality, let  $\lambda_{1,h} > \lambda_{2,h} > \cdots > \lambda_{r,h} > 0$ . Here, we emphasize that  $\lambda_{i,h}$  depends on  $h$ , though in other places when  $h$  is fixed we will omit  $h$  in the notation.

Assumption 1 is similar to those on the noise imposed in Lam et al. (2011), Lam and Yao (2012), Han et al. (2020). It accommodates general patterns of dependence among individual time series fibers, but also allows a presentation of the main results with manageable analytical complexity. The normality assumption, which ensures fast statistical error rates in our analysis, is imposed for technical convenience. In theory, it can be supplanted by a sub-Gaussian condition, or replaced with more general distributions with heavier tails. However, adopting such weaker conditions would significantly complicate the formulae, statistical outcomes, and requisite conditions within our time series framework. This added complexity would likely detract from the paper's readability, without providing additional statistical insights. Our primary goal is to maintain the readers' focus on the core content of the paper, and thus, we have chosen to assume additive Gaussian errors. This

choice simplifies the exposition without compromising the fundamental tenets and the findings of our study.

Assumption 2 is standard. It allows a very general class of time series models, including causal ARMA processes with continuously distributed innovations; see also Bradley (2005), Fan and Yao (2003), Rosenblatt (2012), Tong (1990), Tsay (2005), Tsay and Chen (2018), among others. The restriction  $\gamma_1 \leq 1$  is introduced only for presentation convenience. Assumption 2 requires that the tail probability of  $f_{it}$  decays exponentially fast. In particular, when  $\gamma_2 = 2$ ,  $f_{it}$  is sub-Gaussian.

Assumption 3 is sufficient to guarantee that all the factor loading vectors  $\mathbf{a}_{ik}$  can be uniquely identified up to the sign change. The parameters  $\lambda_i$  can be viewed as an analogue of eigenvalues in the order- $2K$  tensor  $\Sigma_h$ . Similar to the eigen decomposition of a matrix, if some  $\lambda_i$  are equal, estimation of the loading vectors  $\mathbf{a}_{ik}$  may suffer from label shift across  $i$ . When  $h$  is fixed and  $\mathbb{E}f_{i,t}f_{i,t-h} \asymp 1$ ,  $\lambda_i \asymp w_i^2$ . The signal strength of each factor is measured by  $\lambda_i$ .

Let us first study the behavior of the cPCA estimators in Algorithm 1. Theorem 1 presents the performance bounds, which depends on the coherence (the degree of non-orthogonality) of the factor loading vectors.

Let

$$\lambda_* = \min_{1 \leq i \leq r+1} \{\lambda_{i-1} - \lambda_i\} \quad (19)$$

with  $\lambda_0 = \infty$ ,  $\lambda_{r+1} = 0$ , be the minimum gap between the signal strengths of the factors.

**Theorem 1.** *Suppose Assumptions 1, 2, 3 hold. Let  $1/\gamma = 1/\gamma_1 + 2/\gamma_2$ ,  $h \leq T/4$  and  $\delta < 1$  with  $\delta$  defined in (10). In an event with probability at least  $1 - (Tr)^{-C_1} - e^{-d}$ , the following error bound holds for the estimation of the loading vectors  $\mathbf{a}_{ik}$  using Algorithm 1 (cPCA).*

$$\|\hat{\mathbf{a}}_{ik}^{\text{cPCA}} \hat{\mathbf{a}}_{ik}^{\text{cPCA}\top} - \mathbf{a}_{ik} \mathbf{a}_{ik}^\top\|_S \leq \left(1 + \frac{2\lambda_1}{\lambda_*}\right) \delta + \frac{C_2 R^{(0)}}{\lambda_*}, \quad (20)$$

for all  $1 \leq i \leq r$ ,  $1 \leq k \leq K$ , where  $C_1, C_2$  are some positive constants, and

$$R^{(0)} = \max_{1 \leq i \leq r} w_i^2 \left( \sqrt{\frac{r + \log T}{T}} + \frac{(r + \log T)^{1/\gamma}}{T} \right) + \sigma^2 \sqrt{\frac{d}{T}} + \sigma \max_{1 \leq i \leq r} w_i \sqrt{\frac{d}{T}}. \quad (21)$$

**Remark 12.** We note that the eigengap  $\lambda_*$  in Algorithm 1 (cPCA) is not a requisite for the iterative Algorithm 2 (ISO). Algorithm 1 (cPCA) necessitates a significant separation among the different singular values  $\lambda_i$ 's. This condition can be relaxed through the use of random slicing (Anandkumar et al., 2014c, Auddy and Yuan, 2023a), a widely recognized method for initialization in tensor CP decomposition. In our framework, the core step of random slicing is the construction of a projected auto-covariance tensor  $\Sigma_h \times_k g_k \times_{K+k} \tilde{g}_k$ , where  $g_k$  and  $\tilde{g}_k$  are independently generated Gaussian random vectors. Due to the randomness of  $g_k$  and  $\tilde{g}_k$ , even if all  $\lambda_i$ 's are equal, the singular

values of  $\boldsymbol{\Sigma}_h \times_k g_k \times_{K+k} \tilde{g}_k$  will inherently differ. Furthermore, we can generate a sufficiently large eigengap between the top two singular values of the projected auto-covariance tensor through multiple rounds of random slicing, so that the leading component of the projected auto-covariance tensor is identifiable. Since  $\boldsymbol{\Sigma}_h \times_k g_k \times_{K+k} \tilde{g}_k$  is an order  $2K - 2$  tensor, we can still employ cPCA and utilize the benefits of higher-order coherence in Proposition 1 when  $K > 2$ . The existing results in Theorem 1 can be extended to such settings, although it would require more sophisticated theoretical analysis.

The first term in the upper bound (20) is induced by the non-orthogonality of the loading vectors  $\mathbf{a}_{ik}$ , which can be viewed as bias. The second term in (20) comes from a concentration bound for the random noise, and thus can be interpreted as stochastic error. By Proposition 1, it implies that a larger  $K$  (e.g. higher order tensors) leads to smaller bias and higher statistical accuracy of cPCA. If  $\delta \gtrsim R^{(0)}/\lambda_1$ , then the error bound (20) is dominated by the bias related to  $\delta$ , otherwise it is dominated by the stochastic error. Equation (21) shows that  $R^{(0)}$  in the stochastic error comes from the fluctuation of the factor process  $f_{it}$  (the first two terms) and the noise  $\mathcal{E}_t$  in (1) (the other two terms). When  $\sum_{i=1}^r \lambda_i \asymp r\lambda_1 \asymp rw_1^2$  and  $R^{(0)}/\lambda_1 + T/d \lesssim 1$ , the terms related to the noise becomes  $\sqrt{r/T}/\sqrt{\text{SNR}}$ , where the signal-to-noise ratio (SNR) is

$$\text{SNR} := \mathbb{E} \left\| \sum_{i=1}^r w_i f_{it} \otimes_{k=1}^K \mathbf{a}_{ik} \right\|_{\text{HS}}^2 / \mathbb{E} \|\mathcal{E}_t\|_{\text{HS}}^2 = \sum_{i=1}^r w_i^2 / (\sigma^2 d) \asymp r\lambda_1 / (\sigma^2 d). \quad (22)$$

Roughly speaking though not completely correct, the term  $\lambda_i - \lambda_{i+1}$  can be viewed as the gap of  $i$ -th and  $(i+1)$ -th largest eigenvalues of  $\boldsymbol{\Sigma}_h^*$  with  $\boldsymbol{\Sigma}_h^*$  given in (8). In particular, if  $\lambda_1 \asymp \dots \asymp \lambda_r \asymp w_1^2$ , then  $\lambda_* \asymp w_1^2/r$ . In this case, the bound (20) can be simplified to

$$\begin{aligned} & \|\hat{\mathbf{a}}_{ik}^{\text{cPCA}} \hat{\mathbf{a}}_{ik}^{\text{cPCA}\top} - \mathbf{a}_{ik} \mathbf{a}_{ik}^\top\|_{\text{S}} \\ & \leq C_3 r \delta + C_4 r \left( \sqrt{\frac{r + \log T}{T}} + \frac{(r + \log T)^{1/\gamma}}{T} \right) + \frac{C_4 \sigma^2 r \sqrt{d}}{w_1^2 \sqrt{T}} + \frac{C_4 \sigma r \sqrt{d}}{w_1 \sqrt{T}}. \end{aligned} \quad (23)$$

Then, by (23) and Proposition 1, the consistency of the cPCA estimators only requires the incoherence parameter to be at most  $\vartheta_{\max} \lesssim r^{-2/K}$ .

Next, let us consider the statistical performance of the iterative algorithm (Algorithm 2) after cPCA initialization, *i.e.* HOPE estimators. As discussed earlier, the operation in (13) achieves dimension reduction by projecting  $\mathcal{X}_t$  into a vector and retains only one of the  $r$  factor terms, hence eliminates the interaction effects between different factors. As we update the estimation of each individual loading vector  $\mathbf{a}_{ik}$  separately in the algorithm, ideally this would remove the bias part in (20) which is due to the non-orthogonality of the loading vectors, and replace the eigengap  $\lambda_*$  in (20) by  $\lambda_i$ , as (15) only involves one eigenvector. It also leads to the elimination of the first

two terms of  $R^{(0)}$ . As mentioned in Section 3, when updating  $\hat{\mathbf{a}}_{ik}^{(m)}$ , we take advantages of the multiplicative nature of the project error  $\xi_{ij}^{(m)}$  in (16), and the rapid growth of such benefits as the iteration number  $m$  grows. Thus we expect that the rate of HOPE estimators would become

$$\max_{1 \leq i \leq r} \max_{1 \leq k \leq K} \|\hat{\mathbf{a}}_{ik} \hat{\mathbf{a}}_{ik}^\top - \mathbf{a}_{ik} \mathbf{a}_{ik}^\top\|_S \leq C_{0,K} R^{(\text{ideal})}, \quad (24)$$

where

$$R_{k,i}^{(\text{ideal})} = \frac{\sigma^2}{\lambda_i} \sqrt{\frac{d_k}{T}} + \sqrt{\frac{\sigma^2 d_k}{\lambda_i T}}, \quad \text{and} \quad R^{(\text{ideal})} = \max_{1 \leq i \leq r} \max_{1 \leq k \leq K} R_{k,i}^{(\text{ideal})}. \quad (25)$$

Note that  $R_{k,i}^{(\text{ideal})}$  replaces all  $d = d_1 \dots d_K$  in the noise component of the stochastic error in (20) by  $d_k$  due to dimension reduction. The following theorem provides conditions under which this ideal rate is indeed achieved.

Let the statistical error bound of the initialization used in Algorithm 2 be  $\psi_0$ . For cPCA,

$$\psi_0 = \frac{\lambda_1 \delta + R^{(0)}}{\lambda_*}, \quad (26)$$

where  $\lambda_*$  is the eigengap defined in (19) and  $R^{(0)}$  is defined in (21).

**Theorem 2.** *Suppose Assumptions 1, 2, 3 hold. Assume that  $\delta_{\max} = \max_{k \leq K} \delta_k < 1$  with  $\delta_k$  defined in (9), and  $r = O(T)$ . Let  $1/\gamma = 1/\gamma_1 + 2/\gamma_2$ ,  $h \leq T/4$ , and  $d = d_1 \dots d_K$ . Suppose that for a proper numeric constant  $C_{1,K}$  depending on  $K$  only, we have*

$$\sqrt{1 - \delta_{\max}} - (r^{1/2} + 1)\psi_0/\sqrt{1 - 1/(4r)} > 0, \quad (27)$$

$$C_{1,K} \left( \frac{\lambda_1}{\lambda_r} \right) \psi_0^{2K-3} + C_{1,K} \sqrt{\frac{\lambda_1}{\lambda_r}} \left( \sqrt{\frac{r + \log T}{T}} + \frac{(r + \log T)^{1/\gamma}}{T} \right) \psi_0^{K-2} \leq \rho < 1 \quad (28)$$

Then, after at most  $M = O(\log \log(\psi_0/R^{(\text{ideal})}))$  iterations of Algorithm 2, in an event with probability at least  $1 - (Tr)^{-C} - \sum_k e^{-d_k}$ , the HOPE estimator satisfies

$$\|\hat{\mathbf{a}}_{ik}^{\text{iso}} \hat{\mathbf{a}}_{ik}^{\text{iso}\top} - \mathbf{a}_{ik} \mathbf{a}_{ik}^\top\|_S \leq C_{0,K} R^{(\text{ideal})}, \quad (29)$$

for all  $1 \leq i \leq r$ ,  $1 \leq k \leq K$ , where  $C_{0,K}$  is a constant depending on  $K$  only and  $C$  is a positive numeric constant.

The detailed proof of the theorem is in Appendix A. The key idea of the analysis of HOPE is to show that the iterative estimator has an error contraction effect in each iteration. Theorem 2 implies that HOPE will achieve a faster statistical error rate than the typical  $O_{\mathbb{P}}(T^{-1/2})$  whenever  $\lambda_r \gg \sigma^2 \max_k d_k$ . As  $\text{vec}(\mathcal{X}_t)$  has  $d$  elements, the strong factors setting in the literature (Chen et al., 2022, Han et al., 2020, Lam et al., 2011) typically assumes  $\text{SNR} \asymp 1$ . In our case it is similar to assuming the signal strength  $\mathbb{E} \|\sum_{i=1}^r w_i \text{fit} \otimes_{k=1}^K \mathbf{a}_{ik}\|_{\text{HS}}^2 \asymp \sigma^2 d$ . When  $r$  is fixed and  $\lambda_1 \asymp \dots \asymp \lambda_r$ , the statistical error rate will be reduced to  $O_{\mathbb{P}}(T^{-1/2} d_{-k}^{-1/2})$ , where  $d_{-k} = \prod_{j \neq k} d_j$ .

**Remark 13 (Iteration complexity).** Theorem 2 implies that Algorithm 2 achieves the desired estimation error  $R^{(\text{ideal})}$  after at most  $M = O(\log \log(\psi_0/R^{(\text{ideal})}))$  number of iterations. In this sense, after at most double-logarithmic number of iterations, the iterative estimator in Algorithm 2 converges to a neighborhood of the true parameter  $\mathbf{a}_{ik}$ , up to a statistical error with a rate  $O(R^{(\text{ideal})})$ . We observe that Algorithm 2 typically converges within very few steps in practical implementations.

**Remark 14.** Condition (27) requires  $r^{1/2}\psi_0$  to be small. It is a relatively strong condition due to the extra multiplier  $r^{1/2}$  on the error of the initial estimators. This is a technical issue due to the need to invert the estimated  $\mathbf{A}_k^\top \mathbf{A}_k$  in our analysis to construct the mode- $k$  projection in Algorithm 2. In fact the  $r^{1/2}$  term may be eliminated by applying a shrinkage procedure on the singular values of  $\hat{\mathbf{A}}_k$  after obtaining the updates of  $\hat{\mathbf{a}}_{ik}$ ,  $1 \leq i \leq r$ , similar to the procedure proposed by Anandkumar et al. (2014c).

Furthermore, the condition given by (28) originates from the multiplicative nature of the projection error  $\xi_{ij}^{(m)}$ , as seen in (16) for  $i \neq j$ . If  $\psi_0$  signifies the error bound for cPCA estimators, then condition (28) is satisfied when  $(\lambda_1/\lambda_r)\psi_0^{2K-3} \lesssim 1$ . In comparison, the iterative algorithm of Anandkumar et al. (2014c) requires that the initialization fulfills  $\psi_0 \lesssim \lambda_r/\lambda_1 + 1/\sqrt{d_{\min}}$ , a condition that is more stringent than (28). The ratio  $\lambda_1/\lambda_r$  in (28) is unavoidable. When updating the estimates of  $\mathbf{a}_{ik}$  in Algorithm 2, we need to remove the effect of other factors ( $j \neq i$ ) on the  $i$ -th factor, which introduces the ratio of factor strengths  $\lambda_1/\lambda_r$  in the analysis.

In particular, if  $\lambda_1 = \dots = \lambda_r$ , the shrinkage procedure can reduce conditions (27) and (28) to

$$C_{1,K}\psi_0 < 1, \tag{30}$$

where  $\psi_0$  is the cPCA error bound in (26). It ensures that, with high probability,  $\|\hat{\mathbf{a}}_{ik}^{(0)}\hat{\mathbf{a}}_{ik}^{(0)\top} - \mathbf{a}_{ik}\mathbf{a}_{ik}^\top\|_{\text{S}}$  are sufficiently small, so that the cPCA initialization is sufficiently close to the ground truth as in (30).

**Remark 15 (Comparison with general tensor CP-decomposition methods).** To estimate  $\mathbf{a}_{ik}$  in (5), one can use the standard tensor CP-decomposition algorithms, such as those in Anandkumar et al. (2014c), Hao et al. (2020), Sun et al. (2017), without utilizing the special features of TFM-cp. The randomized initialization estimators in these algorithms typically require the incoherence condition  $\vartheta_{\max} \lesssim \text{poly} \log(d_{\min})/\sqrt{d_{\min}}$ . In contrast, the condition for ISO needs  $\vartheta_{\max} \lesssim r^{-5/(2K)}$ , which is weaker when  $r = o(d_{\min}^{K/5})$ . Similarly, we prove that the cPCA yields useful estimates when  $r^2\vartheta_{\max}^K$  is small, or  $\vartheta_{\max} \lesssim r^{-2/K}$ . In other words, as long as  $r$  is not exceedingly large (e.g.  $r = o(d_{\min}^{K/5})$ ), both cPCA and ISO permit a more lenient incoherence condition among the CP basis. Furthermore, the high-order coherence in TFM-cp leads to an impressive computational super-linear convergence rate of Algorithm 2, which is faster than the computational

linear convergence rate of the iterative projection algorithm in Han et al. (2020) or other variants of alternating least squares approaches in the literature, that are at most linear with the required number of iterations  $M = O(\log(\psi_0/R^{(\text{ideal})}))$ .

**Remark 16 (Comparison between TFM-cp and TFM-tucker Models).** As discussed in Remark 3, TFM-cp can be written as a TFM-tucker with a special structure. One can ignore the special structure and treat it a generic TFM-tucker in (3) and estimate the loading spaces spanned by  $\{\mathbf{a}_{ik}, 1 \leq i \leq r\}$  using the iterative estimation algorithm in Han et al. (2020). In fact, ISO (as detailed in Algorithm 2) can be viewed as an enhancement of the iterative algorithm presented in Han et al. (2020) to utilize the special structure of TFM-cp. This is achieved by permitting non-orthogonality in  $\mathbf{A}_k$  and estimating each  $\mathbf{a}_{ik}, 1 \leq i \leq r$ , individually.

Here we provide a brief comparison in the estimation accuracy between the estimators under these two settings to show the impact of the additional structure in TFM-cp. Note that for TFM-tucker, only the linear space spanned by  $\mathbf{A}_k$  can be estimated hence the estimation accuracy is based on a specific space representation, different from that for the TFM-cp. For simplicity, we consider the case  $\lambda_1 \asymp \dots \asymp \lambda_r$ .

(i) The iterative refinement algorithm (Algorithm 2) for TFM-cp requires similar conditions on the initial estimators as the iterative projection algorithms for TFM-tucker. Under many situations, both methods only require the initialization to retain a large portion of the signal, but not the consistency.

(ii) The statistical error rate of HOPE in (29) is the same as the upper bound of the iterative projection algorithms for estimation of the fixed rank TFM-tucker, c.f. Corollary 3.1 and 3.2 in Han et al. (2020), which is shown to have the minimax optimality. It follows that HOPE also achieves the minimax rate-optimal estimation error under fixed  $r$ .

(iii) When the rank  $r$  diverges and  $\text{SNR} \asymp 1$  where  $\text{SNR}$  is defined in (22), the estimation error of the loading spaces by the iterative estimation procedures, iTOPUP and TIPUP-iTOPUP procedures in Han et al. (2020) applied to the specific TFM-tucker model implied by the TFM-cp model, is of the order  $O_{\mathbb{P}}(\max_k r^{3K/2-1} T^{-1/2} d_{-k}^{-1/2})$ , a rate that is always larger than  $O_{\mathbb{P}}(\max_k r^{1/2} T^{-1/2} d_{-k}^{-1/2})$ , the error rate of HOPE for TFM-cp model. The iTIPUP procedure for TFM-tucker model is  $O_{\mathbb{P}}(\max_k r^{1/2+(K-1)\zeta} T^{-1/2} d_{-k}^{-1/2})$  where  $\zeta$  controls the level of signal cancellation (see Han et al. (2020) for details). When there is no signal cancellation,  $\zeta = 0$ , the rate of the two procedures are the same. Note that iTIPUP only estimates the loading space, while HOPE provides estimates of the unique loading vectors. The error rate of HOPE is better when  $\zeta > 0$ . This demonstrates that HOPE is able to utilize the specific structure in TFM-cp to achieve more accurate estimation than simply applying the estimation procedures designed for general TFM-tucker.

(iv) It can be seen that, computationally, the complexities for the initialization of both TFM-cp and TFM-tucker are the same, yet, the per iteration complexity of TFM-cp is lower than that of TFM-tucker by a factor of  $r^{2K-2}$  where  $r_1 = \dots = r_K = r$  in TFM-tucker model.

**Theorem 3.** *Suppose Assumptions 1, 2, 3 hold. Assume that  $\delta_k < 1$  with  $\delta_k$  defined in (9),  $\sigma^2 \lesssim \lambda_r$  and condition (27) holds. Let  $d_{\max} = \max_k d_k$ . Then the HOPE estimator in Algorithm 2 using a specific  $h$  satisfies:*

$$w_i^{-1} \left| \widehat{w}_i^{\text{iso}} \widehat{f}_{it}^{\text{iso}} - w_i f_{it} \right| = O_{\mathbb{P}} \left( \sqrt{\frac{\sigma^2}{\lambda_r}} + \sqrt{\frac{\sigma^2 d_{\max}}{\lambda_r T}} \right) \quad (31)$$

and

$$w_i^{-1} w_j^{-1} \left| \frac{1}{T - h_*} \sum_{t=h_*+1}^T \widehat{w}_i^{\text{iso}} \widehat{w}_j^{\text{iso}} \widehat{f}_{it-h_*}^{\text{iso}} \widehat{f}_{jt}^{\text{iso}} - \frac{1}{T - h_*} \sum_{t=h_*+1}^T w_i w_j f_{it-h_*} f_{jt} \right| = O_{\mathbb{P}} \left( \sqrt{\frac{\sigma^2 d_{\max}}{\lambda_r T}} \right) \quad (32)$$

for  $1 \leq i, j \leq r, 1 \leq t \leq T$  and all  $1 < h_* \leq T/4$ .

Theorem 3 specifies the convergence rate for the estimated factors  $f_{it}$ . When  $\lambda_r \gg \sigma^2 d_{\max} + T$ ,  $w_i^{-1} |\widehat{w}_i^{\text{iso}} \widehat{f}_{it}^{\text{iso}} - w_i f_{it}|$  is much smaller than the parametric rate  $T^{-1/2}$ . If all the factors are strong (Lam et al., 2011) such that  $\lambda_1 \asymp \lambda_r \asymp \sigma^2 d$ , (31) implies that  $w_i^{-1} |\widehat{w}_i^{\text{iso}} \widehat{f}_{it}^{\text{iso}} - w_i f_{it}| = O_{\mathbb{P}}(d^{-1/2} + d_{\max}^{1/2} d^{-1/2} T^{-1/2})$ . Then, as long as  $d_k \rightarrow \infty$  and  $K \geq 2$ , the estimated factors are consistent, even under a fixed  $T$ . In comparison, the convergence rate of the estimated factors in Theorem 1 of Bai (2003) for vector factor models is  $O_{\mathbb{P}}(d^{-1/2} + T^{-1})$ . Moreover, (32) shows that the error rates for the sample auto-cross-moment of the estimated factors to the true sample auto-cross-moment is also  $o_{\mathbb{P}}(T^{-1/2})$  when  $\lambda_r \gg \sigma^2 d_{\max}$ . This implies that it is a valid option to use the estimated factor processes as the true factor processes to model the dynamics of the factors. When the estimation of these time series models only required auto-correlation and partial auto-correction functions, the results are expected to be the same as using the true factor process, without loss of efficiency. The statistical rates in Theorem 3 lay a foundation for further modeling of the estimated factor processes with vast repository of linear and nonlinear options.

## 5 Simulation Studies

### 5.1 Alternative algorithms for estimation of TFM-cp

Here we present two alternative estimation algorithms for TFM-cp, by extending the popular rank one alternating least square (ALS) algorithm of Anandkumar et al. (2014c) and orthogonalized

alternating least square (OALS) of [Sharan and Valiant \(2017\)](#) designed for CP decomposition of noisy tensors, because  $\widehat{\Sigma}_h$  in (5) is indeed in a CP form, but with repeated components. In addition, we use cPCA estimates for initialization, instead of randomized initialization used for general CP decomposition. We will denote the algorithms as cALS (Algorithm 3) and cOALS (Algorithm 4), respectively. The simulation study below shows that, although cALS and cOALS perform better than the straightforward implementation of ALS and OALS with randomized initialization, they do not perform as well as the proposed HOPE algorithm. Hence we do not investigate their theoretical properties in this paper.

---

**Algorithm 3** cPCA-initialized Rank One Alternating Least Square (cALS)

---

**Input:** Observations  $\mathcal{X}_t \in \mathbb{R}^{d_1 \times \dots \times d_K}$  for  $t = 1, \dots, T$ , the number of factors  $r$ , the time lag  $h$ , the cPCA initial estimate  $(\widehat{\mathbf{a}}_{i1}^{\text{cpca}}, \dots, \widehat{\mathbf{a}}_{iK}^{\text{cpca}})$ ,  $1 \leq i \leq r$ , the tolerance parameter  $\epsilon > 0$ , and the maximum number of iterations  $M$ .

- 1: Compute  $\widehat{\Sigma}_h$  defined in (6).
  - 2: Initialize unit vectors  $\widehat{\mathbf{a}}_{ik}^{(0)} = \widehat{\mathbf{a}}_{ik}^{\text{cpca}}$  for  $1 \leq k \leq K$ ,  $1 \leq i \leq r$ . Set  $m = 0$ .
  - 3: **for**  $i = 1$  to  $r$ .
  - 4:     **repeat**
  - 5:         Set  $m = m + 1$ .
  - 6:         **for**  $k = 1$  to  $K$ .
  - 7:             Compute  $\widetilde{\mathbf{a}}_{ik}^{(m)} = \widehat{\Sigma}_h \times_{\ell=1}^{k-1} \widehat{\mathbf{a}}_{i\ell}^{(m)\top} \times_{\ell=k}^K \widehat{\mathbf{a}}_{i\ell}^{(m-1)\top} \times_{\ell=K+1}^{K+k-1} \widehat{\mathbf{a}}_{i\ell}^{(m)\top} \times_{\ell=K+k+1}^{2K} \widehat{\mathbf{a}}_{i\ell}^{(m-1)\top}$ ,  
            where  $\widehat{\mathbf{a}}_{i\ell}^{(m-1)} = \widehat{\mathbf{a}}_{i\ell-K}^{(m-1)}$  for  $\ell > K$ .
  - 8:             Compute  $\widehat{\mathbf{a}}_{ik}^{(m)} = \widetilde{\mathbf{a}}_{ik}^{(m)} / \|\widetilde{\mathbf{a}}_{ik}^{(m)}\|_2$ .
  - 9:         **end for**
  - 10:         **until**  $m = M$  or  $\max_k \|\widehat{\mathbf{a}}_{ik}^{(m)} \widehat{\mathbf{a}}_{ik}^{(m)\top} - \widehat{\mathbf{a}}_{ik}^{(m-1)} \widehat{\mathbf{a}}_{ik}^{(m-1)\top}\|_S \leq \epsilon$ .
  - 11:         Let  $\widehat{\mathbf{a}}_{ik}^{\text{cALS}} = \widehat{\mathbf{a}}_{ik}^{(m)}$ ,  $1 \leq k \leq K$ .
  - 12:     **end for**
- Output:**  $\widehat{\mathbf{a}}_{ik}^{\text{cALS}}$ ,  $i = 1, \dots, r$ ,  $k = 1, \dots, K$ .
- 

## 5.2 Simulation

In this section, we compare the empirical performance of different procedures of estimating the loading vectors of TFM-cp, under various simulation setups. We consider the cPCA initialization (Algorithm 1) alone, the iterative procedure HOPE, and the intermediate output from the iterative procedure when the number of iteration is 1 after initialization. The one step procedure will be denoted as 1HOPE. We also check the performance of the alternative algorithms ALS, OALS, cALS, and cOALS as described above. The estimation error shown is given by  $\max_{i,k} \|\widehat{\mathbf{a}}_{ik} \widehat{\mathbf{a}}_{ik}^\top - \mathbf{a}_{ik} \mathbf{a}_{ik}^\top\|_S$ .

---

**Algorithm 4** cPCA-initialized Orthogonalized Alternating Least Square (cOALS)

---

**Input:** Observations  $\mathcal{X}_t \in \mathbb{R}^{d_1 \times \dots \times d_K}$  for  $t = 1, \dots, T$ , the number of factors  $r$ , the time lag  $h$ , the cPCA initial estimate  $(\hat{\mathbf{a}}_{i1}^{\text{cpca}}, \dots, \hat{\mathbf{a}}_{iK}^{\text{cpca}})$ ,  $1 \leq i \leq r$ , the tolerance parameter  $\epsilon > 0$ , the maximum number of iterations  $M$ .

- 1: Compute  $\hat{\Sigma}_h$  defined in (6).
- 2: Initialize unit vectors  $\hat{\mathbf{a}}_{ik}^{(0)} = \hat{\mathbf{a}}_{ik}^{\text{cpca}}$  for  $1 \leq k \leq K$ ,  $1 \leq i \leq r$ . Set  $\hat{\mathbf{A}}_k^{(0)} = (\hat{\mathbf{a}}_{1k}^{(0)}, \dots, \hat{\mathbf{a}}_{rk}^{(0)})$  and  $m = 0$ .
- 3: **repeat**
- 4:     Set  $m = m + 1$ .
- 5:     Find QR decomposition of  $\hat{\mathbf{A}}_k^{(m-1)}$ , set  $\hat{\mathbf{A}}_k^{(m-1)} = \mathbf{Q}_k^{(m-1)} \mathbf{R}_k^{(m-1)}$  for  $1 \leq k \leq K$ .
- 6:     **for**  $k = 1$  to  $K$ .
- 7:         Compute  $\hat{\mathbf{A}}_k^{(m)} = \text{mat}_k(\hat{\Sigma}_h)(*_\ell^{2K} \mathbf{Q}_\ell^{(m-1)})$ , where  $\mathbf{Q}_\ell^{(m-1)} = \mathbf{Q}_{\ell-K}^{(m-1)}$  for  $\ell > K$  and  $*$  is the Khatri–Rao product.
- 8:     **end for**
- 9: **until**  $m = M$  or  $\max_i \max_k \|\hat{\mathbf{a}}_{ik}^{(m)} \hat{\mathbf{a}}_{ik}^{(m)\top} - \hat{\mathbf{a}}_{ik}^{(m-1)} \hat{\mathbf{a}}_{ik}^{(m-1)\top}\|_S \leq \epsilon$ .

**Output:**  $\hat{\mathbf{a}}_{ik}^{\text{cOALS}} = \hat{\mathbf{a}}_{ik}^{(m)}$ ,  $i = 1, \dots, r$ ,  $k = 1, \dots, K$ .

---

We demonstrate the performance of all procedures under TFM-cp with  $K = 2$  (matrix time series) with

$$\mathcal{X}_t = \sum_{i=1}^r w f_{it} \mathbf{a}_{i1} \otimes \mathbf{a}_{i2} + \mathcal{E}_t. \quad (33)$$

For  $K = 2$  with model (33), we consider the following three experimental configurations:

- I. Set  $r = 2$ ,  $d_1 = d_2 = 40$ ,  $T = 400$ ,  $w = 6$  and vary  $\delta$  in the set  $[0, 0.5]$ . The purpose of this setting is to verify the theoretical bounds of cPCA and HOPE in terms of the coherence parameter  $\delta$ .
- II. Set  $r = 2$ ,  $d_1 = d_2 = 40$ ,  $\delta = 0.2$ . We vary the sample size  $T$  and the signal strength  $w$  to investigate the impact of  $\delta$  against signal strength and sample size.
- III. Set  $r = 3$ ,  $d_1 = d_2 = 40$ ,  $T = 400$ ,  $w = 8$  and vary  $\delta$  to check the sensitivities of  $\delta$  for all the proposed algorithms and compare with randomized initialization.

Results from an additional simulation settings under  $K = 2$  and  $K = 3$  cases are given in Appendix B. We repeat all the experiments 100 times. For simplicity, we set  $h = 1$ .

The loading vectors are generated as follows. First, the elements of matrices  $\tilde{\mathbf{A}}_k = (\tilde{\mathbf{a}}_{1k}, \dots, \tilde{\mathbf{a}}_{rk}) \in \mathbb{R}^{d_k \times r}$ ,  $1 \leq k \leq K$ , are generated from i.i.d.  $N(0, 1)$  and then orthonormalized through QR decomposition. Then if  $\delta = 0$ , set  $\mathbf{A}_k = \tilde{\mathbf{A}}_k$ , otherwise, set  $\mathbf{a}_{1k} = \tilde{\mathbf{a}}_{1k}$  and  $\mathbf{a}_{ik} = (\tilde{\mathbf{a}}_{1k} + \theta \tilde{\mathbf{a}}_{ik}) / \|\tilde{\mathbf{a}}_{1k} + \theta \tilde{\mathbf{a}}_{ik}\|_2$

for all  $i \geq 2$  and  $1 \leq k \leq K$ , with  $\vartheta = \delta/(r-1)$  and  $\theta = (\vartheta^{-2/K} - 1)^{1/2}$ . The commonly used incoherence measure (Anandkumar et al., 2014c, Hao et al., 2020) under this construction is  $\vartheta_{\max} = (1 + \theta^2)^{-1/2} = \vartheta^{1/K}$ .

The noise  $\mathcal{E}_t$  in the model is white  $\mathcal{E}_t \perp \mathcal{E}_{t+h}$ ,  $h > 0$ , and generated according to  $\mathcal{E}_t = \Psi_1^{1/2} Z_t \Psi_2^{1/2}$  where all of the elements in the  $d_1 \times d_2$  matrix  $Z_t$  are i.i.d.  $N(0, 1)$ . Furthermore,  $\Psi_1$ ,  $\Psi_2$  are the covariance matrices along each mode with the diagonal elements being 1 and all the off-diagonal elements being  $\psi_1$ ,  $\psi_2$ . Throughout this section, we set the off-diagonal entries of the covariance matrices of the noise as  $\psi_1 = \psi_2$ .

Under Configurations I and II with  $r = 2$ , the factor processes  $f_{1t}$  and  $f_{2t}$  are generated as two independent AR(1) processes, following  $f_{1t} = 0.8f_{1t-1} + e_{1t}$ ,  $f_{2t} = 0.6f_{2t-1} + e_{2t}$ . Under Configuration III and Configurations IV and V in Appendix B, with  $r = 3$ ,  $f_{1t}, f_{2t}, f_{3t}$  are generated as independent AR(1) processes, with  $f_{1t} = 0.8f_{1t-1} + e_{1t}$ ,  $f_{2t} = 0.7f_{2t-1} + e_{2t}$ ,  $f_{3t} = 0.6f_{3t-1} + e_{3t}$ . Here, all of the innovations follow i.i.d.  $N(0, 1)$ . The factors are not normalized.

Figure 1 shows the boxplots of the estimation errors for cPCA and HOPE under configuration I, for different  $\delta$ . It can be seen that the performance of cPCA deteriorates as  $\delta$  increases, while that of HOPE remains almost unchanged. The median of the cPCA estimation errors increases almost linearly with  $\delta$ , with a  $R^2$  of 0.977. This linear effect of  $\delta$  on the performance bounds of cPCA is confirmed by the theoretical results in (20).

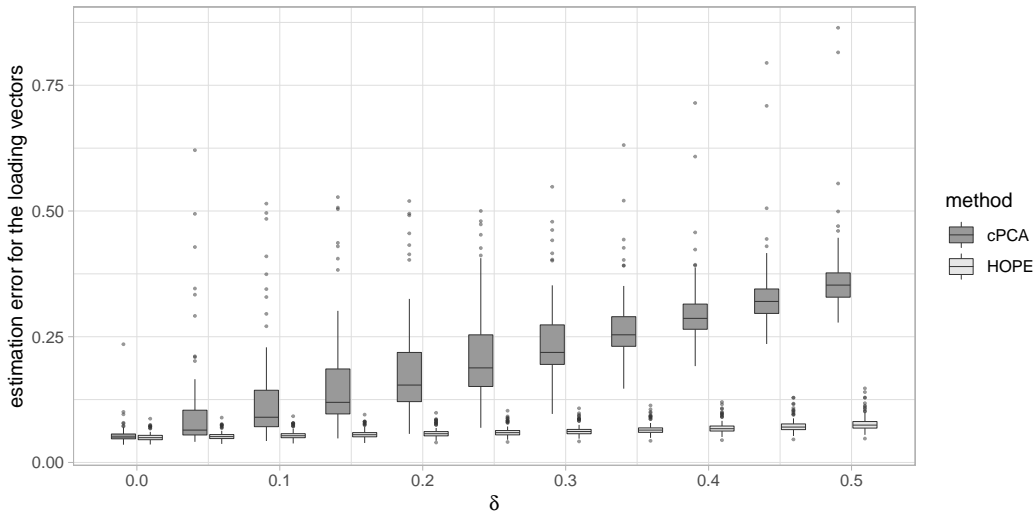


Figure 1: Boxplots of the estimation error over 100 replications under experiment configuration I with different  $\delta$ .

The experiment of Configuration II is conducted to verify the theoretical bounds on different sample sizes  $T$  and signal strengths  $w$ . Figures 2 and 3 show the logarithm of the estimation errors

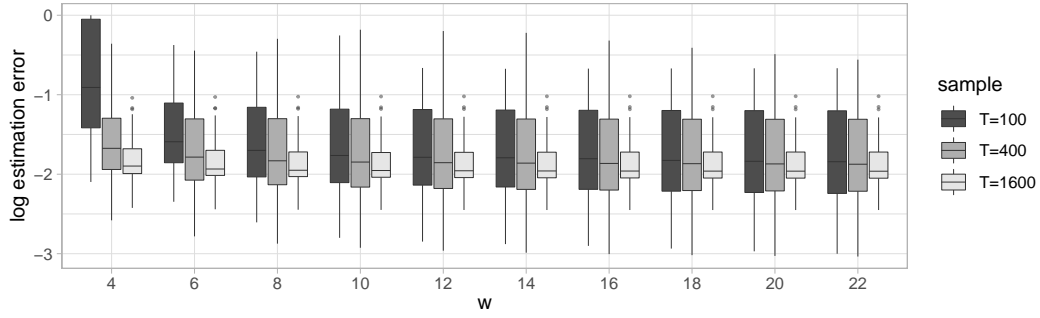


Figure 2: Boxplots of the logarithm of the estimation error for cPCA under experiment configuration II.

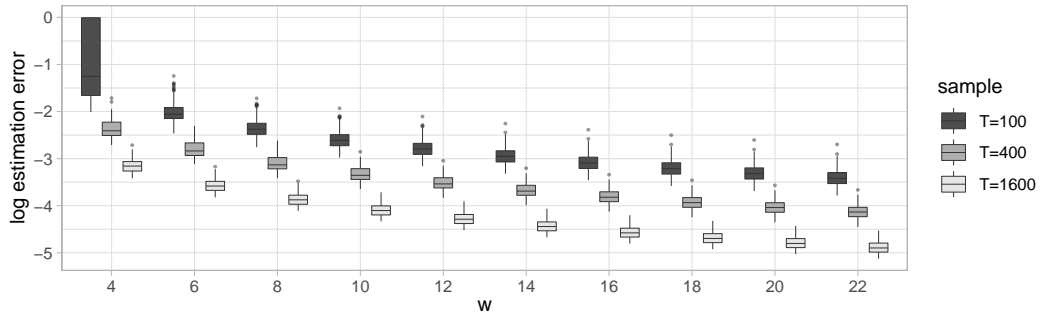


Figure 3: Boxplots of the logarithm of the estimation error for HOPE under experiment configuration II.

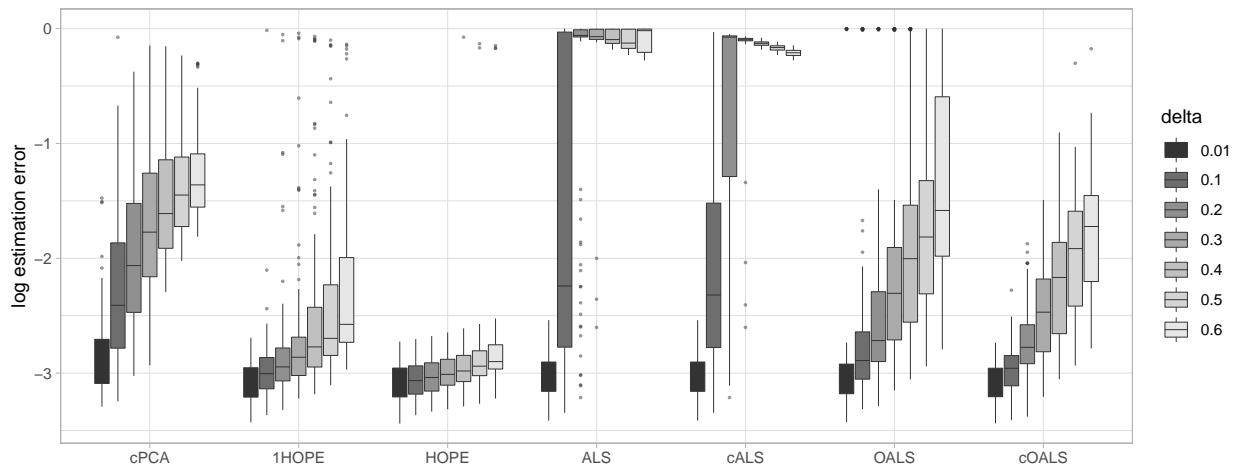


Figure 4: Boxplots of the logarithm of the estimation error under experiment configuration III. Seven methods with seven choices of  $\delta$  are considered in total.

under different  $(w, T)$  combinations. It can be seen from Figure 2 that the estimation error of cPCA decreases to a lower bound as  $w$  and  $T$  increases. The lower bound is associated with the bias term in (20) that cannot be reduced by a larger  $w$  and  $T$ . This is the baseline error due to the non-orthogonality. In contrast, the phenomenon of HOPE is very different. Figure 3 shows that the performance improves monotonically as  $w$  or  $T$  increases. Again, this is consistent with the theoretical bounds in (29).

Figure 4 shows the boxplots of the logarithm of the estimation errors for 7 different methods with choices of  $\delta$  under configuration III. ALS and OALS are implemented with  $L = 200$  random initiations. It can be seen that HOPE outperforms all the other methods. Again, the choice of  $\delta$  does not affect the performance of HOPE significantly. One-step method (1HOPE) is better than the cPCA alone, and the iterative method HOPE is in turn better than the one-step method. When the coherence  $\delta$  decreases, all methods perform better, but the advantage of HOPE over one-step method and the advantage of one-step method over the cPCA initialization become smaller. For the extremely small  $\delta = 0.01$ , all loading vectors are almost orthogonal to each other. In this case, all the iterative procedures, including the one-step HOPE, perform similarly. In addition, ALS and cALS are always the worst under the cases  $\delta \geq 0.1$ . The hybrid methods cALS and cOALS improve the original randomized initialized ALS and OALS significantly, showing the advantages of the cPCA initialization. It is worth noting that cOALS has comparable performance with 1HOPE and HOPE when  $\delta$  is small.

## 6 Applications

In this section, we demonstrate the use of TFM-cp model using the taxi traffic data set used in Chen et al. (2022). The data set was collected by the Taxi & Limousine Commission of New York City, and published at <https://www1.nyc.gov/site/tlc/about/tlc-trip-record-data.page>. Within Manhattan Island, it contains 69 predefined pick-up and drop-off zones and 24 hourly period for each day from January 1, 2009 to December 31, 2017. The total number of rides moving among the zones within each hour is recorded, yielding a  $\mathcal{X}_t \in \mathbb{R}^{69 \times 69 \times 24}$  tensor for each day, using the hour of day as the third dimension.

One natural way to model the hourly traffic data is to consider  $\mathbf{X}_t \in \mathbb{R}^{69 \times 69}$  for  $t = 1, \dots, 24 \times N$ , where  $N$  is the total number of days. It is apparent that such hourly data have two types of seasonality: weekly seasonality and daily seasonality. We handle the weekly seasonality by separating the time series into two parts: business-day series and non-business-day series. The length of the business-day series is 2,262 days, and that of the non-business-day is 1,025 days. The daily seasonality is a more interesting and important issue. It is clear that taxi usage heavily

depends on time of the day (morning and evening rush hours, lunch hours etc). Seasonal time series models have been extensively studied for univariate time series (Box and Jenkins, 1976, Reinsel, 2003, Shumway and Stoffer, 2006, Tsay, 2005), but these parametric models are difficult to be extended to deal with high dimensional matrix time series. Segmenting the 24-hour day into distinct intervals, such as morning rush hours and business hours, loses the detailed hourly information and requires pre-determined segmentation scheme (Zhang and Wang, 2019, Zhu et al., 2022). Here we adopt the nonparametric approach by stacking the hourly observations into a (multi-dimensional) daily observation. This is equivalent to turning hourly observations into daily 24-dimensional vector observations in the univariate time series case, a commonly used approach. By jointly modeling the 24-hourly observations within the day together, the detailed daily pattern can be captured more accurately and more flexibly without a parametric model assumption. This way, the daily pattern is built into the model simultaneously, and the interaction among the geographic and temporal patterns will be revealed.

After some exploratory analysis, we decide to use the TFM-cp with  $r = 4$  factors for both business-day series and non-business-day series, and estimate the model with  $h = 1$ . For the non-business-day series, TFM-cp explains 63.0% of the variability in the data. In comparison, treating the tensor time series as a 114,264 ( $= 69 \times 69 \times 24$ ) dimensional vector time series, the traditional vector factor model with 4 factors explains about 90.0% variability, but uses  $4 \times 114,264$  parameters for the loading matrix. Chen et al. (2022) used TFM-tucker with  $4 \times 4 \times 4$  core factor tensor process. Using iTIPUP estimator of Han et al. (2020), TFM-tucker explains 80.1% variability. Similarly, for the business-day series, the explained fractions of variability by the TFM-cp with 4 factors, vector factor model with 4 factors, and TFM-tucker with  $4 \times 4 \times 4$  core factor tensor are 68.1%, 90.9%, 84.0%, respectively. Comparison of model complexity between TFM-cp and TFM-tucker is substantially more complex compared to that of traditional tensor decomposition, owing to the stochastic nature of the latent factor process. Since both models are estimated through the sample autocovariance tensor, we may count, under each model, the number of parameters required in the population version of the autocovariance tensor. Both models require  $(69 + 69 + 24) \times 4$  number of parameters in terms of loading matrices or vectors, though the degree of freedom for TFM-tucker is slightly smaller due to orthonormal requirements of the loading matrices. However, for the lag-1 autocovariance of the factor processes, TFM-cp only requires 4 parameters (for the four uncorrelated factor process) while TFM-tucker requires  $(4 \times 4 \times 4)^2$  parameters (minus certain savings from rotation ambiguity). More importantly, TFM-cp harbors a much smaller dimensional factor process ( $\mathbf{f}_t \in \mathbb{R}^4$ ) than TFM-tucker ( $\mathcal{F}_t \in \mathbb{R}^{4 \times 4 \times 4}$ ), thereby simplifying subsequent modeling of the latent factor process.

The literature on Markov process models, for example Zhang and Wang (2019), Zhu et al.

(2022), regards each trip as a transition from the pickup location to the drop-off location, rendering the data as a collection of fragmented sample paths representative of a city-wide Markov process. When one aggregates the individual trips within a time period to form a traffic volume matrix, the model, with an assumed fixed (reduced rank) Markov transition matrix, essentially induces an order-1 autoregressive model on the volume matrix time series. Therefore, the distinction between the Markov process models and the CP factor models parallels that between autoregressive models and factor models.

Figures 5 and 6 show the heatmap of the estimated loading vectors  $(\mathbf{a}_{11}, \dots, \mathbf{a}_{41})$  (related to pick-up locations) and  $(\mathbf{a}_{12}, \dots, \mathbf{a}_{42})$  (related to drop-off locations) of the 69 zones in Manhattan, respectively, for the business-day series. Table 1 shows the corresponding loading vectors  $(\mathbf{a}_{13}, \dots, \mathbf{a}_{43})$  on the time of day dimension. For a more meaningful interpretation, we have re-scaled the loading vectors  $\mathbf{a}_{ik}$  and the factors  $w_i f_{it}$  such that  $\|\mathbf{a}_{ik}\|_1 = 1$ , for  $1 \leq i \leq 4, 1 \leq k \leq 3$ . Figure 7 shows the estimated four factors  $(w_i f_{it})$  for business day series in 1,000. (Please note the significant difference in scale). For a more detailed examination, we show the four factor series in the third year (year 2011) in Figure 15 in Appendix C.

It is seen that the estimated loading vectors and the factors are predominantly positive, although there are a few small negative values which we will ignore. When the loading vectors are scaled to sum to 1 (hence percentages), the model has the following interesting interpretation. First, the expected daily total volume  $(\sum_{i,j,k} X_{t,ijk})$  is the sum of the four factors  $w_1 f_{1t} + \dots + w_4 f_{4t}$ . Hence the daily traffic volumes essentially consist of taxi rides following four different patterns, each corresponding to the rank-1 tensor  $\mathbf{a}_{i1} \otimes \mathbf{a}_{i2} \otimes \mathbf{a}_{i3}$ ,  $i = 1, \dots, 4$ . One may also imagine that there are four types of taxi users in the city, each following one specific traffic pattern (of course an individual may take multiple trips in a day and follow different patterns for each trip).

It is interesting to study the component of the rank-1 tensor  $\mathbf{a}_{i1} \otimes \mathbf{a}_{i2} \otimes \mathbf{a}_{i3}$ . Specifically,  $\mathbf{a}_{i3}$  shows how the total volume of traffic pattern  $i$  ( $w_i f_{it}$ ) is distributed to different hours of the day. For example, Table 1 shows that 16% of pattern 2 volume  $w_2 f_{2t}$  is allotted to between 7am and 8am, while only 3% of pattern 4 volume  $w_4 f_{4t}$  is allotted to that hour. The rank-1 matrix  $\mathbf{a}_{i1} \mathbf{a}_{i2}^\top$  shows the spatial pattern of traffic pattern  $i$ , where  $\mathbf{a}_{i1}$  shows the percentage of pattern  $i$  volume ( $w_i f_{it}$ ) at each hour being picked up in each location, and  $\mathbf{a}_{i2}$  shows the percentage of pattern  $i$  volume  $w_i f_{it}$  being dropped-off in each location, and  $a_{i1k} a_{i2\ell}$  is the percentage of pattern  $i$  volume  $w_i f_{it}$  from location  $k$  to location  $\ell$ . This spatial pattern does not change through the day, but the volume in each hour is controlled by  $\mathbf{a}_{i3} w_i f_{it}$ .

From Table 1, it is seen that Factor 1 (or traffic pattern 1) roughly corresponds to the evening hours of 6pm to 12am, by the loading vector  $\mathbf{a}_{13}$ , with main activities in the SoHu and lower east side as both the pick-up and drop-off locations. From the estimated factor series plot in Figure 7,

it seems that this traffic pattern (pattern 1) has the largest overall volume, but with a very strong yearly seasonal pattern and a large daily variation. Intuitively people use less taxi service when the weather is nice, hence the volume is relatively small in summer and early fall, even though there are more evening activities in the summer. The large daily variation is due to a weekly effect. Figure 8 shows the 3-month business-day period from January 1 to March 31 in year 2011, in which the vertical line marks the end of working week (Friday or the day before holiday). It is clearly seen that, for this mainly evening-activity traffic pattern, the volume in the end of working week is almost twice as large as that in the beginning of the working week.

Again from Table 1, it is seen that Factor 2 (or traffic pattern 2) roughly corresponds to the morning rush hours of 6am to 12am, by the loading vector  $\mathbf{a}_{23}$ , with main activities in the midtown area as the pick-up locations, and Times square and 5th Avenue as the drop-off locations. About 23.1% (defined as  $\sum_t w_2 f_{2t} / \sum_t \sum_i w_i f_{it}$ ) of the total traffic follows this pattern. From Figure 7, it is seen that Factor 2 is quite stable throughout the year, which is again intuitively understandable as the traffic pattern is mainly used by the steady population of people commuting to work in morning rush hours. There is a large number of (small value) outliers, most of them corresponding to the business days before or after major holidays. It can be seen more clearly from Figure 15 in Appendix C.

For Factors 3 and 4, the areas that load heavily on the factors for pick-up are quite similar to that for drop-off, i.e., upper east side (with affluent neighborhoods and museums) on Factor 3, and upper west side (with affluent neighborhoods and performing arts) on Factor 4. The conventional business hours are heavily and almost exclusively loaded on these factors. From Figure 7, it seems that both patterns have a yearly seasonal effect, small in the summer and early fall, which can be seen more clearly in Figure 15 in Appendix C. Their volumes are relatively small than that of Factors 1 and 2.

We note that TFM-cp representation is unique which facilitates a more “unique” interpretation. On the other hand, TFM-tucker is subject to arbitrary rotation. Using TFM-tucker to analyze the same data set, Chen et al. (2022) used varimax rotation to obtain one specific representation of their estimated model and provided interesting interpretations. Their results are quite different from that of TFM-cp. First, since TFM-tucker representation requires orthonormal loading matrices, the discovered patterns in the loading matrices are forced to be different. For example, the daily patterns revealed in Chen et al. (2022) have quite distinct periods, while Table 1 shows more intertwined (non-orthogonal) patterns. Second, TFM-tucker requires  $4 \times 4 \times 4$  factor processes. The column loading vectors in each loading matrices work on all these factors, instead of on only one factor as in TFM-cp. The interpretation of these loading vectors are more convoluted. For example, in TFM-tucker, the volume from all four heavily loaded pick-up areas identified by  $\mathbf{a}_{i1}, i = 1, \dots, 4$

can be traveling to all four heavily loaded drop-off areas  $\mathbf{a}_{i2}, i = 1, \dots, 4$ . But in TFM-cp, the rank-1 matrix  $\mathbf{a}_{i1}\mathbf{a}_{i2}^\top$  shows the exact proportion of pattern  $i$  traffic from each of the pick-up area identified by  $\mathbf{a}_{i1}$  to the drop-off area  $\mathbf{a}_{i2}$ . In particular, it is seen that  $\mathbf{a}_{i1}$  is very similar to  $\mathbf{a}_{i2}$  for  $i = 1, 3, 4$ . This observation suggests that our TFM-cp model may offer better intuitive understanding as it aligns with the expectation that most taxi traffic activities are likely confined within specific areas. This comparison further underscores the distinct analytical insights offered by the TFM-cp model in capturing the spatial-temporal dynamics of urban taxi traffic.

For the non-business day series, the estimated loading vectors  $(\mathbf{a}_{11}, \dots, \mathbf{a}_{41})$  (related to pick-up locations),  $(\mathbf{a}_{12}, \dots, \mathbf{a}_{42})$  (related to drop-off locations),  $(\mathbf{a}_{13}, \dots, \mathbf{a}_{43})$  (on the hour of day dimension), the estimated factors  $(w_1f_{1t}, \dots, w_4f_{4t})$  are showed in Figures 9, 10, Table 2, and Figure 11, respectively. Understandably the morning rush hour pattern in the business day series (Factor 2) disappears here but the night-time pattern (Factor 1) now lasts deep into the early hours, comparing Tables 1 and 2. From Figure 11, it is seen that there exist two different yearly seasonal patterns. Factors 3 and 4 are similar to that of business day series, with small volumes in the summer and fall, again confirming that the use of taxi service is relatively low when the weather is good for walking in the city. On the other hand, the volume of Factor 2 is typically small in the winter time. The volumes of night-life pattern in Factor 1 remain to be volatile. It has many small-value outliers, mostly on the day before a business day (Sundays or the end of holiday.) These can be seen more clearly in the more detailed Figure 12, which shows the estimated factors of all the non-business days in Year 2011 (year 3), with vertical lines indicating the day before a business day (dashed lines for Sundays and solid lines for Mondays of long weekend when Tuesday is the start of business week.) This is again intuitively understandable, because people tend not to stay out too late if they need to work the next day.

The pick-up and drop-off locations that heavily load on Factors 1, 3, 4 are similar to that for Factors 1, 3, 4 in the business day series. The daytime hours load on Factors 3 and 4, and the night life hours from 12am to 4am load on Factor 1. As for the second factor, it loads heavily on midtown area for pick-up, on the lower west side near Chelsea (with many restaurants and bars) for drop-off, on the afternoon/evening hours between 1pm to 8pm as the dominating periods.

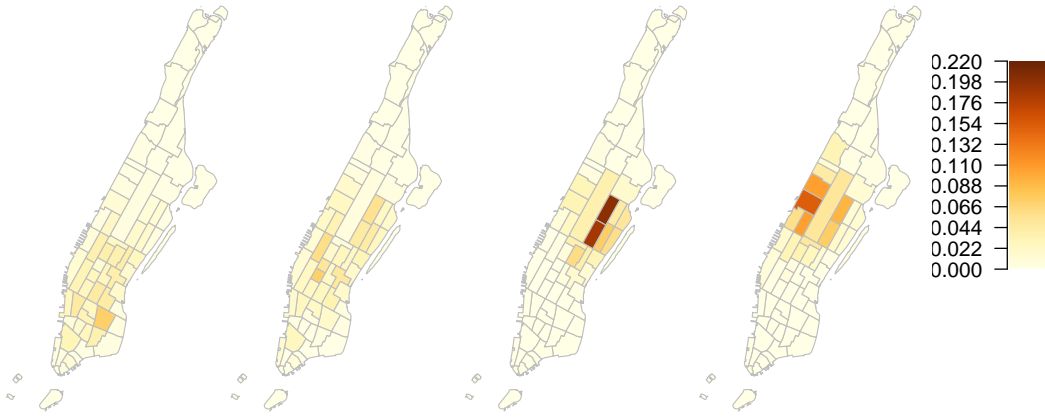


Figure 5: Loadings on four pickup factors for business day series.



Figure 6: Loadings on four dropoff factors for business day series.

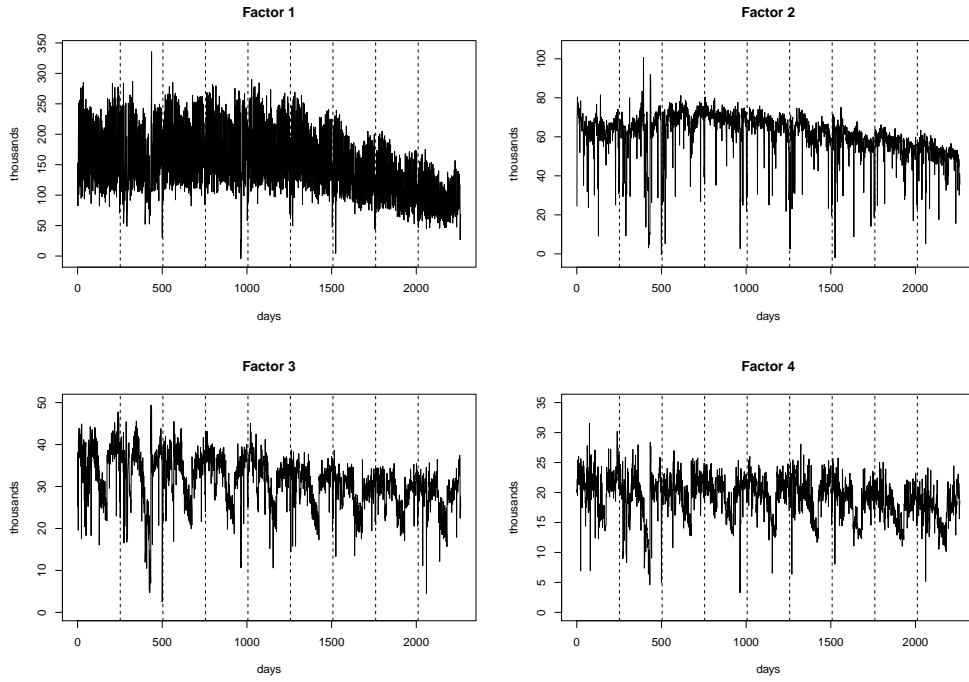


Figure 7: Estimated four factors for business day series.

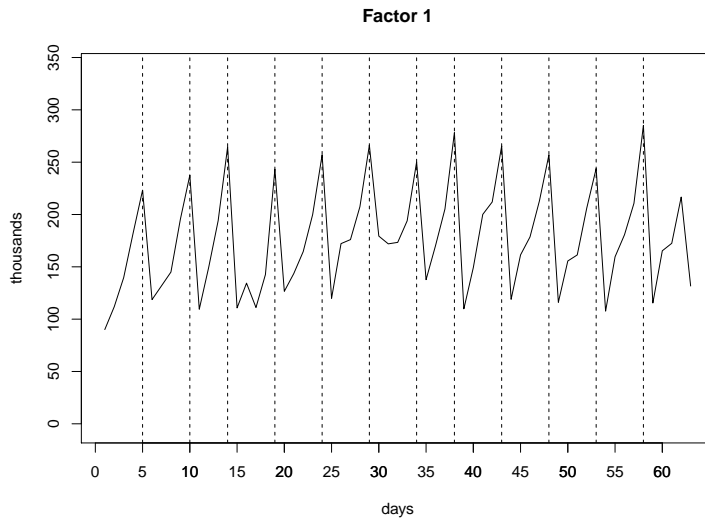


Figure 8: Estimated Factor 1 for business day series in the 3-months business-day period from January 1 to March 31 in year 2011. Vertical lines mark the end of business week.

	0am	2	4	6	8	10	12pm	2	4	6	8	10	12am											
$i = 1$	5	3	2	1	1	1	1	2	2	3	3	3	3	4	4	4	3	5	7	8	9	9	9	8
$i = 2$	0	0	0	0	1	3	12	16	13	11	7	6	5	4	4	3	2	2	3	3	2	2	1	1
$i = 3$	1	0	0	0	0	0	2	5	7	6	6	7	7	7	7	8	6	7	7	6	4	3	2	1
$i = 4$	1	1	0	0	0	0	1	3	5	4	5	5	6	6	7	7	6	8	9	8	6	5	4	3

Table 1: Estimated four loading vectors  $\mathbf{a}_{i3} \in \mathbb{R}^{24}$  ( $i = 1, \dots, 4$ ), for hour of day mode. Business day. Values are in percentage.

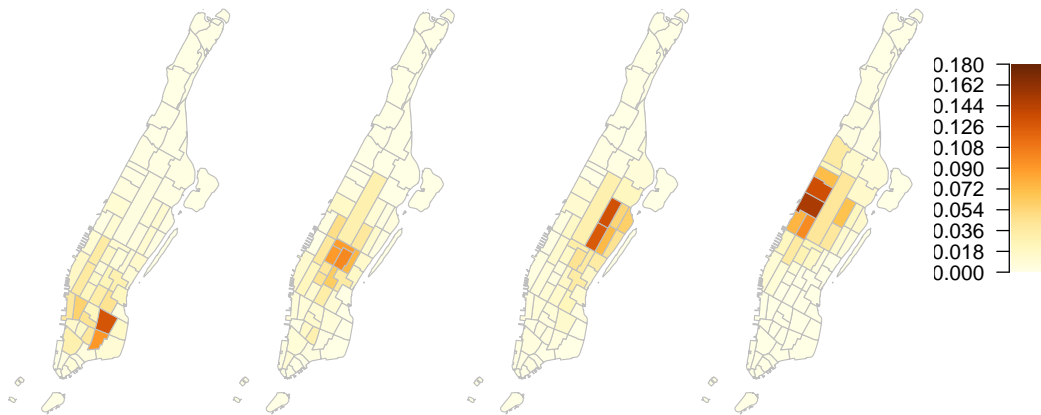


Figure 9: Loadings on four pick-up factors for non-business day series.

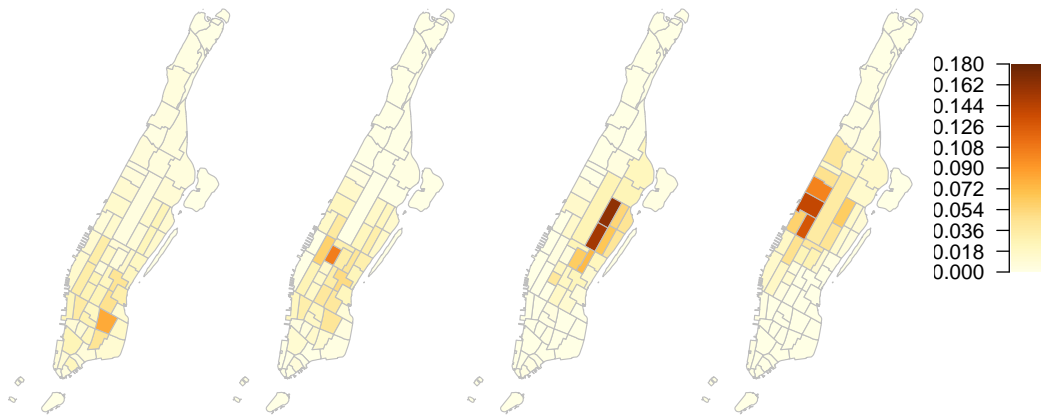


Figure 10: Loadings on four drop-off factors for non-business day series.

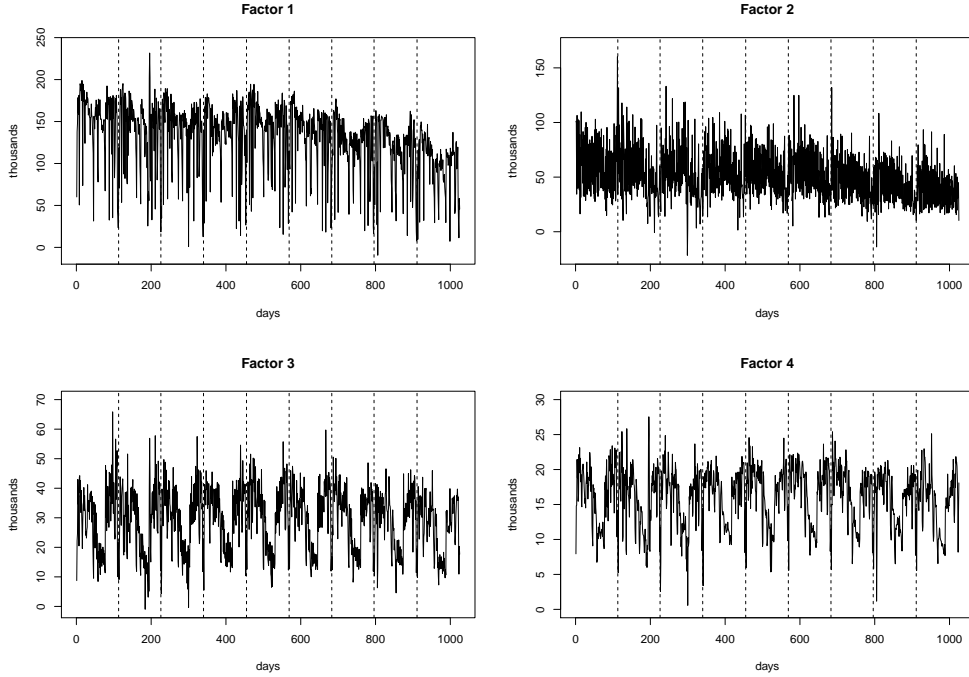


Figure 11: Estimated four factors for non-business day series.

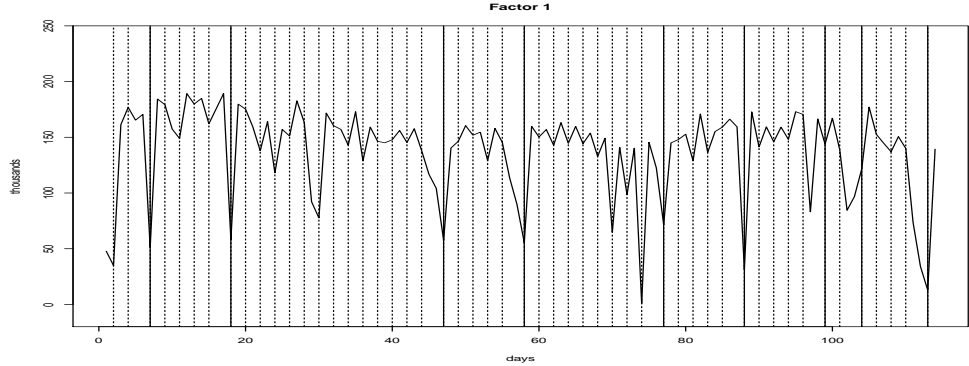


Figure 12: Estimated Factor 1 for non-business day series in Year 2011 with vertical lines indicating the day before a business day (dashed lines for Sundays and solid lines for Mondays of a long weekend).

We remark that this example is just for illustration and showcasing the interpretation of the proposed tensor factor model. Again we note that for the TFM-tucker model, one needs to identify a proper representation of the loading space in order to interpret the model. In [Chen et al. \(2022\)](#), varimax rotation was used to find the most sparse loading matrix representation to model interpretation. For TFM-cp, the model is unique hence interpretation can be made directly. Interpretation

	0am	2	4	6	8	10	12pm	2	4	6	8	10	12am											
$i = 1$	10	10	9	7	3	1	1	1	1	2	2	3	3	3	3	3	4	5	5	5	5	6		
$i = 2$	4	3	2	1	1	1	1	1	2	2	3	4	6	8	7	6	5	6	8	10	6	5	5	4
$i = 3$	2	1	1	1	0	0	1	2	3	6	7	8	8	8	8	7	6	6	5	4	3	2	2	
$i = 4$	3	2	1	1	1	0	1	1	3	5	6	7	7	7	7	6	6	7	7	5	4	4	3	

Table 2: Estimated four loading vectors  $\mathbf{a}_{i3} \in \mathbb{R}^{24}$  ( $i = 1, \dots, 4$ ) for hour of day mode. Non-Business day. Values are in percentage.

is impossible for the vector factor model in such a high dimensional case.

## 7 Discussion

In this paper, we propose a tensor factor model with a low rank CP structure and develop its corresponding estimation procedures. The estimation procedure takes advantage of the special structure of the model, resulting in faster convergence rate and more accurate estimations comparing to the standard procedures designed for the more general TFM-tucker, and the more general tensor CP decomposition. Numerical study illustrates the finite sample properties of the proposed estimators. The results show that HOPE uniformly outperforms the other methods, when the observations follow the specified TFM-cp.

The HOPE in this paper is based on CP decomposition of the second moment tensor  $\Sigma_h = \sum_{i=1}^r \lambda_i (\otimes_{k=1}^K \mathbf{a}_{ik})^{\otimes 2}$ , an order  $2K$  tensor. The intuition that higher order tensors tend to have smaller coherence among the CP components leads to the consideration of using higher order cross-moments to have more orthogonal CP components. For example, let the  $m$ -th cross moment tensor with lags  $0 = h_1 < \dots < h_m$  be

$$\Sigma_{h_1 \dots h_m}^{(m)} = \mathbb{E} [\otimes_{j=1}^m \mathcal{X}_{t-h_j}].$$

When the factor processes  $f_{it}$ ,  $i = 1, \dots, r$  are independent across different  $i$  in TFM-cp, a naive 4-th cross moment tensor to estimate  $\mathbf{a}_{ik}$  is

$$\begin{aligned} & \Sigma_{h_1 h_2 h_3 h_4}^{(4)} - \Sigma_{h_1 h_2}^{(2)} \otimes \Sigma_{h_3 h_4}^{(2)} - \mathbb{E}[\mathcal{X}_{t-h_1} \otimes \mathcal{X}_{t-h_2}^* \otimes \mathcal{X}_{t-h_3} \otimes \mathcal{X}_{t-h_4}^*] - \mathbb{E}[\mathcal{X}_{t-h_1} \otimes \mathcal{X}_{t-h_2}^* \otimes \mathcal{X}_{t-h_3}^* \otimes \mathcal{X}_{t-h_4}] \\ &= \sum_{i=1}^r \lambda_{i, h_1 h_2 h_3 h_4}^{(4)} (\otimes_{k=1}^K \mathbf{a}_{ik})^{\otimes 4}, \end{aligned}$$

with  $\{\mathcal{X}_t^*\}$  being an independent coupled process of  $\{\mathcal{X}_t\}$  and when  $h_j = (j-1)h$ ,

$$\lambda_{i, h_1 h_2 h_3 h_4}^{(4)} = \mathbb{E} \prod_{j=0}^3 f_{i, t-jh} - [\mathbb{E} f_{i, t} f_{i, t-h}]^2 - [\mathbb{E} f_{i, t} f_{i, t-2h}]^2 - [\mathbb{E} f_{i, t} f_{i, t-h}][\mathbb{E} f_{i, t} f_{i, t-3h}].$$

This naive 4-th cross moment tensor has more orthogonal CP bases. In light tailed case, simulation shows that it is much worse than the second moment tensor, due to the reduced signal strength  $\lambda_{i,h_1h_2h_3h_4}^{(4)}$ . However, for heavy tailed and skewed data, this procedure would be helpful. It would be an interesting and challenging problem to develop an efficient higher cross moment tensor to improve the statistical and computational performance. We leave this for future research.

Our primary consideration was directed towards the CP factor model in a time series setting, as the need of effectively analyzing tensor time series has arisen in many applications, and CP factor model is an efficient approach for such analysis. Without a specified (parametric) model for the latent factor processes (an topic currently under investigation), we focus on the auto-covariance and auto-cross-moment tensor for effective estimation of the proposed model. This is the main contribution of the paper. However, the proposed cPCA and ISO can be used directly in or be extended to many other problems involving CP decomposition of certain type of tensors. For example, in many problems where higher order moments can be introduced to reduce incoherence, the cPCA and ISO algorithms may offer better initialization and outperform conventional tensor power iteration methods. One specific example is the kurtosis tensor in independent component analysis in [Auddy and Yuan \(2023a\)](#). Another possible extension is highlighted in Remark 12 where we pointed out how cPCA can be modified to deal with situations when a few leading singular values of the auto-cross-moment tensor are the same.

## References

- Ahn, S. C. and Horenstein, A. R. (2013). Eigenvalue ratio test for the number of factors. *Econometrica*, 81(3):1203–1227.
- Allman, E. S., Matias, C., and Rhodes, J. A. (2009). Identifiability of parameters in latent structure models with many observed variables. *The Annals of Statistics*, 37(6A):3099 – 3132.
- Alter, O. and Golub, G. H. (2005). Reconstructing the pathways of a cellular system from genome-scale signals by using matrix and tensor computations. *Proceedings of the National Academy of Sciences*, 102(49):17559–17564.
- Anandkumar, A., Ge, R., Hsu, D., and Kakade, S. M. (2014a). A tensor approach to learning mixed membership community models. *Journal of Machine Learning Research*, 15(1):2239–2312.
- Anandkumar, A., Ge, R., Hsu, D., Kakade, S. M., and Telgarsky, M. (2014b). Tensor decompositions for learning latent variable models. *Journal of Machine Learning Research*, 15:2773–2832.

- Anandkumar, A., Ge, R., and Janzamin, M. (2014c). Guaranteed non-orthogonal tensor decomposition via alternating rank-1 updates. *arXiv preprint arXiv:1402.5180*.
- Auddy, A. and Yuan, M. (2023a). Large dimensional independent component analysis: Statistical optimality and computational tractability. *arXiv preprint arXiv:2303.18156*.
- Auddy, A. and Yuan, M. (2023b). Perturbation bounds for (nearly) orthogonally decomposable tensors with statistical applications. *Information and Inference: A Journal of the IMA*, 12(2):1044–1072.
- Auffinger, A., Arous, G. B., and Černý, J. (2013). Random matrices and complexity of spin glasses. *Communications on Pure and Applied Mathematics*, 66(2):165–201.
- Bai, J. (2003). Inferential theory for factor models of large dimensions. *Econometrica*, 71(1):135–171.
- Bai, J. and Ng, S. (2002). Determining the number of factors in approximate factor models. *Econometrica*, 70(1):191–221.
- Bai, J. and Ng, S. (2007). Determining the number of primitive shocks in factor models. *Journal of Business & Economic Statistics*, 25(1):52–60.
- Bai, J. and Wang, P. (2014). Identification theory for high dimensional static and dynamic factor models. *Journal of Econometrics*, 178(2):794–804.
- Bai, J. and Wang, P. (2015). Identification and bayesian estimation of dynamic factor models. *Journal of Business & Economic Statistics*, 33(2):221–240.
- Bekker, P. (1986). A note on the identification of restricted factor loading matrices. *Psychometrika*, 51:607–611.
- Bi, X., Qu, A., and Shen, X. (2018). Multilayer tensor factorization with applications to recommender systems. *The Annals of Statistics*, 46(6B):3308–3333.
- Box, G. and Jenkins, G. (1976). *Time Series Analysis, Forecasting and Control*. Holden Day: San Francisco.
- Bradley, R. C. (2005). Basic properties of strong mixing conditions. a survey and some open questions. *Probability Surveys*, 2:107–144.
- Chamberlain, G. and Rothschild, M. (1983). Arbitrage, factor structure, and mean-variance analysis on large asset markets. *Econometrica*, 51(5):1281–1304.

- Chang, J., He, J., Yang, L., and Yao, Q. (2023). Modelling matrix time series via a tensor cp-decomposition. *Journal of the Royal Statistical Society Series B: Statistical Methodology*, 85(1):127–148.
- Chen, E. Y. and Fan, J. (2023). Statistical inference for high-dimensional matrix-variate factor models. *Journal of the American Statistical Association*, 118(542):1038–1055.
- Chen, E. Y., Tsay, R. S., and Chen, R. (2019). Constrained factor models for high-dimensional matrix-variate time series. *Journal of the American Statistical Association*, pages 1–37.
- Chen, E. Y., Xia, D., Cai, C., and Fan, J. (2024). Semi-parametric tensor factor analysis by iteratively projected singular value decomposition. *Journal of the Royal Statistical Society Series B: Statistical Methodology*, page qkae001.
- Chen, R., Yang, D., and Zhang, C.-H. (2022). Factor models for high-dimensional tensor time series. *Journal of the American Statistical Association*, 117(537):94–116.
- Comon, P., Luciani, X., and De Almeida, A. L. (2009). Tensor decompositions, alternating least squares and other tales. *Journal of Chemometrics: A Journal of the Chemometrics Society*, 23(7-8):393–405.
- De Lathauwer, L., De Moor, B., and Vandewalle, J. (2000). On the best rank-1 and rank- $(r_1, r_2, \dots, r_n)$  approximation of higher-order tensors. *SIAM Journal on Matrix Analysis and Applications*, 21(4):1324–1342.
- Fan, J., Liao, Y., and Mincheva, M. (2011). High dimensional covariance matrix estimation in approximate factor models. *The Annals of Statistics*, 39(6):3320.
- Fan, J., Liao, Y., and Mincheva, M. (2013). Large covariance estimation by thresholding principal orthogonal complements. *Journal of the Royal Statistical Society: Series B (Statistical Methodology)*, 75(4):603–680.
- Fan, J., Liao, Y., and Wang, W. (2016). Projected principal component analysis in factor models. *The Annals of Statistics*, 44(1):219–254.
- Fan, J. and Yao, Q. (2003). *Nonlinear Time Series: Nonparametric and Parametric Methods*. Springer Series in Statistics. Springer-Verlag, New York.
- Forni, M., Hallin, M., Lippi, M., and Reichlin, L. (2000). The generalized dynamic-factor model: Identification and estimation. *The Review of Economics and Statistics*, 82(4):540–554.

- Forni, M., Hallin, M., Lippi, M., and Reichlin, L. (2004). The generalized dynamic factor model consistency and rates. *Journal of Econometrics*, 119(2):231–255.
- Forni, M., Hallin, M., Lippi, M., and Reichlin, L. (2005). The generalized dynamic factor model: one-sided estimation and forecasting. *Journal of the American Statistical Association*, 100(471):830–840.
- Fosdick, B. K. and Hoff, P. D. (2014). Separable factor analysis with applications to mortality data. *Annals of Applied Statistics*, 8(1):120.
- Hallin, M. and Liška, R. (2007). Determining the number of factors in the general dynamic factor model. *Journal of the American Statistical Association*, 102(478):603–617.
- Han, R., Shi, P., and Zhang, A. R. (2023). Guaranteed functional tensor singular value decomposition. *Journal of the American Statistical Association*, pages 1–13.
- Han, Y., Chen, R., Yang, D., and Zhang, C.-H. (2020). Tensor factor model estimation by iterative projection. *arXiv preprint arXiv:2006.02611*.
- Han, Y., Chen, R., and Zhang, C.-H. (2022). Rank determination in tensor factor model. *Electronic Journal of Statistics*, 16(1):1726–1803.
- Hao, B., Zhang, A., and Cheng, G. (2020). Sparse and low-rank tensor estimation via cubic sketchings. *IEEE Transactions on Information Theory*, 66(9):5927–5964.
- Håstad, J. (1990). Tensor rank is NP-complete. *Journal of Algorithms*, 11(4):644–654.
- Hillar, C. J. and Lim, L.-H. (2013). Most tensor problems are np-hard. *Journal of the ACM (JACM)*, 60(6):1–39.
- Hoff, P. D. (2011). Separable covariance arrays via the tucker product, with applications to multivariate relational data. *Bayesian Analysis*, 6(2):179–196.
- Hoff, P. D. (2015). Multilinear tensor regression for longitudinal relational data. *Annals of Applied Statistics*, 9(3):1169.
- Huang, B., Mu, C., Goldfarb, D., and Wright, J. (2015). Provable models for robust low-rank tensor completion. *Pacific Journal of Optimization*, 11(2):339–364.
- Jain, P. and Oh, S. (2014). Learning mixtures of discrete product distributions using spectral decompositions. In *Conference on Learning Theory*, pages 824–856. PMLR.

- Kolda, T. G. and Bader, B. W. (2009). Tensor decompositions and applications. *SIAM Review*, 51(3):455–500.
- Kuleshov, V., Chaganty, A., and Liang, P. (2015). Tensor factorization via matrix factorization. In *Artificial Intelligence and Statistics*, pages 507–516. PMLR.
- Lam, C. and Yao, Q. (2012). Factor modeling for high-dimensional time series: inference for the number of factors. *The Annals of Statistics*, 40(2):694–726.
- Lam, C., Yao, Q., and Bathia, N. (2011). Estimation of latent factors for high-dimensional time series. *Biometrika*, 98(4):901–918.
- Liu, J., Musialski, P., Wonka, P., and Ye, J. (2012). Tensor completion for estimating missing values in visual data. *IEEE Transactions on Pattern Analysis and Machine Intelligence*, 35(1):208–220.
- Liu, Y., Shang, F., Fan, W., Cheng, J., and Cheng, H. (2014). Generalized higher-order orthogonal iteration for tensor decomposition and completion. In *Advances in Neural Information Processing Systems*, pages 1763–1771.
- Merlevède, F., Peligrad, M., and Rio, E. (2011). A bernstein type inequality and moderate deviations for weakly dependent sequences. *Probability Theory and Related Fields*, 151(3-4):435–474.
- Neudecker, H. (1990). On the identification of restricted factor loading matrices: An alternative condition. *Journal of Mathematical Psychology*, 34(2):237–241.
- Omberg, L., Golub, G. H., and Alter, O. (2007). A tensor higher-order singular value decomposition for integrative analysis of dna microarray data from different studies. *Proceedings of the National Academy of Sciences*, 104(47):18371–18376.
- Pan, J. and Yao, Q. (2008). Modelling multiple time series via common factors. *Biometrika*, 95(2):365–379.
- Pena, D. and Box, G. E. (1987). Identifying a simplifying structure in time series. *Journal of the American statistical Association*, 82(399):836–843.
- Reinsel, G. C. (2003). *Elements of Multivariate Time Series Analysis*. Springer.
- Richard, E. and Montanari, A. (2014). A statistical model for tensor PCA. In *Advances in Neural Information Processing Systems*, volume 27.
- Rosenblatt, M. (2012). *Markov Processes, Structure and Asymptotic Behavior: Structure and Asymptotic Behavior*, volume 184. Springer Science & Business Media.

- Sharan, V. and Valiant, G. (2017). Orthogonalized ALS: A theoretically principled tensor decomposition algorithm for practical use. In *International Conference on Machine Learning*, pages 3095–3104. PMLR.
- Shumway, R. and Stoffer, D. (2006). *Time Series Analysis and Its Applications: With R Examples*. Springer.
- Stock, J. H. and Watson, M. W. (2002). Forecasting using principal components from a large number of predictors. *Journal of the American Statistical Association*, 97(460):1167–1179.
- Sun, W. W. and Li, L. (2017). STORE: sparse tensor response regression and neuroimaging analysis. *Journal of Machine Learning Research*, 18(1):4908–4944.
- Sun, W. W., Lu, J., Liu, H., and Cheng, G. (2017). Provable sparse tensor decomposition. *Journal of the Royal Statistical Society: Series B (Statistical Methodology)*, 3(79):899–916.
- Tong, H. (1990). *Non-linear Time Series: a Dynamical System Approach*. Oxford University Press.
- Tsay, R. S. (2005). *Analysis of Financial Time Series*, volume 543. John Wiley & Sons.
- Tsay, R. S. and Chen, R. (2018). *Nonlinear Time Series Analysis*, volume 891. John Wiley & Sons.
- Wang, D., Liu, X., and Chen, R. (2019). Factor models for matrix-valued high-dimensional time series. *Journal of Econometrics*, 208(1):231–248.
- Wang, M. and Li, L. (2020). Learning from binary multiway data: Probabilistic tensor decomposition and its statistical optimality. *Journal of Machine Learning Research*, 21(154):1–38.
- Wang, M. and Song, Y. (2017). Tensor decompositions via two-mode higher-order SVD (HOSVD). In *Artificial Intelligence and Statistics*, pages 614–622. PMLR.
- Wang, P.-A. and Lu, C.-J. (2017). Tensor decomposition via simultaneous power iteration. In *International Conference on Machine Learning*, pages 3665–3673. PMLR.
- Wedin, P.-Å. (1972). Perturbation bounds in connection with singular value decomposition. *BIT Numerical Mathematics*, 12(1):99–111.
- Zhang, A. and Wang, M. (2019). Spectral state compression of markov processes. *IEEE Transactions on Information Theory*, 66(5):3202–3231.
- Zhang, A. and Xia, D. (2018). Tensor SVD: Statistical and computational limits. *IEEE Transactions on Information Theory*, 64(11):7311–7338.

Zhou, H., Li, L., and Zhu, H. (2013). Tensor regression with applications in neuroimaging data analysis. *Journal of the American Statistical Association*, 108(502):540–552.

Zhu, Z., Li, X., Wang, M., and Zhang, A. (2022). Learning markov models via low-rank optimization. *Operations Research*, 70(4):2384–2398.

# Supplementary Material to “CP Factor Model for Dynamic Tensors”

Yuefeng Han, Dan Yang, Cun-Hui Zhang and Rong Chen

University of Notre Dame, The University of Hong Kong, and Rutgers University

## A Proofs

### A.1 Proofs of main theorems

Let  $[n]$  denote the set  $\{1, 2, \dots, n\}$ . For a matrix  $A = (a_{ij}) \in \mathbb{R}^{m \times n}$ , write the SVD as  $A = U\Sigma V^\top$ , where  $\Sigma = \text{diag}(\sigma_1(A), \sigma_2(A), \dots, \sigma_{\min\{m,n\}}(A))$ , with the singular values  $\sigma_1(A) \geq \sigma_2(A) \geq \dots \geq \sigma_{\min\{m,n\}}(A) \geq 0$  in descending order. For nonempty  $J \subseteq [K]$ ,  $\text{mat}_J(\mathcal{A})$  is the mode  $J$  matrix unfolding which maps  $\mathcal{A}$  to  $m_J \times m_{-J}$  matrix with  $m_J = \prod_{j \in J} m_j$  and  $m_{-J} = m/m_J$ , e.g.  $\text{mat}_{\{1,2\}}(\mathcal{A}) = \text{mat}_3^\top(\mathcal{A})$  for  $K = 3$ . Denote  $a \wedge b = \min\{a, b\}$  and  $a \vee b = \max\{a, b\}$ .

**Proof of Proposition 1.** Recall that  $\mathbf{A} = (\mathbf{a}_1, \dots, \mathbf{a}_r) \in \mathbb{R}^{d \times r}$ ,  $\delta = \|\mathbf{A}^\top \mathbf{A} - I_r\|_S$  and  $\delta_k = \|\mathbf{A}_k^\top \mathbf{A}_k - I_r\|_S$ . Because  $\mathbf{A}^\top \mathbf{A} = (\mathbf{A}_1^\top \mathbf{A}_1) \circ \dots \circ (\mathbf{A}_K^\top \mathbf{A}_K)$  is the Hadamard product of correlation matrices, the spectrum of  $\mathbf{A}^\top \mathbf{A}$  is contained inside the spectrum limits of  $\mathbf{A}_k^\top \mathbf{A}_k$  for each  $k$ , so that

$$\delta \leq \min_{1 \leq k \leq K} \delta_k.$$

Because  $\mathbf{A}^\top \mathbf{A} - I_r$  is symmetric, its spectrum norm is bounded by its  $\ell_1$  norm,

$$\delta \leq \max_{j \leq r} \sum_{i \neq j} |\mathbf{a}_i^\top \mathbf{a}_j| \leq (r-1)\vartheta \leq (r-1) \prod_{k=1}^K \vartheta_k$$

due to  $|\mathbf{a}_i^\top \mathbf{a}_j| = \prod_{k=1}^K |\mathbf{a}_{ik}^\top \mathbf{a}_{jk}| = \prod_{k=1}^K |\sigma_{ij,k}|$ . Moreover, for any  $j \leq r$  and  $1 \leq k_1 < k_2 \leq K$ ,

$$\begin{aligned} \sum_{i \neq j} \prod_{k=1}^K |\sigma_{ij,k}| &\leq \sum_{i \neq j} |\sigma_{ij,k_1} \sigma_{ij,k_2}| \max_{i \neq j} \prod_{k \neq k_1, k \neq k_2} |\sigma_{ij,k}| \\ &\leq \left( \prod_{k=1}^K \eta_{jk} \right) r^{-(K-2)/2} \max_{i \neq j} \prod_{k \neq k_1, k \neq k_2} \sqrt{r} |\sigma_{ij,k}| / \eta_{jk} \end{aligned}$$

as  $\eta_{jk} = (\sum_{i \neq j} \sigma_{ij,k}^2)^{1/2}$ . The proof is complete as  $k_1$  and  $k_2$  are arbitrary.  $\square$

**Proof of Theorem 1.** Recall  $\widehat{\Sigma}_h = \sum_{t=h+1}^T \mathcal{X}_{t-h} \otimes \mathcal{X}_t$ ,  $\lambda_i = w_i^2 \cdot \mathbb{E} f_{i,t-h} f_{i,t}$ ,  $\mathbf{a}_i = \text{vec}(\mathbf{a}_{i1} \otimes \mathbf{a}_{i2} \otimes \dots \otimes \mathbf{a}_{iK})$ ,  $d = d_1 d_2 \dots d_K$ . Let  $\mathbf{e}_t = \text{vec}(\mathcal{E}_t)$ . Write

$$\widetilde{\Sigma} := \text{mat}_{[K]}(\widehat{\Sigma}_h) = \sum_{i=1}^r \lambda_i \mathbf{a}_i \mathbf{a}_i^\top + \Psi^* = \mathbf{A} \mathbf{A} \mathbf{A}^\top + \Psi^*,$$

where  $\mathbf{A} = \text{diag}(\lambda_1, \dots, \lambda_r)$ . Assume  $\mathbf{A}$  has SVD  $\mathbf{A} = \widetilde{U} \widetilde{D} \widetilde{V}^\top$ , with  $\widetilde{D} = \text{diag}(\widetilde{\sigma}_1, \dots, \widetilde{\sigma}_r)$ . Let  $\mathbf{U} = \widetilde{U} \widetilde{V}^\top = (\mathbf{u}_1, \dots, \mathbf{u}_r)$ . Then,  $\mathbf{U}^\top \mathbf{U} = \mathbf{I}_r$ . Note that  $(\widetilde{\Sigma}/2 + \widetilde{\Sigma}^\top)/2$  is guaranteed to be symmetric. Without loss of generality, assume  $\widetilde{\Sigma}$  is symmetric.

By (10),  $\|\mathbf{A}^\top \mathbf{A} - \mathbf{I}_r\|_S = \|\widetilde{D}^2 - \mathbf{I}_r\|_S \leq \delta$ . It follows that  $\max_{1 \leq i \leq r} |\widetilde{\sigma}_i^2 - 1| \leq \delta$ . As  $\delta < 1$ , basic calculation shows that  $\max_i |\widetilde{\sigma}_i - 1| \leq \delta/(2 - \delta)$ . Thus,

$$\|\mathbf{A} - \mathbf{U}\|_S = \|\widetilde{D} - \mathbf{I}_r\|_S \leq \delta/(2 - \delta) < \delta < 1.$$

This yields

$$\max_i \|\mathbf{a}_i - \mathbf{u}_i\|_2 \leq \delta < 1.$$

It follows that  $\max_i (2 - 2\mathbf{a}_i^\top \mathbf{u}_i) \leq \delta^2$ . Since  $1 - x^2 \leq 2 - 2x$ , we have

$$\|\mathbf{a}_i \mathbf{a}_i^\top - \mathbf{u}_i \mathbf{u}_i^\top\|_S = \sqrt{1 - (\mathbf{a}_i^\top \mathbf{u}_i)^2} \leq \sqrt{2 - 2(\mathbf{a}_i^\top \mathbf{u}_i)} \leq \delta < 1. \quad (34)$$

Let the top  $r$  eigenvectors of  $\widetilde{\Sigma}$  be  $\widehat{\mathbf{U}} = (\widehat{\mathbf{u}}_1, \dots, \widehat{\mathbf{u}}_r) \in \mathbb{R}^{d \times r}$ . Note that  $\lambda_1 > \lambda_2 > \dots > \lambda_r > \lambda_{r+1} = 0$ . By Wedin's perturbation theorem (Wedin, 1972) and Lemma 2, for any  $1 \leq i \leq r$ ,

$$\|\widehat{\mathbf{u}}_i \widehat{\mathbf{u}}_i^\top - \mathbf{u}_i \mathbf{u}_i^\top\|_S \leq \frac{2\|\mathbf{A} \mathbf{A} \mathbf{A}^\top - \mathbf{U} \mathbf{A} \mathbf{U}^\top + \Psi^*\|_S}{\min\{\lambda_{i-1} - \lambda_i, \lambda_i - \lambda_{i+1}\}} \leq \frac{2\lambda_1 \delta + 2\|\Psi^*\|_S}{\min\{\lambda_{i-1} - \lambda_i, \lambda_i - \lambda_{i+1}\}}. \quad (35)$$

Combining (34) and (35), we have

$$\|\widehat{\mathbf{u}}_i \widehat{\mathbf{u}}_i^\top - \mathbf{a}_i \mathbf{a}_i^\top\|_S \leq \delta + \frac{2\lambda_1 \delta + 2\|\Psi^*\|_S}{\min\{\lambda_{i-1} - \lambda_i, \lambda_i - \lambda_{i+1}\}}. \quad (36)$$

We formulate each  $\widehat{\mathbf{u}}_i \in \mathbb{R}^d$  to be a  $K$ -way tensor  $\widehat{\mathbf{U}}_i \in \mathbb{R}^{d_1 \times \dots \times d_K}$ . Let  $\widehat{\mathbf{U}}_{ik} = \text{mat}_k(\widehat{\mathbf{U}}_i)$ , which is viewed as an estimate of  $\mathbf{a}_{ik} \text{vec}(\otimes_{\ell \neq k}^K \mathbf{a}_{i\ell})^\top \in \mathbb{R}^{d_k \times (d/d_k)}$ . Then  $\widehat{\mathbf{a}}_{ik}^{\text{cpca}}$  is the top left singular vector of  $\widehat{\mathbf{U}}_{ik}$ . By Lemma 3,

$$\|\widehat{\mathbf{a}}_{ik}^{\text{cpca}} \widehat{\mathbf{a}}_{ik}^{\text{cpca}\top} - \mathbf{a}_{ik} \mathbf{a}_{ik}^\top\|_S^2 \wedge (1/2) \leq \|\widehat{\mathbf{u}}_i \widehat{\mathbf{u}}_i^\top - \mathbf{a}_i \mathbf{a}_i^\top\|_S^2. \quad (37)$$

Substituting (36) and Lemma 1 into the above equation, since  $\|\Psi^*\|_S / \min\{\lambda_{i-1} - \lambda_i, \lambda_i - \lambda_{i+1}\} \lesssim 1$ , we have the desired results.  $\square$

**Lemma 1.** Suppose Assumptions 1, 2 hold and  $\delta < 1$ . Let  $\tilde{\Sigma} = \sum_{i=1}^r \lambda_i \mathbf{a}_i \mathbf{a}_i^\top + \Psi^*$  and  $1/\gamma = 1/\gamma_1 + 2/\gamma_2$ . In an event with probability at least  $1 - (Tr)^{-c}/2 - e^{-d}/6$ , we have

$$\begin{aligned} \|\Psi^*\|_S &\leq C \max_{1 \leq i \leq r} w_i^2 \left( \sqrt{\frac{r + \log T}{T}} + \frac{(r + \log T)^{1/\gamma}}{T} \right) + \frac{C\sigma^2(d + \sqrt{dT})}{T} \\ &\quad + C\sigma \max_{1 \leq i \leq r} w_i \sqrt{\frac{d}{T}}. \end{aligned} \quad (38)$$

*Proof.* Let  $\Upsilon_0 = T^{-1} \sum_{t=1}^T \sum_{i,j=1}^r w_i w_j f_{it} f_{jt} \mathbf{a}_i \mathbf{a}_j^\top$ ,  $\bar{\mathbb{E}}(\cdot) = \mathbb{E}(\cdot | f_{it}, 1 \leq i \leq r, 1 \leq t \leq T)$ . Define  $e_t = \text{vec}(\mathcal{E}_t)$ . Write

$$\begin{aligned} \tilde{\Sigma} &= \frac{1}{T-h} \sum_{t=h+1}^T \text{vec}(\mathcal{X}_{t-h}) \text{vec}(\mathcal{X}_t)^\top \\ &= \sum_{i=1}^r \lambda_i \mathbf{a}_i \mathbf{a}_i^\top + \sum_{i,j=1}^r \frac{1}{T-h} \sum_{t=h+1}^T w_i w_j (f_{i,t-h} f_{j,t} - \mathbb{E} f_{i,t-h} f_{j,t}) \mathbf{a}_i \mathbf{a}_j^\top + \frac{1}{T-h} \sum_{t=h+1}^T e_{t-h} e_t^\top \\ &\quad + \frac{1}{T-h} \sum_{t=h+1}^T \sum_{i=1}^r w_i f_{i,t-h} \mathbf{a}_i e_t^\top + \frac{1}{T-h} \sum_{t=h+1}^T \sum_{i=1}^r w_i f_{i,t} e_{t-h} \mathbf{a}_i^\top \\ &:= \sum_{i=1}^r \lambda_i \mathbf{a}_i \mathbf{a}_i^\top + \Delta_1 + \Delta_2 + \Delta_3 + \Delta_4. \end{aligned}$$

That is,  $\Psi^* = \Delta_1 + \Delta_2 + \Delta_3 + \Delta_4$ .

We first bound  $\|\Delta_1\|_S$ . Let

$$\Theta_h = \sum_{t=h+1}^T \begin{pmatrix} f_{1,t-h} f_{1,t} & f_{1,t-h} f_{2,t} & \cdots & f_{1,t-h} f_{r,t} \\ \vdots & \vdots & \ddots & \vdots \\ f_{r,t-h} f_{1,t} & f_{r,t-h} f_{2,t} & \cdots & f_{r,t-h} f_{r,t} \end{pmatrix}. \quad (39)$$

Then

$$\Delta_1 = (w_1 \mathbf{a}_1, \dots, w_r \mathbf{a}_r) \left( \frac{\Theta_h - \mathbb{E} \Theta_h}{T-h} \right) (w_1 \mathbf{a}_1, \dots, w_r \mathbf{a}_r)^\top.$$

For any unit vector  $u$  in  $\mathbb{R}^r$ , there exist  $u_j \in \mathbb{R}^r$  with  $\|u_j\|_2 \leq 1$ ,  $j = 1, \dots, N_{r,\epsilon}$  such that  $\max_{\|u\|_2 \leq 1} \min_{1 \leq j \leq N_{r,\epsilon}} \|u - u_j\|_2 \leq \epsilon$ . The standard volume comparison argument implies that the covering number  $N_{r,\epsilon} = \lceil (1 + 2/\epsilon)^r \rceil$ . Then, there exist  $u_j, v_{j'} \in \mathbb{R}^r$ ,  $1 \leq j, j' \leq N_{r,1/3} := 7^r$ , such that  $\|u_j\|_2 = \|v_{j'}\|_2 = 1$  and

$$\|\Theta_h - \mathbb{E} \Theta_h\|_S - \max_{1 \leq j, j' \leq N_{r,1/3}} |u_j^\top (\Theta_h - \mathbb{E} \Theta_h) v_{j'}| \leq (2/3) \|\Theta_h - \mathbb{E} \Theta_h\|_S.$$

It follows that

$$\|\Theta_h - \mathbb{E} \Theta_h\|_S \leq 3 \max_{1 \leq j, j' \leq N_{r,1/3}} |u_j^\top (\Theta_h - \mathbb{E} \Theta_h) v_{j'}|.$$

As  $1/\gamma = 1/\gamma_1 + 2/\gamma_2$ , by Theorem 1 in [Merlevède et al. \(2011\)](#),

$$\begin{aligned} \mathbb{P}(|u_j^\top(\Theta_h - \mathbb{E}\Theta_h)v_j| \geq x) &\leq T \exp\left(-\frac{x^\gamma}{c_1}\right) + \exp\left(-\frac{x^2}{c_2T}\right) \\ &\quad + \exp\left(-\frac{x^2}{c_3T} \exp\left(\frac{x^{\gamma(1-\gamma)}}{c_4(\log x)^\gamma}\right)\right). \end{aligned} \quad (40)$$

Hence,

$$\begin{aligned} \mathbb{P}(\|\Theta_h - \mathbb{E}\Theta_h\|_S/3 \geq x) &\leq N_{r,1/3}^2 T \exp\left(-\frac{x^\gamma}{c_1}\right) + N_{r,1/3}^2 \exp\left(-\frac{x^2}{c_2T}\right) \\ &\quad + N_{r,1/3}^2 \exp\left(-\frac{x^2}{c_3T} \exp\left(\frac{x^{\gamma(1-\gamma)}}{c_4(\log x)^\gamma}\right)\right). \end{aligned}$$

As  $h$  is fixed and  $T \geq 4h$ , choosing  $x = \sqrt{T(r + \log T)} + (r + \log T)^{1/\gamma}$ , in an event  $\Omega_1$  with probability at least  $1 - (Tr)^{-C_1/2}$ ,

$$\left\| \frac{\Theta_h - \mathbb{E}\Theta_h}{T - h} \right\|_S \leq C \sqrt{\frac{r + \log(T)}{T}} + \frac{C(r + \log T)^{1/\gamma}}{T}.$$

It follows that, in the event  $\Omega_1$ ,

$$\begin{aligned} \|\Delta_1\|_S &\leq \|\mathbf{A}\|_S^2 \max_{1 \leq i \leq r} w_i^2 \cdot \left\| \frac{\Theta_h - \mathbb{E}\Theta_h}{T - h} \right\|_S \\ &\leq C \max_{1 \leq i \leq r} w_i^2 \left( \sqrt{\frac{r + \log T}{T}} + \frac{(r + \log T)^{1/\gamma}}{T} \right), \end{aligned}$$

and, as  $\mathbb{E}f_{i,t}^2 = 1$ ,

$$\begin{aligned} \|\Upsilon_0\|_S &\leq \left\| \sum_{i=1}^r w_i^2 \mathbf{a}_i \mathbf{a}_j^\top \right\|_S + \left\| \frac{1}{T} \sum_{t=1}^T \sum_{i,j=1}^r w_i w_j (f_{i,t} f_{j,t} - \mathbb{E}f_{i,t} f_{j,t}) \mathbf{a}_i \mathbf{a}_j^\top \right\|_S \\ &\leq \|\mathbf{A}\|_S^2 \max_{1 \leq i \leq r} w_i^2 + \left\| \frac{1}{T} \sum_{t=1}^T \sum_{i,j=1}^r w_i w_j (f_{i,t} f_{j,t} - \mathbb{E}f_{i,t} f_{j,t}) \mathbf{a}_i \mathbf{a}_j^\top \right\|_S \\ &\leq (1 + \delta)^2 \max_{1 \leq i \leq r} w_i^2 + C \max_{1 \leq i \leq r} w_i^2 \left( \sqrt{\frac{r + \log T}{T}} + \frac{(r + \log T)^{1/\gamma}}{T} \right) \\ &:= \Delta_\Upsilon. \end{aligned} \quad (41)$$

Note that  $\Delta_\Upsilon \lesssim \max_{1 \leq i \leq r} w_i^2$ .

For  $\|\Delta_2\|_S$ , we split the sum into two terms over the index sets,  $S_1 = \{(h, 2h] \cup (3h, 4h] \cup \dots\} \cap (h, T]$  and its complement  $S_2$  in  $(h, T]$ , so that  $\{e_{t-h}, t \in S_a\}$  is independent of  $\{e_t, t \in S_a\}$  for each  $a = 1, 2$ . Let  $n_a = |S_a|$ . By Lemma 5(i),

$$\mathbb{P}\left(\left\| \sum_{t \in S_a} e_{t-h} e_t^\top \right\|_S \geq \sigma^2(d + 2\sqrt{dn_a}) + \sigma^2 x(x + 2\sqrt{n_a} + 2\sqrt{d})\right) \leq 2e^{-\frac{x^2}{2}}.$$

With  $x \asymp \sqrt{d}$ , in an event  $\Omega_2$  with probability at least  $1 - e^{-d}/18$ ,

$$\|\Delta_2\|_S \leq \sum_{a=1,2} \left\| \sum_{t \in S_a} \frac{e_{t-h} e_t^\top}{T-h} \right\|_S \leq \frac{C\sigma^2(d + \sqrt{dT})}{T}.$$

For  $\Delta_3$ , by Assumption 1, for any  $u$  and  $v$  in  $\mathbb{R}^d$  we have

$$\mathbb{E} \left\{ u^\top \left( \frac{1}{\sqrt{T}} \sum_{t=h+1}^T \sum_{i=1}^r w_i f_{i,t-h} \mathbf{a}_i e_t^\top \right) v \right\}^2 \leq \sigma^2 \|\Upsilon_0\|_S \|u\|_2^2 \|v\|_2^2.$$

Thus for vectors  $u_i$  and  $v_i$  with  $\|u_i\|_2 = \|v_i\|_2 = 1$ ,  $i = 1, 2$ ,

$$\begin{aligned} & \sigma^{-2} \|\Upsilon_0\|_S^{-1} \mathbb{E} \left( u_1^\top \left( \frac{1}{\sqrt{T}} \sum_{t=h+1}^T \sum_{i=1}^r w_i f_{i,t-h} \mathbf{a}_i e_t^\top \right) v_1 - u_2^\top \left( \frac{1}{\sqrt{T}} \sum_{t=h+1}^T \sum_{i=1}^r w_i f_{i,t-h} \mathbf{a}_i e_t^\top \right) v_2 \right)^2 \\ & \leq (\|u_1 - u_2\|_2 \|v_1\|_2 + \|u_2\|_2 \|v_1 - v_2\|_2)^2 \\ & \leq 2 (\|u_1 - u_2\|_2^2 + \|v_1 - v_2\|_2^2) \\ & = 2 \mathbb{E} \{ (u_1 - u_2)^\top \xi + (v_1 - v_2)^\top \zeta \}^2, \end{aligned}$$

where  $\xi$  and  $\zeta$  are iid  $N(0, I_d)$  vectors. The Sudakov- Fernique inequality yields

$$\sigma^{-2} \|\Upsilon_0\|_S^{-1} \mathbb{E} \left\| \frac{1}{\sqrt{T}} \sum_{t=h+1}^T \sum_{i=1}^r w_i f_{i,t-h} \mathbf{a}_i e_t^\top \right\|_S \leq \sqrt{2} \mathbb{E} \sup_{\|u\|_2 = \|v\|_2 = 1} |u^\top \xi + v^\top \zeta| \leq \sqrt{2} \mathbb{E} (\|\xi\|_2 + \|\zeta\|_2)$$

As  $\mathbb{E}\|\xi\|_2 = \mathbb{E}\|\zeta\|_2 \leq \sqrt{d}$ , it follows that

$$\mathbb{E} \left\| \frac{1}{T-h} \sum_{t=h+1}^T \sum_{i=1}^r w_i f_{i,t-h} \mathbf{a}_i e_t^\top \right\|_S \leq \frac{\sigma \sqrt{8Td} \|\Upsilon_0\|_S^{1/2}}{T-h}. \quad (42)$$

Elementary calculation shows that,  $\left\| \sum_{t=h+1}^T \sum_{i=1}^r w_i f_{i,t-h} \mathbf{a}_i e_t^\top \right\|_S$  is a  $\sigma \sqrt{T} \|\Upsilon_0\|_S^{1/2}$  Lipschitz function. Then, by Gaussian concentration inequalities for Lipschitz functions,

$$\mathbb{P} \left( \left\| \frac{1}{T-h} \sum_{t=h+1}^T \sum_{i=1}^r w_i f_{i,t-h} \mathbf{a}_i e_t^\top \right\|_S \geq \frac{\sigma \sqrt{8Td}}{T-h} \|\Upsilon_0\|_S^{1/2} + \frac{\sigma \sqrt{T}}{T-h} \|\Upsilon_0\|_S^{1/2} x \right) \leq 2e^{-\frac{x^2}{2}}.$$

With  $x \asymp \sqrt{d}$ , in an event  $\Omega_3$  with probability at least  $1 - e^{-d}/18$ ,

$$\|\Delta_3\|_S \leq C\sigma \sqrt{\frac{d}{T}} \|\Upsilon_0\|_S^{1/2}.$$

Hence, in the event  $\Omega_1 \cap \Omega_3$ ,

$$\|\Delta_3\|_S \leq C\sigma \sqrt{\frac{d}{T}} \Delta_Y^{1/2}.$$

Similarly,  $\|\Delta_4\|_S \leq C\sigma\sqrt{d/T}\Delta_Y^{1/2}$ .

Therefore, in the event  $\Omega_1 \cap \Omega_2 \cap \Omega_3$  with probability at least  $1 - (Tr)^{-c}/2 - e^{-d}/6$ ,

$$\begin{aligned} \|\Psi^*\|_S &\leq C \max_{1 \leq i \leq r} w_i^2 \left( \sqrt{\frac{r + \log T}{T}} + \frac{(r + \log T)^{1/\gamma}}{T} \right) + \frac{C\sigma^2(d + \sqrt{dT})}{T} \\ &\quad + C \max_{1 \leq i \leq r} w_i \sigma \sqrt{\frac{d}{T}}. \end{aligned}$$

□

**Proof of Theorem 2.** Recall  $\hat{\mathbf{A}}_k^{(m)} = (\hat{\mathbf{a}}_{1k}^{(m)}, \dots, \hat{\mathbf{a}}_{rk}^{(m)}) \in \mathbb{R}^{d_k \times r}$ ,  $\hat{\Sigma}_k^{(m)} = \hat{\mathbf{A}}_k^{(m)\top} \hat{\mathbf{A}}_k^{(m)}$ , and  $\hat{\mathbf{B}}_k^{(m)} = \hat{\mathbf{A}}_k^{(m)} (\hat{\Sigma}_k^{(m)})^{-1} = (\hat{\mathbf{b}}_{1k}^{(m)}, \dots, \hat{\mathbf{b}}_{rk}^{(m)}) \in \mathbb{R}^{d_k \times r}$ . Let  $\bar{\mathbb{E}}(\cdot) = \mathbb{E}(\cdot | f_{it}, 1 \leq i \leq r, 1 \leq t \leq T)$  and  $\bar{\mathbb{P}}(\cdot) = \mathbb{P}(\cdot | f_{it}, 1 \leq i \leq r, 1 \leq t \leq T)$ . Also let

$$\bar{\lambda}_i = \frac{1}{T-h} \sum_{t=h+1}^T w_i^2 f_{i,t-h} f_{i,t}.$$

Without loss of generality, assume  $\hat{\Sigma}_h$  is symmetric. Write

$$\begin{aligned} \hat{\Sigma}_h &= \frac{1}{T-h} \sum_{t=h+1}^T \mathcal{X}_{t-h} \otimes \mathcal{X}_t \\ &= \sum_{i=1}^r \bar{\lambda}_i \otimes_{k=1}^{2K} \mathbf{a}_{ik} + \sum_{i \neq j}^r \frac{1}{T-h} \sum_{t=h+1}^T w_i w_j f_{i,t-h} f_{j,t} \otimes_{k=1}^K \mathbf{a}_{ik} \otimes_{k=K+1}^{2K} \mathbf{a}_{jk} \\ &\quad + \frac{1}{T-h} \sum_{t=h+1}^T \sum_{i=1}^r w_i f_{i,t-h} \otimes_{k=1}^K \mathbf{a}_{ik} \otimes \mathcal{E}_t + \frac{1}{T-h} \sum_{t=h+1}^T \sum_{i=1}^r w_i f_{i,t} \mathcal{E}_{t-h} \otimes_{k=K+1}^{2K} \mathbf{a}_{ik} \\ &\quad + \frac{1}{T-h} \sum_{t=h+1}^T \mathcal{E}_{t-h} \otimes \mathcal{E}_t \\ &:= \sum_{i=1}^r \bar{\lambda}_i \otimes_{k=1}^{2K} \mathbf{a}_{ik} + \Delta_1 + \Delta_2 + \Delta_3 + \Delta_4, \end{aligned} \tag{43}$$

with  $\mathbf{a}_{i,K+k} = \mathbf{a}_{ik}$  for all  $1 \leq k \leq K$ . Let  $\Psi = \Delta_1 + \Delta_2 + \Delta_3 + \Delta_4$ .

By Theorem 1, in an event  $\Omega_0$  with probability at least  $1 - (Tr)^{-c}/2 - e^{-d}/6$ ,

$$\|\hat{\mathbf{a}}_{ik}^{(0)} \hat{\mathbf{a}}_{ik}^{(0)\top} - \mathbf{a}_{ik} \mathbf{a}_{ik}^\top\|_S \leq \delta + \frac{2\lambda_1 \delta + C_1 R^{(0)}}{\min\{\lambda_{i-1} - \lambda_i, \lambda_i - \lambda_{i+1}\}},$$

where

$$R^{(0)} = \max_{1 \leq i \leq r} w_i^2 \left( \sqrt{\frac{r + \log T}{T}} + \frac{(r + \log T)^{1/\gamma}}{T} \right) + \frac{\sigma^2(d + \sqrt{dT})}{T} + \sigma \max_{1 \leq i \leq r} w_i \sqrt{\frac{d}{T}}.$$

Then in the event  $\Omega_0$ ,

$$\psi_0 := \max_i \max_k \|\widehat{\mathbf{a}}_{ik}^{(0)} \widehat{\mathbf{a}}_{ik}^{(0)\top} - \mathbf{a}_{ik} \mathbf{a}_{ik}^\top\|_S \leq \max_i \left( \frac{C'_1 \lambda_1 \delta + C'_1 R^{(0)}}{\min\{\lambda_{i-1} - \lambda_i, \lambda_i - \lambda_{i+1}\}} \right). \quad (44)$$

At  $m$ -th step, let

$$\psi_{m,i,k} := \|\widehat{\mathbf{a}}_{ik}^{(m)} \widehat{\mathbf{a}}_{ik}^{(m)\top} - \mathbf{a}_{ik} \mathbf{a}_{ik}^\top\|_S, \quad \psi_{m,k} := \max_i \psi_{m,i,k}, \quad \psi_m = \max_k \psi_{m,k}. \quad (45)$$

Let  $\mathbf{g}_{i\ell} = \mathbf{b}_{i\ell} / \|\mathbf{b}_{i\ell}\|_2$  and  $\widehat{\mathbf{g}}_{i\ell}^{(m)} = \widehat{\mathbf{b}}_{i\ell}^{(m)} / \|\widehat{\mathbf{b}}_{i\ell}^{(m)}\|_2$ . Given  $\widehat{\mathbf{a}}_{i\ell}^{(m)}$  ( $1 \leq i \leq r, 1 \leq \ell \leq K$ ), the  $(m+1)$ th iteration produces estimates  $\widehat{\mathbf{a}}_{ik}^{(m+1)}$ , which is the top left singular vector of  $\widehat{\Sigma}_h \times_{\ell \in [2K] \setminus \{k, K+k\}} \widehat{\mathbf{b}}_{i\ell}^{(m)\top}$ , or equivalently  $\widehat{\Sigma}_h \times_{\ell \in [2K] \setminus \{k, K+k\}} \widehat{\mathbf{g}}_{i\ell}^{(m)\top}$ . Note that  $\widehat{\Sigma}_h = \sum_{j=1}^r \bar{\lambda}_j \otimes_{\ell=1}^{2K} \mathbf{a}_{j\ell} + \Psi$ , with  $\mathbf{a}_{j,\ell+K} = \mathbf{a}_{j\ell}$ . The “noiseless” version of this update is given by

$$\widehat{\Sigma}_h \times_{\ell \in [2K] \setminus \{k, K+k\}} \mathbf{g}_{i\ell}^\top = \bar{\lambda}_i \mathbf{a}_{ik} \mathbf{a}_{ik}^\top + \Psi \times_{\ell \in [2K] \setminus \{k, K+k\}} \mathbf{g}_{i\ell}^\top. \quad (46)$$

At  $(m+1)$ -th iteration, for any  $1 \leq i \leq r$ , we have

$$\widehat{\Sigma}_h \times_{\ell \in [2K] \setminus \{k, K+k\}} \widehat{\mathbf{g}}_{i\ell}^{(m)\top} = \sum_{j=1}^r \tilde{\lambda}_{j,i} \mathbf{a}_{jk} \mathbf{a}_{jk}^\top + \Psi \times_{\ell \in [2K] \setminus \{k, K+k\}} \widehat{\mathbf{g}}_{i\ell}^{(m)\top},$$

where

$$\tilde{\lambda}_{j,i} = \bar{\lambda}_j \prod_{\ell \in [2K] \setminus \{k, K+k\}} \mathbf{a}_{j\ell}^\top \widehat{\mathbf{g}}_{i\ell}^{(m)}.$$

Let

$$\begin{aligned} \lambda_{j,i} &= \lambda_j \prod_{\ell \in [2K] \setminus \{k, K+k\}} \mathbf{a}_{j\ell}^\top \widehat{\mathbf{g}}_{i\ell}^{(m)}, \\ \alpha &= \sqrt{1 - \delta_{\max}} - (r^{1/2} + 1) \psi_0 / \sqrt{1 - 1/(4r)}, \\ \phi_{m,\ell} &= 1 \wedge \frac{\psi_{m,\ell} \sqrt{2r}}{\alpha \sqrt{1 - 1/(4r)}}, \\ \phi_m &= \max_{\ell} \phi_{m,\ell}. \end{aligned}$$

We may assume without loss of generality  $\mathbf{a}_{j\ell}^\top \widehat{\mathbf{a}}_{j\ell}^{(m)} \geq 0$  for all  $(j, \ell)$ . Basic calculation shows

$$\max_{j \leq r} \|\widehat{\mathbf{a}}_{j\ell}^{(m)} - \mathbf{a}_{j\ell}\|_2 \leq \psi_{m,\ell} / \sqrt{1 - 1/(4r)}, \quad \|\widehat{\mathbf{b}}_{j\ell}^{(m)}\|_2 \leq \|\widehat{\mathbf{B}}_{\ell}^{(m)}\|_S \leq \left( \sqrt{1 - \delta_{\ell}} - \frac{r^{1/2} \psi_0}{\sqrt{1 - 1/(4r)}} \right)^{-1}. \quad (47)$$

Let  $P_\ell = \mathbf{A}_\ell(\mathbf{A}_\ell^\top \mathbf{A}_\ell)^{-1} \mathbf{A}_\ell^\top$  and  $P_\ell^\perp = I_{d_\ell} - P_\ell^\top$ . As  $\widehat{\mathbf{B}}_\ell^{(m)} - \mathbf{B}_\ell = P_\ell^\perp (\widehat{\mathbf{A}}_\ell^{(m)} - \mathbf{A}_\ell) (\widehat{\Sigma}_\ell^{(m)})^{-1} - \mathbf{B}_\ell (\widehat{\mathbf{A}}_\ell^{(m)} - \mathbf{A}_\ell)^\top \widehat{\mathbf{B}}_\ell^{(m)}$ ,

$$\begin{aligned} \|\widehat{\mathbf{b}}_{j\ell}^{(m)} - \mathbf{b}_{j\ell}\|_2^2 &\leq \|\widehat{\mathbf{A}}_\ell^{(m)} - \mathbf{A}_\ell\|_{\mathbb{S}}^2 (\|\widehat{\mathbf{B}}_\ell^{(m)}\|_{\mathbb{S}}^2 + \|\mathbf{B}_\ell\|_{\mathbb{S}}^2) (\|\widehat{\mathbf{b}}_{j\ell}^{(m)}\|_2^2 \wedge \|\mathbf{b}_{j\ell}\|_2^2) \\ &\leq \{r\psi_{m,\ell}^2/(1 - 1/(4r))\} (2/\alpha^2) (\|\widehat{\mathbf{b}}_{j\ell}^{(m)}\|_2^2 \wedge \|\mathbf{b}_{j\ell}\|_2^2) \end{aligned}$$

by the algebraic symmetry between the estimator and estimand. As  $\|\widehat{\mathbf{g}}_{j\ell}^{(m)} - \mathbf{b}_{j\ell}\|_2 \leq \|\widehat{\mathbf{b}}_{j\ell}^{(m)} - \mathbf{b}_{j\ell}\|_2$  for  $\|\widehat{\mathbf{b}}_{j\ell}^{(m)}\|_2 \geq \|\mathbf{b}_{j\ell}\|_2 = 1$ ,

$$\|\widehat{\mathbf{g}}_{j\ell}^{(m)} - \mathbf{b}_{j\ell}/\|\mathbf{b}_{j\ell}\|_2\|_2 \leq (\psi_{m,\ell}/\alpha) \sqrt{2r/(1 - 1/(4r))} \quad (48)$$

by scale invariance. Moreover, (47) provides

$$\max_{i \neq j} |\mathbf{a}_{i\ell}^\top \widehat{\mathbf{g}}_{j\ell}^{(m)}| \leq \psi_{m,\ell}/\sqrt{1 - 1/(4r)}, \quad |\mathbf{a}_{j\ell}^\top \widehat{\mathbf{g}}_{j\ell}^{(m)}| \geq \alpha, \quad (49)$$

as  $\widehat{\mathbf{a}}_{i\ell}^{(m)\top} \widehat{\mathbf{g}}_{j\ell}^{(m)} = I\{i = j\}/\|\widehat{\mathbf{b}}_{j\ell}^{(m)}\|_2$ . Then, for  $j \neq i$ ,

$$\lambda_{j,i}/\lambda_{i,i} \leq (\lambda_1/\lambda_i) \prod_{\ell \neq k}^K \left( \frac{\psi_{m,\ell}/\sqrt{1 - 1/(4r)}}{1 - \psi_{m,\ell}/\sqrt{1 - 1/(4r)}} \right)^2.$$

Employing similar arguments in the proof of Lemma 1, in an event  $\Omega_1$  with probability at least  $1 - (Tr)^{-c}/2$ , we have

$$\left\| \frac{\Theta_h - \mathbb{E}\Theta_h}{T - h} \right\|_{\mathbb{S}} \leq C_1 \left( \sqrt{\frac{r + \log T}{T}} + \frac{(r + \log T)^{1/\gamma}}{T} \right), \quad (50)$$

where  $\Theta_h$  is defined in (39). In the event  $\Omega_1$ , we also have

$$\max_{1 \leq j_1, j_2 \leq r} \left| \frac{1}{T - h} \sum_{t=h+1}^T f_{j_1, t-h} f_{j_2, t} - \mathbb{E} f_{j_1, t-h} f_{j_2, t} \right| \leq C_1 \left( \sqrt{\frac{r + \log T}{T}} + \frac{(r + \log T)^{1/\gamma}}{T} \right).$$

It follows that in the event  $\Omega_1$ , for any  $1 \leq j \leq r$ ,

$$|\bar{\lambda}_j - \lambda_j| \leq C_1 \left( \sqrt{\frac{r + \log T}{T}} + \frac{(r + \log T)^{1/\gamma}}{T} \right) \lambda_j.$$

By Wedin's theorem (Wedin, 1972), in the event  $\Omega_1$ ,

$$\begin{aligned} \|\widehat{\mathbf{a}}_{ik}^{(m+1)} \widehat{\mathbf{a}}_{ik}^{(m+1)\top} - \mathbf{a}_{ik} \mathbf{a}_{ik}^\top\|_{\mathbb{S}} &\leq \frac{2 \left\| \sum_{j \neq i}^r \tilde{\lambda}_{j,i} \mathbf{a}_{jk} \mathbf{a}_{jk}^\top \right\|_{\mathbb{S}} + 2 \|\Psi \times_{\ell \in [2K] \setminus \{k, K+k\}} \widehat{\mathbf{g}}_{i\ell}^{(m)\top}\|_{\mathbb{S}}}{\tilde{\lambda}_{i,i}} \\ &\leq \frac{4 \|\mathbf{A}_k\|_{\mathbb{S}}^2 \max_{j \neq i} |\lambda_{j,i}| + 2 \|\Psi \times_{\ell \in [2K] \setminus \{k, K+k\}} \widehat{\mathbf{g}}_{i\ell}^{(m)\top}\|_{\mathbb{S}}}{\alpha^{2k-2} \lambda_{i,i}}. \end{aligned} \quad (51)$$

To bound the numerator of (51), we write

$$\begin{aligned}\Delta_{1,1,h} &= \sum_{j_2 \neq i}^r \frac{1}{T-h} \sum_{t=h+1}^T w_i w_{j_2} f_{i,t-h} f_{j_2,t} \otimes_{\ell=1}^K \mathbf{a}_{i\ell} \otimes_{\ell=K+1}^{2K} \mathbf{a}_{j_2\ell} \times_{\ell \in [2K] \setminus \{k, K+k\}} \widehat{\mathbf{g}}_{i\ell}^{(m)\top}, \\ \Delta_{1,2,h} &= \sum_{j_1 \neq i}^r \frac{1}{T-h} \sum_{t=h+1}^T w_{j_1} w_i f_{j_1,t-h} f_{it} \otimes_{\ell=1}^K \mathbf{a}_{j_1\ell} \otimes_{\ell=K+1}^{2K} \mathbf{a}_{i\ell} \times_{\ell \in [2K] \setminus \{k, K+k\}} \widehat{\mathbf{g}}_{i\ell}^{(m)\top}, \\ \Delta_{1,3,h} &= \sum_{j_1 \neq j_2 \neq i}^r \frac{1}{T-h} \sum_{t=h+1}^T w_{j_1} w_{j_2} f_{j_1,t-h} f_{j_2,t} \otimes_{\ell=1}^K \mathbf{a}_{j_1\ell} \otimes_{\ell=K+1}^{2K} \mathbf{a}_{j_2\ell} \times_{\ell \in [2K] \setminus \{k, K+k\}} \widehat{\mathbf{g}}_{i\ell}^{(m)\top}.\end{aligned}$$

For any vectors  $\tilde{\mathbf{g}}_{i\ell}, \check{\mathbf{g}}_{i\ell} \in \mathbb{R}^{d_i}$ , define

$$\begin{aligned}\Delta_{2,k,h}(\tilde{\mathbf{g}}_{i\ell}, \ell \neq k) &= \frac{1}{T-h} \sum_{t=h+1}^T w_i f_{it} \mathcal{E}_{t-h} \times_{\ell=1, \ell \neq k}^K \tilde{\mathbf{g}}_{i\ell}^\top \in \mathbb{R}^{d_k}, \\ \Delta_{3,k,h}(\tilde{\mathbf{g}}_{i\ell}, \ell \neq k) &= \frac{1}{T-h} \sum_{t=h+1}^T \mathcal{E}_{t-h} \otimes (w_j f_{jt}, j \neq i)^\top \times_{\ell=1, \ell \neq k}^K \tilde{\mathbf{g}}_{i\ell}^\top \in \mathbb{R}^{d_k \times (r-1)}, \\ \Delta_{4,k,h}(\tilde{\mathbf{g}}_{i\ell}, \ell \neq k) &= \frac{1}{T-h} \sum_{t=h+1}^T w_i f_{i,t-h} \mathcal{E}_t \times_{\ell=1, \ell \neq k}^K \tilde{\mathbf{g}}_{i\ell}^\top \in \mathbb{R}^{d_k}, \\ \Delta_{5,k,h}(\tilde{\mathbf{g}}_{i\ell}, \ell \neq k) &= \frac{1}{T-h} \sum_{t=h+1}^T \mathcal{E}_t \otimes (w_j f_{j,t-h}, j \neq i)^\top \times_{\ell=1, \ell \neq k}^K \tilde{\mathbf{g}}_{i\ell}^\top \in \mathbb{R}^{d_k \times (r-1)}, \\ \Delta_{6,k,h}(\tilde{\mathbf{g}}_{i\ell}, \check{\mathbf{g}}_{i\ell}, \ell \neq k) &= \frac{1}{T-h} \sum_{t=h+1}^T \mathcal{E}_{t-h} \otimes \mathcal{E}_t \times_{\ell=1, \ell \neq k}^K \tilde{\mathbf{g}}_{i\ell}^\top \times_{\ell=K+1, \ell \neq K+k}^{2K} \check{\mathbf{g}}_{i, \ell-K}^\top \in \mathbb{R}^{d_k \times d_k}.\end{aligned}$$

As  $\Delta_{q,k,h}(\tilde{\mathbf{g}}_{i\ell}, \check{\mathbf{g}}_{i\ell}, \ell \neq k)$  is linear in  $\tilde{\mathbf{g}}_{i\ell}, \check{\mathbf{g}}_{i\ell}$ , by (49), the numerator on the right hand side of (51) can be bounded by

$$\begin{aligned}& \|\boldsymbol{\Psi} \times_{\ell \in [2K] \setminus \{k, K+k\}} \widehat{\mathbf{g}}_{i\ell}^{(m)\top}\|_{\mathbb{S}} \\ & \leq \|\Delta_1 \times_{\ell \in [2K] \setminus \{k, K+k\}} \widehat{\mathbf{g}}_{i\ell}^{(m)\top}\|_{\mathbb{S}} + \sum_{q=2,4} \|\Delta_{q,k,h}(\widehat{\mathbf{g}}_{i\ell}^{(m)}, \ell \neq k)\|_{\mathbb{S}} + \|\Delta_{6,k,h}(\widehat{\mathbf{g}}_{i\ell}^{(m)}, \widehat{\mathbf{g}}_{i\ell}^{(m)}, \ell \neq k)\|_{\mathbb{S}} \\ & \quad + \sum_{q=3,5} \|\mathbf{A}_k\|_{\mathbb{S}} \|\Delta_{q,k,h}(\widehat{\mathbf{g}}_{i\ell}^{(m)}, \ell \neq k)\|_{\mathbb{S}} \max_{j \neq i} \prod_{\ell \neq k}^K |\mathbf{a}_{j\ell}^\top \widehat{\mathbf{g}}_{i\ell}^{(m)}| \\ & \leq \sum_{q=1,2,3} \|\Delta_{1,q,h}\|_{\mathbb{S}} + \sum_{q=2,4} \|\Delta_{q,k,h}(\mathbf{g}_{i\ell}, \ell \neq k)\|_{\mathbb{S}} + \sum_{q=2,4} (2K-2) \phi_{m,k} \|\Delta_{q,k,h}\|_{\mathbb{S}, \mathbb{S}} \\ & \quad + \sum_{q=3,5} \|\mathbf{A}_k\|_{\mathbb{S}} \prod_{\ell \neq k}^K (\psi_{m,\ell} / \sqrt{1 - 1/(4r)}) \|\Delta_{q,k,h}(\mathbf{g}_{i\ell}, \ell \neq k)\|_{\mathbb{S}} \\ & \quad + \sum_{q=3,5} \|\mathbf{A}_k\|_{\mathbb{S}} (2K-2) \phi_{m,k} \prod_{\ell \neq k}^K (\psi_{m,\ell} / \sqrt{1 - 1/(4r)}) \|\Delta_{q,k,h}\|_{\mathbb{S}, \mathbb{S}} \\ & \quad + \|\Delta_{6,k,h}(\mathbf{g}_{i\ell}, \mathbf{g}_{i\ell}, \ell \neq k)\|_{\mathbb{S}} + (2K-2) \phi_{m,k} \|\Delta_{6,k,h}\|_{\mathbb{S}, \mathbb{S}},\end{aligned}\tag{52}$$

where

$$\begin{aligned}\|\Delta_{q,k,h}\|_{S,S} &= \max_{\substack{\|\tilde{\mathbf{g}}_{i\ell}\|_2=1, \\ \tilde{\mathbf{g}}_{i\ell} \in \mathbb{R}^{d_\ell}}} \|\Delta_{q,k,h}(\tilde{\mathbf{g}}_{i\ell}, \ell \neq k)\|_S, \quad q = 2, 3, 4, 5, \\ \|\Delta_{6,k,h}\|_{S,S} &= \max_{\substack{\|\tilde{\mathbf{g}}_{i\ell}\|_2=\|\check{\mathbf{g}}_{i\ell}\|_2=1, \\ \tilde{\mathbf{g}}_{i\ell}, \check{\mathbf{g}}_{i\ell} \in \mathbb{R}^{d_\ell}}} \|\Delta_{6,k,h}(\tilde{\mathbf{g}}_{i\ell}, \check{\mathbf{g}}_{i\ell}, \ell \neq k)\|_S.\end{aligned}$$

Note that

$$\Delta_{1,1,h} = w_i \mathbf{a}_{ik} \left( \prod_{\ell \neq k} \mathbf{a}_{i\ell}^\top \hat{\mathbf{g}}_{i\ell}^{(m)} \right) \frac{1}{T-h} \sum_{t=h+1}^T f_{i,t-h} \cdot (f_{j_2,t}, j_2 \neq i) \text{diag} \left( \prod_{\ell \neq k} \mathbf{a}_{j_2\ell}^\top \hat{\mathbf{g}}_{i\ell}^{(m)}, j_2 \neq i \right) (w_{j_2} \mathbf{a}_{j_2k}, j_2 \neq i)^\top.$$

By (50), in the event  $\Omega_1$ ,

$$\begin{aligned}\|\Delta_{1,1,h}\|_S &\leq w_i \max_j w_j \|\mathbf{A}_k\|_S \left\| \frac{\Theta_h - \mathbb{E}\Theta_h}{T-h} \right\|_S \max_{j \neq i} \prod_{\ell \neq k} |\mathbf{a}_{j\ell}^\top \hat{\mathbf{g}}_{i\ell}^{(m)}| \\ &\leq C_1 w_i \max_j w_j \left( \sqrt{\frac{r + \log T}{T}} + \frac{(r + \log T)^{1/\gamma}}{T} \right) \prod_{\ell \neq k} (\psi_{m,\ell} / \sqrt{1 - 1/(4r)}). \quad (53)\end{aligned}$$

Similarly, in the event  $\Omega_1$ ,

$$\|\Delta_{1,2,h}\|_S \leq C_1 w_i \max_j w_j \left( \sqrt{\frac{r + \log T}{T}} + \frac{(r + \log T)^{1/\gamma}}{T} \right) \prod_{\ell \neq k} (\psi_{m,\ell} / \sqrt{1 - 1/(4r)}), \quad (54)$$

$$\|\Delta_{1,3,h}\|_S \leq C_1 \max_j w_j^2 \left( \sqrt{\frac{r + \log T}{T}} + \frac{(r + \log T)^{1/\gamma}}{T} \right) \prod_{\ell \neq k} (\psi_{m,\ell} / \sqrt{1 - 1/(4r)})^2. \quad (55)$$

Let  $\Upsilon_{0,i,k} = T^{-1} \sum_{t=1}^T w_i^2 f_{it}^2 \mathbf{a}_{ik} \mathbf{a}_{ik}^\top$  and  $\Upsilon_{0,-i,k} = T^{-1} \sum_{t=1}^T \sum_{j_1, j_2 \neq i}^r w_{j_1} w_{j_2} f_{j_1 t} f_{j_2 t} \mathbf{a}_{j_1 k} \mathbf{a}_{j_2 k}^\top$ . Then, in the event  $\Omega_1$ ,

$$\|\Upsilon_{0,i,k}\|_S \leq w_i^2 + C_1 w_i^2 \left( \sqrt{\frac{r + \log T}{T}} + \frac{(r + \log T)^{1/\gamma}}{T} \right) := \Delta_{\Upsilon_i} \asymp \lambda_i, \quad (56)$$

$$\|\Upsilon_{0,-i,k}\|_S \leq \max_j w_j^2 + C_1 \max_j w_j^2 \left( \sqrt{\frac{r + \log T}{T}} + \frac{(r + \log T)^{1/\gamma}}{T} \right) := \Delta_{\Upsilon_{-i}} \asymp \lambda_1. \quad (57)$$

We claim that in certain events  $\Omega_1 \cap \Omega_q$ ,  $q = 2, 3, 4, 5, 6$ , with  $\mathbb{P}(\Omega_q) \geq 1 - 6^{-1} \sum_{\ell=1}^K e^{-d_\ell}$ , for any  $1 \leq \ell \leq K$ , the following bounds for  $\|\Delta_{q,k,h}\|_{S,S}$  and  $\|\Delta_{q,k,h}(b_{j\ell}, b_{j\ell}, \ell \neq k)\|_S$  hold,

$$\begin{aligned}\|\Delta_{q,k,h}\|_{S,S} &\leq C_1 \sigma \frac{\sqrt{d_k} + \sqrt{\sum_{\ell \neq k} d_\ell}}{\sqrt{T}} \Delta_{\Upsilon_i}^{1/2}, \quad q = 2, 4, \\ \|\Delta_{q,k,h}\|_{S,S} &\leq C_1 \sigma \frac{\sqrt{d_k} + \sqrt{\sum_{\ell \neq k} d_\ell}}{\sqrt{T}} \Delta_{\Upsilon_{-i}}^{1/2}, \quad q = 3, 5, \\ \|\Delta_{6,k,h}\|_{S,S} &\leq \frac{C_1 \sigma^2 \left( \sum_{k=1}^K d_k + \sqrt{d_k T} + \sqrt{\sum_{\ell \neq k} d_\ell T} \right)}{T},\end{aligned} \quad (58)$$

and

$$\begin{aligned}
\|\Delta_{q,k,h}(\mathbf{g}_{i\ell}, \ell \neq k)\|_S &\leq C_1 \sigma \sqrt{\frac{d_k}{T}} \Delta_{\Upsilon_i}^{1/2}, \quad q = 2, 4, \\
\|\Delta_{q,k,h}(\mathbf{g}_{i\ell}, \ell \neq k)\|_S &\leq C_1 \sigma \sqrt{\frac{d_k}{T}} \Delta_{\Upsilon_{-i}}^{1/2}, \quad q = 3, 5, \\
\|\Delta_{6,k,h}(\mathbf{g}_{i\ell}, \mathbf{g}_{i\ell}, \ell \neq k)\|_S &\leq \frac{C_1 \sigma^2 (d_k + \sqrt{d_k T})}{T}.
\end{aligned} \tag{59}$$

Define

$$R_{k,i}^{(\text{ideal})} = \frac{\sigma^2 (d_k + \sqrt{d_k T})}{T} + \sqrt{\frac{\lambda_i d_k}{T}}, \tag{60}$$

$$R_{i,\phi}^{(\text{ideal})} = R_{k,i}^{(\text{ideal})} + \phi \sum_{\ell \neq k} R_{\ell,i}^{(\text{ideal})}. \tag{61}$$

As  $\mathbf{g}_{i\ell}$  is true and deterministic, it follows from (52), (53), (54), (55), (58), (59), in the event  $\cap_{q=0}^6 \Omega_q$ , for some numeric constant  $C_2 > 0$

$$\begin{aligned}
&\|\Psi \times_{\ell \in [2K] \setminus \{k, K+k\}} \widehat{\mathbf{g}}_{i\ell}^{(m)\top}\|_S \\
&\leq C_2 R_{k,i}^{(\text{ideal})} + C_2 (K-1) \phi_m \sum_{\ell \neq k} R_{\ell,i}^{(\text{ideal})} + \frac{2C_1}{(1 - 1/(4r))^{(K-1)/2}} \sqrt{\lambda_1 \lambda_i} \prod_{\ell \neq k} \psi_{m,\ell} \left( \sqrt{\frac{r + \log T}{T}} + \frac{(r + \log T)^{1/\gamma}}{T} \right) \\
&\quad + \frac{C_1}{(1 - 1/(4r))^{K-1}} \lambda_1 \prod_{\ell \neq k} \psi_{m,\ell}^2 \left( \sqrt{\frac{r + \log T}{T}} + \frac{(r + \log T)^{1/\gamma}}{T} \right).
\end{aligned} \tag{62}$$

Substituting (62) into (51), we have, in the event  $\cap_{q=0}^6 \Omega_q$ ,

$$\begin{aligned}
&\|\widehat{\mathbf{a}}_{ik}^{(m+1)} \widehat{\mathbf{a}}_{ik}^{(m+1)\top} - \mathbf{a}_{ik} \mathbf{a}_{ik}^\top\|_S \\
&\leq \frac{4(1 + \delta_{\max}) \lambda_1 \prod_{\ell \neq k} \psi_{m,\ell}^2}{\alpha^{2K-2} \lambda_i [\sqrt{(1 - \delta_{\max})(1 - 1/(4r))} \alpha]^{2K-2}} + \frac{2C_2 (K-1) R_{i,\phi}^{(\text{ideal})}}{\alpha^{2K-2} \lambda_i} \\
&\quad + \frac{4C_1}{\alpha^{2K-2} (1 - 1/(4r))^{(K-1)/2}} \sqrt{\lambda_1 / \lambda_i} \prod_{\ell \neq k} \psi_{m,\ell} \left( \sqrt{\frac{r + \log T}{T}} + \frac{(r + \log T)^{1/\gamma}}{T} \right) \\
&\quad + \frac{2C_1}{\alpha^{2K-2} (1 - 1/(4r))^{K-1}} (\lambda_1 / \lambda_i) \prod_{\ell \neq k} \psi_{m,\ell}^2 \left( \sqrt{\frac{r + \log T}{T}} + \frac{(r + \log T)^{1/\gamma}}{T} \right) \\
&\leq C_{\alpha,K} (\lambda_1 / \lambda_i) \prod_{\ell \neq k} \psi_{m,\ell}^2 + C_{\alpha,K} \sqrt{\lambda_1 / \lambda_i} \prod_{\ell \neq k} \psi_{m,\ell} \left( \sqrt{\frac{r + \log T}{T}} + \frac{(r + \log T)^{1/\gamma}}{T} \right) + C_{\alpha,K} R_{i,\phi_m}^{(\text{ideal})} / \lambda_i.
\end{aligned} \tag{63}$$

Let  $\phi_0 = (\psi^* / \alpha) \sqrt{2r(1 - 1/(4r))}$  with  $\psi^* = C_{\alpha,K} R^{(\text{ideal})}$ . By induction,  $\phi_{m,k} \leq \phi_0$ . It follows that

$$\begin{aligned}
\psi_{m+1,i,k} &\leq C_{\alpha,K} (\lambda_1 / \lambda_i) \prod_{\ell \neq k} \psi_{m,\ell}^2 + C_{\alpha,K} \sqrt{\lambda_1 / \lambda_i} \prod_{\ell \neq k} \psi_{m,\ell} \left( \sqrt{\frac{r + \log T}{T}} + \frac{(r + \log T)^{1/\gamma}}{T} \right) + C_{\alpha,K} R^{(\text{ideal})} \\
&\leq \epsilon \vee C_{\alpha,K} R^{(\text{ideal})}.
\end{aligned} \tag{64}$$

Hence, we have

$$\psi_{m+,k} \leq \psi_0 \rho^{1+(2K-2)+\dots+(2K-2)^m}$$

with the  $\rho < 1$  in (28), so that the required iteration number is  $O(\log \log(\psi_0/R^{\text{(ideal)}}))$ .

In the end, we divide the rest of the proof into 3 steps to prove (58) for  $q = 2, 3, 4, 5, 6$ . The proof of (59) is similar, thus omitted.

**Step 1.** We prove (58) for the  $\|\Delta_{2,k,h}\|_{S,S}$ . The proof for  $\|\Delta_{4,k,h}\|_{S,S}$  will be similar, thus is omitted. By Lemma 4 (iii), there exist  $\mathbf{g}_{il}^{(\ell)} \in \mathbb{R}^{d_l}$ ,  $1 \leq \ell \leq N_{d_l,1/8} := 17^{d_l}$ , such that  $\|\mathbf{g}_{il}^{(\ell)}\|_2 \leq 1$  and

$$\begin{aligned} \|\Delta_{2,k,h}\|_{S,S} &\leq 2 \max_{\ell \leq N_{d_l,1/8}} \left\| \Delta_{2,k,h}(\mathbf{g}_{il}^{(\ell)}, l \neq k) \right\|_S \\ &= 2 \max_{\ell \leq N_{d_l,1/8}} \left\| \frac{1}{T-h} \sum_{t=h+1}^T w_i f_{it} \mathcal{E}_{t-h} \times_{l=1, l \neq k}^K \mathbf{g}_{il}^{(\ell)\top} \right\|_S. \end{aligned}$$

Employing similar arguments in the proof of Lemma 1, we have

$$\mathbb{E} \left\| \Delta_{2,k,h}(\mathbf{g}_{il}^{(\ell)}, l \neq k) \right\|_S \leq \frac{\sigma \sqrt{8Td_k}}{T-h} \|\Upsilon_{0,i,k}\|_S^{1/2}.$$

Elementary calculation shows that  $\left\| \Delta_{2,k,h}(\mathbf{g}_{il}^{(\ell)}, l \neq k) \right\|_S$  is a  $\sigma \sqrt{T} \|\Upsilon_{0,i,k}\|_S^{1/2}$  Lipschitz function. Then, by Gaussian concentration inequalities for Lipschitz functions,

$$\mathbb{P} \left( \left\| \Delta_{2,k,h}(\mathbf{g}_{il}^{(\ell)}, l \neq k) \right\|_S - \frac{\sigma \sqrt{8Td_k}}{T-h} \|\Upsilon_{0,i,k}\|_S^{1/2} \geq \frac{\sigma \sqrt{T}}{T-h} \|\Upsilon_{0,i,k}\|_S^{1/2} x \right) \leq 2e^{-\frac{x^2}{2}}.$$

Hence,

$$\mathbb{P} \left( \left\| \Delta_{2,k,h} \right\|_{S,S} - \frac{\sigma \sqrt{8Td_k}}{T-h} \|\Upsilon_{0,i,k}\|_S^{1/2} \geq \frac{\sigma \sqrt{T}}{T-h} \|\Upsilon_{0,i,k}\|_S^{1/2} x \right) \leq 4 \prod_{l \neq k} N_{d_l,1/8} e^{-\frac{x^2}{2}}.$$

As  $T \geq 4h$ , this implies with  $x \asymp \sqrt{\sum_{l \neq k} d_l}$  that in an event  $\Omega_2$  with at least probability  $1 - \sum_k e^{-d_k}/6$ ,

$$\|\Delta_{2,k,h}\|_{S,S} \leq C_1 \sigma \frac{\sqrt{d_k} + \sqrt{\sum_{l \neq k}^K d_l}}{\sqrt{T}} \|\Upsilon_{0,i,k}\|_S^{1/2}.$$

It follows that, in the event  $\Omega_1 \cap \Omega_2$ ,

$$\|\Delta_{2,k,h}\|_{S,S} \leq C_1 \sigma \frac{\sqrt{d_k} + \sqrt{\sum_{l \neq k}^K d_l}}{\sqrt{T}} \Delta_{\Upsilon_i}^{1/2}, \quad (65)$$

where  $\Delta_{\Upsilon_i} \asymp \lambda_i$  is defined in (56).

**Step 2.** Inequality (58) for  $\|\Delta_{3,k,h}\|_{S,S}$  and  $\|\Delta_{5,k,h}\|_{S,S}$  follow from the same argument as the above step.

**Step 3.** Now we prove (58) for  $\|\Delta_{6,k,h}\|_{S,S}$ . We split the sum into two terms over the index sets,  $S_1 = \{(h, 2h] \cup (3h, 4h] \cup \dots\} \cap (h, T]$  and its complement  $S_2$  in  $(h, T]$ , so that  $\{\mathcal{E}_{t-h}, t \in S_a\}$  is independent of  $\{\mathcal{E}_t, t \in S_a\}$  for each  $a = 1, 2$ . Let  $n_a = |S_a|$ .

By Lemma 4 (iii), there exist  $\mathbf{g}_{il}^{(\ell)}, \mathbf{g}_{il}^{(\ell')} \in \mathbb{R}^{d_l}$ ,  $1 \leq \ell, \ell' \leq N_{d_l, 1/8} := 17^{d_l}$ , such that  $\|\mathbf{g}_{il}^{(\ell)}\|_2 \leq 1$ ,  $\|\mathbf{g}_{il}^{(\ell')}\|_2 \leq 1$  and

$$\begin{aligned} \|\Delta_{6,k,h}\|_{S,S} &\leq 2 \max_{\ell, \ell' \leq N_{d_l, 1/8}} \left\| \Delta_{6,k,h}(\mathbf{g}_{il}^{(\ell)}, \mathbf{g}_{ik}^{(\ell')}, l \neq k) \right\|_S \\ &= 2 \max_{\ell, \ell' \leq N_{d_l, 1/8}} \left\| \frac{1}{T-h} \sum_{t=h+1}^T \mathcal{E}_{t-h} \otimes \mathcal{E}_t \times_{l=1, l \neq k}^K \mathbf{g}_{il}^{(\ell)\top} \times_{l=k+1, l \neq K+k}^{2K} \mathbf{g}_{i, l-K}^{(\ell')\top} \right\|_S. \end{aligned}$$

Define  $G_a = (\mathcal{E}_{t-h} \times_{l=1, l \neq k}^K \mathbf{g}_{il}^{(\ell)\top}, t \in S_a) \in \mathbb{R}^{d_k \times n_a}$  and  $H_a = (\mathcal{E}_t \times_{l=1, l \neq k}^K \mathbf{g}_{il}^{(\ell')\top}, t \in S_a) \in \mathbb{R}^{d_k \times n_a}$ . Then,  $G_a, H_a$  are two independent Gaussian matrices. Note that

$$\left\| \sum_{t \in S_a} \mathcal{E}_{t-h} \otimes \mathcal{E}_t \times_{l=1, l \neq k}^K \mathbf{g}_{il}^{(\ell)\top} \times_{l=k+1, l \neq K+k}^{2K} \mathbf{g}_{i, l-K}^{(\ell')\top} \right\|_S = \|G_a H_a^\top\|_S.$$

By Lemma 5(i),

$$\mathbb{P} \left( \|G_a H_a\|_S \geq \sigma^2 (d_k + 2\sqrt{d_k n_a}) + \sigma^2 x (x + 2\sqrt{n_a} + 2\sqrt{d_k}) \right) \leq 2e^{-\frac{x^2}{2}}.$$

As  $\sum_{a=1}^2 n_a = T - h$ , it follows from the above inequality,

$$\mathbb{P} \left( \frac{\|\Delta_{6,k,h}\|_{S,S}}{4\sigma^2} \geq \frac{(\sqrt{d_k} + x)^2}{T-h} + \frac{\sqrt{2}(\sqrt{d_k} + x)}{\sqrt{T-h}} \right) \leq 4 \prod_{l \neq k} N_{d_l, 1/8}^2 e^{-\frac{x^2}{2}}.$$

Thus, with  $h \leq T/4$ ,  $x = \sqrt{\sum_{l \neq k} d_l}$ , in an event  $\Omega_6$  with probability at least  $1 - \sum_k e^{-d_k/6}$ ,

$$\|\Delta_{6,k,h}\|_{S,S} \leq \frac{C_1 \sigma^2 \left( \sum_{k=1}^K d_k + \sqrt{d_k T} + \sqrt{\sum_{l \neq k} d_l T} \right)}{T}. \quad (66)$$

□

**Proof of Theorem 3.** Let

$$\begin{aligned} \psi_0 &= \max_{1 \leq i \leq r} \max_{1 \leq k \leq K} \|\widehat{\mathbf{a}}_{ik}^{\text{cpca}} \widehat{\mathbf{a}}_{ik}^{\text{cpca}\top} - \mathbf{a}_{ik} \mathbf{a}_{ik}^\top\|_S, \\ \psi &= \max_{1 \leq i \leq r} \max_{1 \leq k \leq K} \|\widehat{\mathbf{a}}_{ik}^{\text{iso}} \widehat{\mathbf{a}}_{ik}^{\text{iso}\top} - \mathbf{a}_{ik} \mathbf{a}_{ik}^\top\|_S. \end{aligned}$$

As  $\sigma^2 \lesssim \lambda_r$ , Theorem 2 implies that

$$\psi = O_{\mathbb{P}} \left( \sqrt{\frac{\sigma^2 d_{\max}}{\lambda_r T}} \right).$$

We first prove (31). Note that

$$\begin{aligned} \widehat{w}_i^{\text{iso}} \widehat{f}_{it}^{\text{iso}} - w_i f_{it} &= \sum_{j=1}^r w_j f_{jt} \otimes_{k=1}^K \mathbf{a}_{jk} \times_{k=1}^K \widehat{\mathbf{b}}_{ik}^{\text{iso}\top} + \mathcal{E}_t \times_{k=1}^K \widehat{\mathbf{b}}_{ik}^{\text{iso}\top} - w_i f_{it} \\ &= w_i f_{it} \left( \prod_{k=1}^K \mathbf{a}_{ik}^{\top} \widehat{\mathbf{b}}_{ik}^{\text{iso}} - 1 \right) + \sum_{j \neq i} w_j f_{jt} \prod_{k=1}^K \mathbf{a}_{ik}^{\top} \widehat{\mathbf{b}}_{jk}^{\text{iso}} + \mathcal{E}_t \times_{k=1}^K \widehat{\mathbf{b}}_{ik}^{\text{iso}\top} \\ &:= \text{I}_1 + \text{I}_2 + \text{I}_3. \end{aligned}$$

By (49) in the proof of Theorem 2,  $\max_{1 \leq i, j \leq r} \max_{1 \leq k \leq K} |\mathbf{a}_{ik}^{\top} \widehat{\mathbf{b}}_{jk}^{\text{iso}} - \mathbf{1}_{\{i=j\}}| \lesssim \psi$ . It follows that  $\text{I}_1 = O_{\mathbb{P}}(w_i \psi)$ ,  $\text{I}_2 = O_{\mathbb{P}}(\sqrt{\lambda_1} r \psi^K)$  and  $\text{I}_3 = O_{\mathbb{P}}(\sigma)$ . Since  $\lambda_* \lesssim \lambda_r$ ,  $\lambda_r + (r-1)\lambda_* \lesssim \lambda_1$  and  $d_{\max} r \lesssim d$ , condition (27) leads to  $(\lambda_1/\lambda_r)^{1/2} r \psi^{K-1} \lesssim (\lambda_1/\lambda_r)^{1/2} \psi_0^{K-1} \lesssim 1$ . Then  $\text{I}_2 = O_{\mathbb{P}}(\lambda_r^{1/2} \psi)$ . Hence  $w_i^{-1} |\widehat{w}_i^{\text{iso}} \widehat{f}_{it}^{\text{iso}} - w_i f_{it}| = O_{\mathbb{P}}(\psi + \sigma w_i^{-1})$ , which completes the proof.

Next, we prove (32). Note that

$$\begin{aligned} &\frac{1}{T-h} \sum_{t=h+1}^T \widehat{w}_i^{\text{iso}} \widehat{w}_j^{\text{iso}} \widehat{f}_{it-h}^{\text{iso}} \widehat{f}_{jt}^{\text{iso}} - \frac{1}{T-h} \sum_{t=h+1}^T w_i w_j f_{it-h} f_{jt} \\ &= \frac{1}{T-h} \sum_{t=h+1}^T \mathcal{E}_{t-h} \otimes \mathcal{E}_t \times_{k=1}^K \widehat{\mathbf{b}}_{ik}^{\text{iso}\top} \times_{k=K+1}^{2K} \widehat{\mathbf{b}}_{jk}^{\text{iso}\top} + \frac{1}{T-h} \sum_{t=h+1}^T w_i w_j f_{it-h} f_{jt} \left( \prod_{k=1}^K \mathbf{a}_{ik}^{\top} \widehat{\mathbf{b}}_{ik}^{\text{iso}} \prod_{k=1}^K \mathbf{a}_{jk}^{\top} \widehat{\mathbf{b}}_{jk}^{\text{iso}} - 1 \right) \\ &\quad + \frac{1}{T-h} \sum_{t=h+1}^T \sum_{\ell_1 \neq i, \ell_2 \neq j} w_{\ell_1} w_{\ell_2} f_{\ell_1 t-h} f_{\ell_2 t} \prod_{k=1}^K (\mathbf{a}_{\ell_1 k}^{\top} \widehat{\mathbf{b}}_{ik}^{\text{iso}}) \prod_{k=1}^K (\mathbf{a}_{\ell_2 k}^{\top} \widehat{\mathbf{b}}_{jk}^{\text{iso}}) \\ &\quad + \frac{1}{T-h} \sum_{t=h+1}^T \sum_{\ell_2 \neq j} w_i w_{\ell_2} f_{it-h} f_{\ell_2 t} \cdot \prod_{k=1}^K (\mathbf{a}_{ik}^{\top} \widehat{\mathbf{b}}_{ik}^{\text{iso}}) \prod_{k=1}^K (\mathbf{a}_{\ell_2 k}^{\top} \widehat{\mathbf{b}}_{jk}^{\text{iso}}) \\ &\quad + \frac{1}{T-h} \sum_{t=h+1}^T \sum_{\ell_1 \neq i} w_{\ell_1} w_j f_{\ell_1 t-h} f_{jt} \cdot \prod_{k=1}^K (\mathbf{a}_{\ell_1 k}^{\top} \widehat{\mathbf{b}}_{ik}^{\text{iso}}) \prod_{k=1}^K (\mathbf{a}_{jk}^{\top} \widehat{\mathbf{b}}_{jk}^{\text{iso}}) \\ &\quad + \frac{1}{T-h} \sum_{t=h+1}^T w_i f_{it-h} \mathcal{E}_t \times_{k=1}^K \widehat{\mathbf{b}}_{jk}^{\text{iso}\top} \cdot \prod_{k=1}^K \mathbf{a}_{ik}^{\top} \widehat{\mathbf{b}}_{ik}^{\text{iso}} + \frac{1}{T-h} \sum_{t=h+1}^T w_j f_{jt} \mathcal{E}_{t-h} \times_{k=1}^K \widehat{\mathbf{b}}_{ik}^{\text{iso}\top} \cdot \prod_{k=1}^K \mathbf{a}_{jk}^{\top} \widehat{\mathbf{b}}_{jk}^{\text{iso}} \\ &\quad + \frac{1}{T-h} \sum_{t=h+1}^T \sum_{\ell_1 \neq i} w_{\ell_1} f_{\ell_1 t-h} \mathcal{E}_t \times_{k=1}^K \widehat{\mathbf{b}}_{jk}^{\text{iso}\top} \cdot \prod_{k=1}^K \mathbf{a}_{\ell_1 k}^{\top} \widehat{\mathbf{b}}_{ik}^{\text{iso}} \\ &\quad + \frac{1}{T-h} \sum_{t=h+1}^T \sum_{\ell_2 \neq j} w_{\ell_2} f_{\ell_2 t} \mathcal{E}_{t-h} \times_{k=1}^K \widehat{\mathbf{b}}_{ik}^{\text{iso}\top} \cdot \prod_{k=1}^K \mathbf{a}_{\ell_2 k}^{\top} \widehat{\mathbf{b}}_{jk}^{\text{iso}} \\ &:= \text{II}_1 + \text{II}_2 + \text{II}_3 + \text{II}_4 + \text{II}_5 + \text{II}_6 + \text{II}_7 + \text{II}_8 + \text{II}_9. \end{aligned}$$

Employing the same arguments in the proof of Theorem 2, as  $d_{\max}r \lesssim d$ , we can show

$$\begin{aligned}
\Pi_1 &= O_{\mathbb{P}} \left( \frac{\sigma^2}{\sqrt{T}} + \sqrt{r}\psi \cdot \sigma^2 \sqrt{\frac{d_{\max}}{T}} \right) = O_{\mathbb{P}} \left( \frac{\sigma^2}{\sqrt{T}} + \lambda_r \psi \right), \\
\Pi_2 &= O_{\mathbb{P}} (w_i w_j \psi), \\
\Pi_3 &= O_{\mathbb{P}} (\lambda_1 r^2 \psi^{2K}), \\
\Pi_4 &= O_{\mathbb{P}} (w_i \sqrt{\lambda_1} r \psi^K), \\
\Pi_5 &= O_{\mathbb{P}} (w_j \sqrt{\lambda_1} r \psi^K), \\
\Pi_6 &= O_{\mathbb{P}} \left( \frac{\sigma w_i}{\sqrt{T}} + w_i \sqrt{r} \psi \sqrt{\frac{\sigma^2 d_{\max}}{T}} \right) = O_{\mathbb{P}} \left( \frac{\sigma w_i}{\sqrt{T}} + w_i \sqrt{\lambda_r} \psi \right), \\
\Pi_7 &= O_{\mathbb{P}} \left( \frac{\sigma w_j}{\sqrt{T}} + w_j \sqrt{r} \psi \sqrt{\frac{\sigma^2 d_{\max}}{T}} \right) = O_{\mathbb{P}} \left( \frac{\sigma w_j}{\sqrt{T}} + w_j \sqrt{\lambda_r} \psi \right), \\
\Pi_8 &= \Pi_9 = O_{\mathbb{P}} \left( \sqrt{\lambda_1} r \psi^K \frac{\sigma}{\sqrt{T}} + \sqrt{\lambda_1} r \psi^{K+1} \sqrt{\frac{\sigma^2 d_{\max}}{T}} \right).
\end{aligned}$$

As derived before  $(\lambda_1/\lambda_r)^{1/2} r \psi^{K-1} \lesssim (\lambda_1/\lambda_r)^{1/2} \psi_0^{K-1} \lesssim 1$ , we have  $\Pi_3 = O_{\mathbb{P}}(\lambda_r \psi^2)$ , and  $\Pi_8 = \Pi_9 = O_{\mathbb{P}}(\sigma T^{-1/2} \lambda_r^{1/2} \psi + \lambda_r \psi^2)$ . Therefore,

$$\begin{aligned}
& w_i^{-1} w_j^{-1} \left| \frac{1}{T-h} \sum_{t=h+1}^T \hat{w}_i^{\text{iso}} \hat{w}_j^{\text{iso}} \hat{f}_{it-h}^{\text{iso}} \hat{f}_{it}^{\text{iso}} - \frac{1}{T-h} \sum_{t=h+1}^T w_i w_j f_{it-h} f_{it} \right| \\
&= O_{\mathbb{P}} \left( \psi + \psi^2 + \sqrt{\frac{\sigma^2}{\lambda_r T}} \right) = O_{\mathbb{P}} \left( \sqrt{\frac{\sigma^2 d_{\max}}{\lambda_r T}} \right).
\end{aligned}$$

□

## A.2 Technical Lemmas

We collect all technical lemmas that has been used in the theoretical proofs throughout the paper in this section. We denote the Kronecker product  $\odot$  as  $A \odot B \in \mathbb{R}^{m_1 m_2 \times r_1 r_2}$ , for any two matrices  $A \in \mathbb{R}^{m_1 \times r_1}, B \in \mathbb{R}^{m_2 \times r_2}$ . For any two  $m \times r$  matrices with orthonormal columns, say,  $U$  and  $\hat{U}$ , suppose the singular values of  $U^\top \hat{U}$  are  $\sigma_1 \geq \sigma_2 \geq \dots \geq \sigma_r \geq 0$ . A natural measure of distance between the column spaces of  $U$  and  $\hat{U}$  is then

$$\|\hat{U} \hat{U}^\top - U U^\top\|_{\text{S}} = \sqrt{1 - \sigma_r^2} = \|\sin \Theta(U, \hat{U})\|_{\text{S}},$$

which equals to the sine of the largest principal angle between the column spaces of  $U$  and  $\hat{U}$ .

**Lemma 2.** Let  $d_1 \geq r$  and  $A \in \mathbb{R}^{d_1 \times r}$  with  $\|A^\top A - I_r\|_S \leq \delta$ . Then, there exists an orthonormal  $U \in \mathbb{R}^{d_1 \times r}$  such that  $\|A\Lambda A^\top - U\Lambda U^\top\|_S \leq \delta\|\Lambda\|_S$  for all nonnegative-definite matrices  $\Lambda$  in  $\mathbb{R}^{r \times r}$ . Moreover, for  $d_2 \geq r$  and  $B \in \mathbb{R}^{d_2 \times r}$  with  $\|B^\top B - I_r\|_S \leq \delta$ , there exists an orthonormal  $V \in \mathbb{R}^{d_2 \times r}$  such that  $\|B\Lambda B^\top - V\Lambda V^\top\|_S \leq \|B^\top B - I_r\|_S\|\Lambda\|_S$  for all nonnegative-definite matrices  $\Lambda$  in  $\mathbb{R}^{r \times r}$  and  $\|AQB^\top - UQV^\top\|_S \leq \sqrt{2}\delta\|Q\|_S$  for all  $r \times r$  matrices  $Q$ .

*Proof.* Let  $A = \tilde{U}_1 \tilde{D}_1 \tilde{U}_2^\top$  and  $B = \tilde{V}_1 \tilde{D}_2 \tilde{V}_2^\top$  be respectively the SVD of  $A$  and  $B$  with  $\tilde{D}_1 = \text{diag}(\tilde{\sigma}_{11}, \dots, \tilde{\sigma}_{1r})$  and  $\tilde{D}_2 = \text{diag}(\tilde{\sigma}_{21}, \dots, \tilde{\sigma}_{2r})$ . Let  $U = \tilde{U}_1 \tilde{U}_2^\top$  and  $V = \tilde{V}_1 \tilde{V}_2^\top$ . We have  $\|\tilde{D}_1^2 - I_r\|_S = \|A^\top A - I_r\|_S \leq \delta$  and  $\|\tilde{D}_2^2 - I_r\|_S = \|B^\top B - I_r\|_S \leq \delta$ . Moreover,

$$\begin{aligned} \|AQB^\top - UQV^\top\|_S^2 &= \max_{\|u_1\|_2 = \|u_2\|_2 = 1} |u_1^\top (\tilde{D}_1 \tilde{U}_2^\top Q \tilde{V}_2 \tilde{D}_2 - \tilde{U}_2^\top Q \tilde{V}_2) u_2|^2 \\ &\leq 2\|Q\|_S^2 \max_{\|u_1\|_2 = \|u_2\|_2 = 1} \|\tilde{D}_2 u_2 u_1^\top \tilde{D}_1 - u_2 u_1^\top\|_F^2 \\ &= 2\|Q\|_S^2 \max_{\|u_1\|_2 = \|u_2\|_2 = 1} \sum_{i=1}^r \sum_{j=1}^r u_{1i}^2 u_{2j}^2 (\tilde{\sigma}_{1i} \tilde{\sigma}_{2j} - 1)^2 \end{aligned}$$

with  $u_\ell = (u_{\ell 1}, \dots, u_{\ell r})^\top$ ,  $\sqrt{(1-\delta)_+} \leq \tilde{\sigma}_{\ell j} \leq \sqrt{1+\delta}$ ,  $\ell = 1, 2$ . The maximum on the right-hand side above is attained at  $\tilde{\sigma}_{\ell j} = \sqrt{(1-\delta)_+}$  or  $\sqrt{1+\delta}$  by convexity. As  $(\sqrt{(1-\delta)_+} \sqrt{1+\delta} - 1)^2 \leq \delta^4 \wedge 1$ , we have  $\|AQB^\top - UQV^\top\|_S^2 \leq 2\|Q\|_S^2 \delta^2$ . For nonnegative-definite  $\Lambda$  and  $B = A$ ,  $\|A\Lambda A^\top - U\Lambda U^\top\|_S = \|\tilde{D}_1 \tilde{U}_2^\top \Lambda \tilde{U}_2 \tilde{D}_1 - \tilde{U}_2^\top \Lambda \tilde{U}_2\|_S$  and

$$|u^\top (\tilde{D}_1 \tilde{U}_2^\top \Lambda \tilde{U}_2 \tilde{D}_1 - \tilde{U}_2^\top \Lambda \tilde{U}_2) u| = \left| \sum_{j=1}^2 \tau_j v_j^\top \tilde{U}_2^\top \Lambda \tilde{U}_2 v_j \right| \leq \begin{cases} \|\Lambda\|_S (|\tau_1| \vee |\tau_2|), & \tau_1 \tau_2 < 0, \\ \|\Lambda\|_S (|\tau_1 + \tau_2|), & \tau_1 \tau_2 \geq 0, \end{cases}$$

where  $\sum_{j=1}^2 \tau_j v_j v_j^\top$  is the eigenvalue decomposition of  $\tilde{D}_1 u u^\top \tilde{D}_1 - u u^\top$ . Similar to the general case,  $(|\tau_1| \vee |\tau_2|)^2 \leq \tau_1^2 + \tau_2^2 = \|\tilde{D}_1 u u^\top \tilde{D}_1 - u u^\top\|_F^2 \leq \delta^2$  and  $|\tau_1 + \tau_2| = |\text{tr}(\tilde{D}_1 u u^\top \tilde{D}_1 - u u^\top)| \leq \|\tilde{D}_1 \tilde{D}_1 - I_r\|_S \leq \delta$ . Hence,  $\|A\Lambda A^\top - U\Lambda U^\top\|_S \leq \|\Lambda\|_S \delta$ .  $\square$

**Lemma 3.** Let  $M \in \mathbb{R}^{d_1 \times d_2}$  be a matrix with  $\|M\|_F = 1$  and  $a$  and  $b$  be unit vectors respectively in  $\mathbb{R}^{d_1}$  and  $\mathbb{R}^{d_2}$ . Let  $\hat{a}$  be the top left singular vector of  $M$ . Then,

$$(\|\hat{a}\hat{a}^\top - a a^\top\|_S^2) \wedge (1/2) \leq \|\text{vec}(M)\text{vec}(M)^\top - \text{vec}(ab^\top)\text{vec}(ab^\top)^\top\|_S^2. \quad (67)$$

*Proof.* Let  $\sum_{j=1}^r \sigma_j u_j v_j^\top$  be the SVD of  $M$  with singular values  $\sigma_1 \geq \dots \geq \sigma_r$  where  $r$  is the rank of  $M$ . Because  $\text{vec}(u_j v_j^\top)$  are orthonormal in  $\mathbb{R}^{d_1 d_2}$ ,

$$\text{vec}(M)^\top \text{vec}(ab^\top) = a^\top M b = \sum_{j=1}^r \sigma_j (u_j^\top a) (v_j^\top b)$$

with  $\sum_{j=1}^r \sigma_j^2 = \|M\|_{\mathbb{F}}^2 = 1$ ,  $\sum_{j=1}^r (u_j^\top a)^2 \leq \|a\|_2^2 = 1$  and  $\sum_{j=1}^r (v_j^\top b)^2 \leq \|b\|_2^2 = 1$ . Because  $\sigma_1 \geq \dots \geq \sigma_r$ ,

$$|a^\top Mb| \leq \sigma_1 \left( \sum_{j=1}^r (u_j^\top a)^2 \right)^{1/2} \left( \sum_{j=1}^r (v_j^\top b)^2 \right)^{1/2} = \sigma_1$$

Similarly, by Cauchy-Schwarz,

$$|a^\top Mb|^2 \leq \sum_{j=1}^r \sigma_j^2 (u_j^\top a)^2 \leq \sigma_1^2 (u_1^\top a)^2 + (1 - \sigma_1^2) (1 - (u_1^\top a)^2). \quad (68)$$

When  $(u_1^\top a)^2 \geq 1/2$ , the maximum on the right-hand side above is achieved at  $\sigma_1^2 = 1$ , so that  $|a^\top Mb|^2 \leq (u_1^\top a)^2$ ; Otherwise, the right-hand side of (68) is maximized at  $\sigma_1^2 = |a^\top Mb|^2$ , so that  $|a^\top Mb|^2 \leq 1 - |a^\top Mb|^2$ . Thus,  $|a^\top Mb|^2 > 1/2$  implies  $|a^\top Mb|^2 \leq (u_1^\top a)^2$ . By the property of spectral norm, this is equivalent to (67).  $\square$

The following two lemmas were proved in Han et al. (2020).

**Lemma 4.** *Let  $d, d_j, d_*, r \leq d \wedge d_j$  be positive integers,  $\epsilon > 0$  and  $N_{d,\epsilon} = \lfloor (1 + 2/\epsilon)^d \rfloor$ .*

(i) *For any norm  $\|\cdot\|$  in  $\mathbb{R}^d$ , there exist  $M_j \in \mathbb{R}^d$  with  $\|M_j\| \leq 1$ ,  $j = 1, \dots, N_{d,\epsilon}$ , such that  $\max_{\|M\| \leq 1} \min_{1 \leq j \leq N_{d,\epsilon}} \|M - M_j\| \leq \epsilon$ . Consequently, for any linear mapping  $f$  and norm  $\|\cdot\|_*$ ,*

$$\sup_{M \in \mathbb{R}^d, \|M\| \leq 1} \|f(M)\|_* \leq 2 \max_{1 \leq j \leq N_{d,1/2}} \|f(M_j)\|_*.$$

(ii) *Given  $\epsilon > 0$ , there exist  $U_j \in \mathbb{R}^{d \times r}$  and  $V_{j'} \in \mathbb{R}^{d' \times r}$  with  $\|U_j\|_{\mathbb{S}} \vee \|V_{j'}\|_{\mathbb{S}} \leq 1$  such that*

$$\max_{M \in \mathbb{R}^{d \times d'}, \|M\|_{\mathbb{S}} \leq 1, \text{rank}(M) \leq r} \min_{j \leq N_{dr,\epsilon/2}; j' \leq N_{d'r,\epsilon/2}} \|M - U_j V_{j'}^\top\|_{\mathbb{S}} \leq \epsilon.$$

Consequently, for any linear mapping  $f$  and norm  $\|\cdot\|_*$  in the range of  $f$ ,

$$\sup_{\substack{M, \tilde{M} \in \mathbb{R}^{d \times d'}, \|M - \tilde{M}\|_{\mathbb{S}} \leq \epsilon \\ \|M\|_{\mathbb{S}} \vee \|\tilde{M}\|_{\mathbb{S}} \leq 1 \\ \text{rank}(M) \vee \text{rank}(\tilde{M}) \leq r}} \frac{\|f(M - \tilde{M})\|_*}{\epsilon 2^{I_{r < d \wedge d'}}} \leq \sup_{\substack{\|M\|_{\mathbb{S}} \leq 1 \\ \text{rank}(M) \leq r}} \|f(M)\|_* \leq 2 \max_{\substack{1 \leq j \leq N_{dr,1/8} \\ 1 \leq j' \leq N_{d'r,1/8}}} \|f(U_j V_{j'}^\top)\|_*. \quad (69)$$

(iii) *Given  $\epsilon > 0$ , there exist  $U_{j,k} \in \mathbb{R}^{d_k \times r_k}$  and  $V_{j',k} \in \mathbb{R}^{d'_k \times r_k}$  with  $\|U_{j,k}\|_{\mathbb{S}} \vee \|V_{j',k}\|_{\mathbb{S}} \leq 1$  such that*

$$\max_{\substack{M_k \in \mathbb{R}^{d_k \times d'_k}, \|M_k\|_{\mathbb{S}} \leq 1 \\ \text{rank}(M_k) \leq r_k, \forall k \leq K}} \min_{\substack{j_k \leq N_{d_k r_k, \epsilon/2} \\ j'_k \leq N_{d'_k r_k, \epsilon/2}, \forall k \leq K}} \left\| \bigodot_{k=2}^K M_k - \bigodot_{k=2}^K (U_{j_k, k} V_{j'_k, k}^\top) \right\|_{\text{op}} \leq \epsilon(K-1).$$

For any linear mapping  $f$  and norm  $\|\cdot\|_*$  in the range of  $f$ ,

$$\sup_{\substack{M_k, \tilde{M}_k \in \mathbb{R}^{d_k \times d'_k}, \|M_k - \tilde{M}_k\|_{\mathbb{S}} \leq \epsilon \\ \text{rank}(M_k) \vee \text{rank}(\tilde{M}_k) \leq r_k \\ \|M_k\|_{\mathbb{S}} \vee \|\tilde{M}_k\|_{\mathbb{S}} \leq 1, \forall k \leq K}} \frac{\|f(\bigodot_{k=2}^K M_k - \bigodot_{k=2}^K \tilde{M}_k)\|_*}{\epsilon(2K-2)} \leq \sup_{\substack{M_k \in \mathbb{R}^{d_k \times d'_k} \\ \text{rank}(M_k) \leq r_k \\ \|M_k\|_{\mathbb{S}} \leq 1, \forall k}} \|f(\bigodot_{k=2}^K M_k)\|_* \quad (70)$$

and

$$\sup_{\substack{M_k \in \mathbb{R}^{d_k \times d'_k}, \|M_k\|_S \leq 1 \\ \text{rank}(M_k) \leq r_k \quad \forall k \leq K}} \left\| f\left(\odot_{k=2}^K M_k\right) \right\|_* \leq 2 \max_{\substack{1 \leq j_k \leq N_{d_k r_k, 1/(8K-8)} \\ 1 \leq j'_k \leq N_{d'_k r_k, 1/(8K-8)}}} \left\| f\left(\odot_{k=2}^K U_{j_k, k} V_{j'_k, k}^\top\right) \right\|_*. \quad (71)$$

**Lemma 5.** (i) Let  $G \in \mathbb{R}^{d_1 \times n}$  and  $H \in \mathbb{R}^{d_2 \times n}$  be two centered independent Gaussian matrices such that  $\mathbb{E}(u^\top \text{vec}(G))^2 \leq \sigma^2 \quad \forall u \in \mathbb{R}^{d_1 n}$  and  $\mathbb{E}(v^\top \text{vec}(H))^2 \leq \sigma^2 \quad \forall v \in \mathbb{R}^{d_2 n}$ . Then,

$$\|GH^\top\|_S \leq \sigma^2(\sqrt{d_1 d_2} + \sqrt{d_1 n} + \sqrt{d_2 n}) + \sigma^2 x(x + 2\sqrt{n} + \sqrt{d_1} + \sqrt{d_2})$$

with at least probability  $1 - 2e^{-x^2/2}$  for all  $x \geq 0$ .

(ii) Let  $G_i \in \mathbb{R}^{d_1 \times d_2}$ ,  $H_i \in \mathbb{R}^{d_3 \times d_4}$ ,  $i = 1, \dots, n$ , be independent centered Gaussian matrices such that  $\mathbb{E}(u^\top \text{vec}(G_i))^2 \leq \sigma^2 \quad \forall u \in \mathbb{R}^{d_1 d_2}$  and  $\mathbb{E}(v^\top \text{vec}(H_i))^2 \leq \sigma^2 \quad \forall v \in \mathbb{R}^{d_3 d_4}$ . Then,

$$\begin{aligned} \left\| \text{mat}_1 \left( \sum_{i=1}^n G_i \otimes H_i \right) \right\|_S &\leq \sigma^2(\sqrt{d_1 n} + \sqrt{d_1 d_3 d_4} + \sqrt{nd_2 d_3 d_4}) \\ &\quad + \sigma^2 x(x + \sqrt{n} + \sqrt{d_1} + \sqrt{d_2} + \sqrt{d_3 d_4}) \end{aligned}$$

with at least probability  $1 - 2e^{-x^2/2}$  for all  $x \geq 0$ .

## B Additional Simulation Results

Here we provide two additional simulation results. One under TFM-cp with  $K = 2$  (matrix time series) with

$$\mathcal{X}_t = \sum_{i=1}^r w f_{it} \mathbf{a}_{i1} \otimes \mathbf{a}_{i2} + \mathcal{E}_t, \quad (72)$$

and the other one  $K = 3$  with

$$\mathcal{X}_t = \sum_{i=1}^r w f_{it} \otimes_{k=1}^3 \mathbf{a}_{ik} + \mathcal{E}_t. \quad (73)$$

For  $K = 2$  with model (72), we consider the following additional experimental configuration:

- IV. Set  $r = 3$ ,  $d_1 = d_2 = 40$ ,  $\delta = 0.1$  to compare the performance of different methods and to reveal the effect of sample size  $T$  and signal strength  $w$ .

For  $K = 3$ , under model (73), we implement the following configuration:

- V. Set  $r = 3$ ,  $d_1 = d_2 = d_3 = 20$ ,  $\delta = 0.2$ . The sample size  $T$  and signal strength  $w$  are varied, similar to configuration II in Section 5.2

We repeat all the experiments 100 times. For simplicity, we set  $h = 1$ .

To see more clearly the impact of  $T$  and  $w$ , we show the boxplots of the logarithm of the estimation errors in Figures 13 and 14. Here we use different sample sizes, with the coherence fixed

at  $\delta = 0.1$  (resp.  $\delta = 0.2$ ) and three  $w$  values:  $w = 4, 8, 12$  (resp.  $w = 5, 10, 15$ ) in the matrix factor model (72) (resp. in the tensor factor model (73)). We observe that the performance of all methods improves as the the sample size or the signal increases. Again, HOPE uniformly outperforms the other methods. When the sample size is large and signal is strong, the one-step method is similar to the iterative method HOPE after convergence. The message is almost the same as in Figure 4 for the comparison of cPCA, 1HOPE and HOPE. When  $w = 4$  in Figure 13 (resp.  $w = 5$  in Figure 14), both HOPE and cOALS perform almost the same. When  $w = 8, 12$  (resp.  $w = 10, 15$ ), cOALS is only slightly worse than HOPE. This observation provides empirical advantages of cOALS, and motivates us to investigate its theoretical properties in the future.

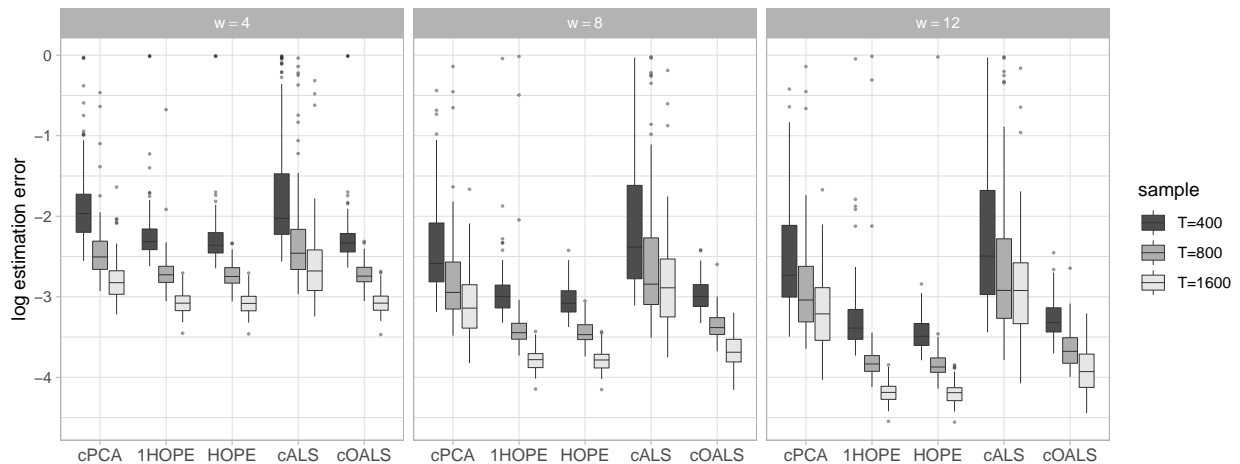


Figure 13: Boxplots of the logarithm of the estimation error under experiment configuration IV. Five methods with three choices of sample size  $T$  are considered in total. Three columns correspond to three signal strengths  $w = 4, 8, 12$ .

## C Additional Figures for the Taxi Example

Here we show the estimated factors for year 2011 (the third year in the series under study), in order to see finer details than those shown in Figures 7 and 11.

For business day series, the weekly pattern in Factor 1 is clearly seen. Factor 2 is mainly used by morning hours, potentially by commuters going to offices. The volume is quite stable, except some significant (small value) outliers, most of them corresponding to the working day before or after holidays (e.g. July 4 holiday, thanksgiving holiday, and end of year holiday seasons). For unknown reasons (possibly weather related), there are also more (small value) outliers in January. It is seen in other years as well. The impact of summer/early fall is mostly seen in Factors 3 and

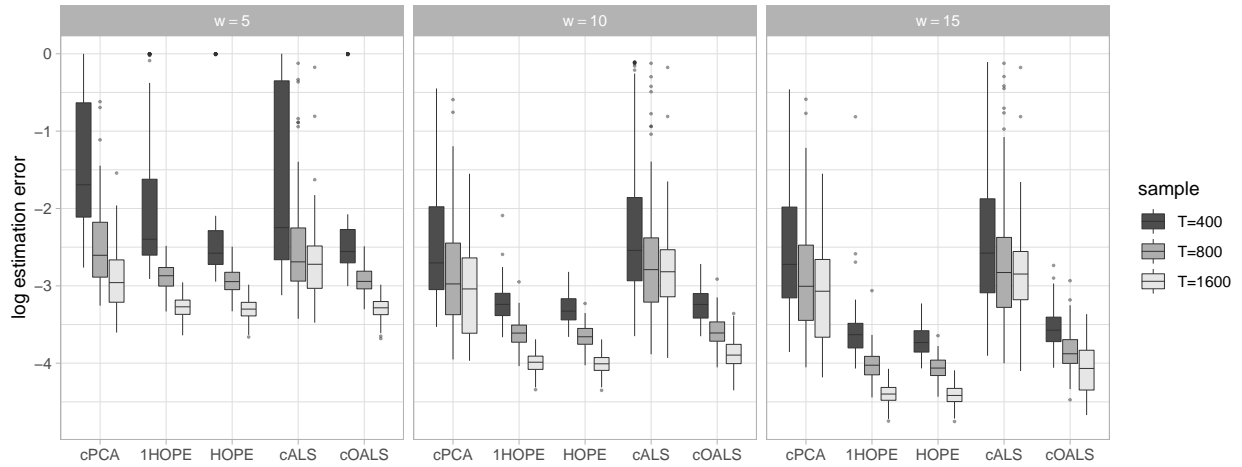


Figure 14: Boxplots of the logarithm of the estimation error under experiment configuration V. Five methods with three choices of sample size  $T$  are considered in total. Three columns correspond to three signal strengths  $w = 5, 10, 15$ .

4, though these two factors are relatively small comparing to the first two factors.

For non-business day series, the factor series are more volatile, with more dominant summer effect.

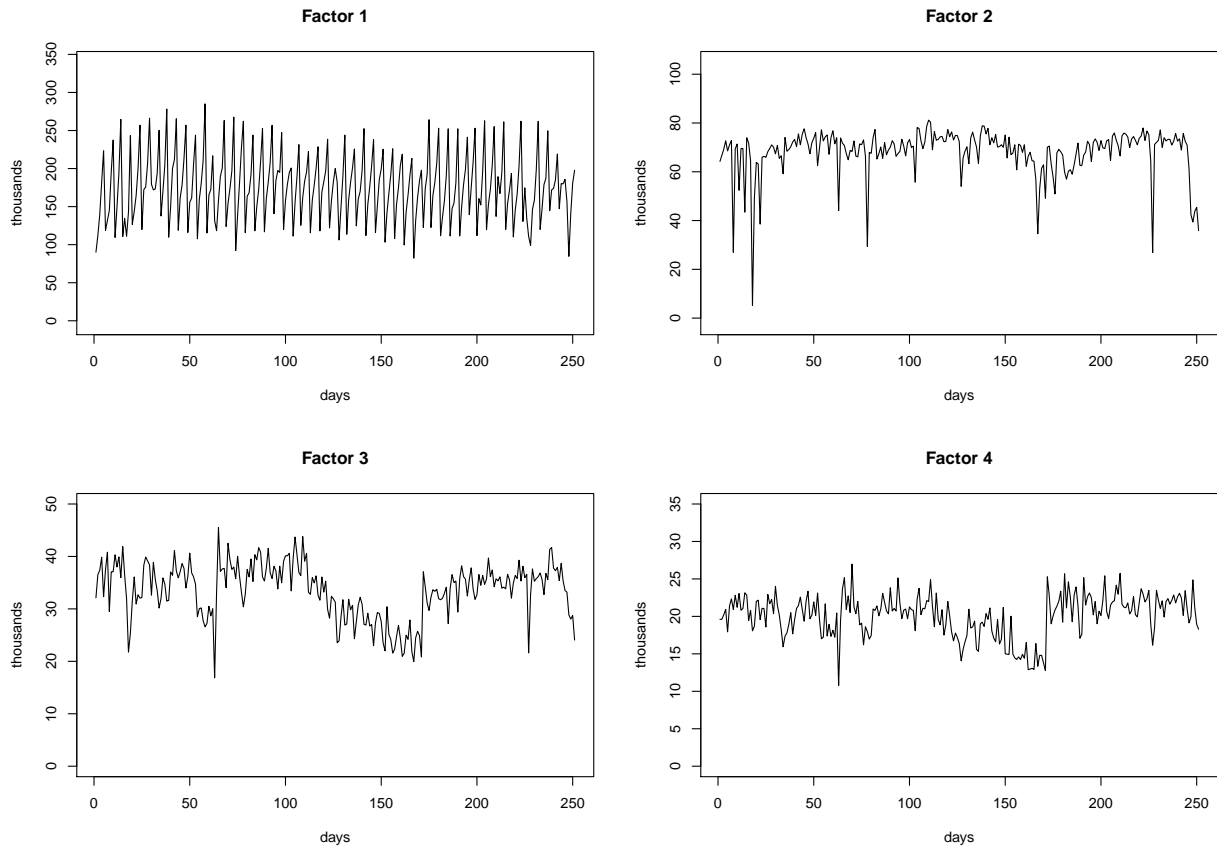


Figure 15: Estimated four factors (in 1,000) for business day series in year 2011.

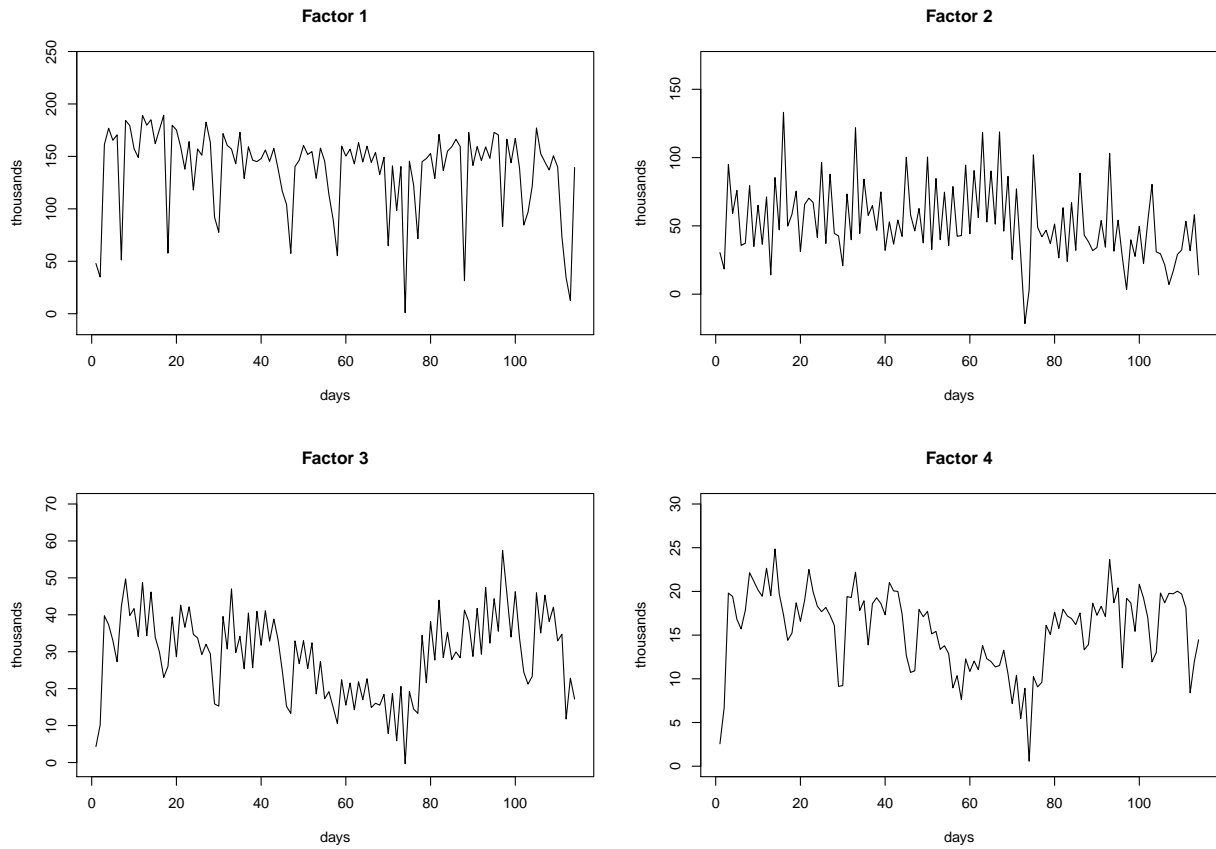


Figure 16: Estimated four factors (in 1,000) for non-business day series in year 2011.